AD-A041 782 TENNESSEE UNIV SPACE INST TULLAHOMA F/G 21/5
INVESTIGATION OF FEASIBLE NOZZLE CONFIGURATIONS FOR NOISE REDUC--ETC(U)
MAR 77 B H GOETHERT, J R MAUS, W A DUNNILL DOT-FA72WA-3053
UNCLASSIFIED FAA-RD-75-162-3 NL

1 OF 2
ADA
041782

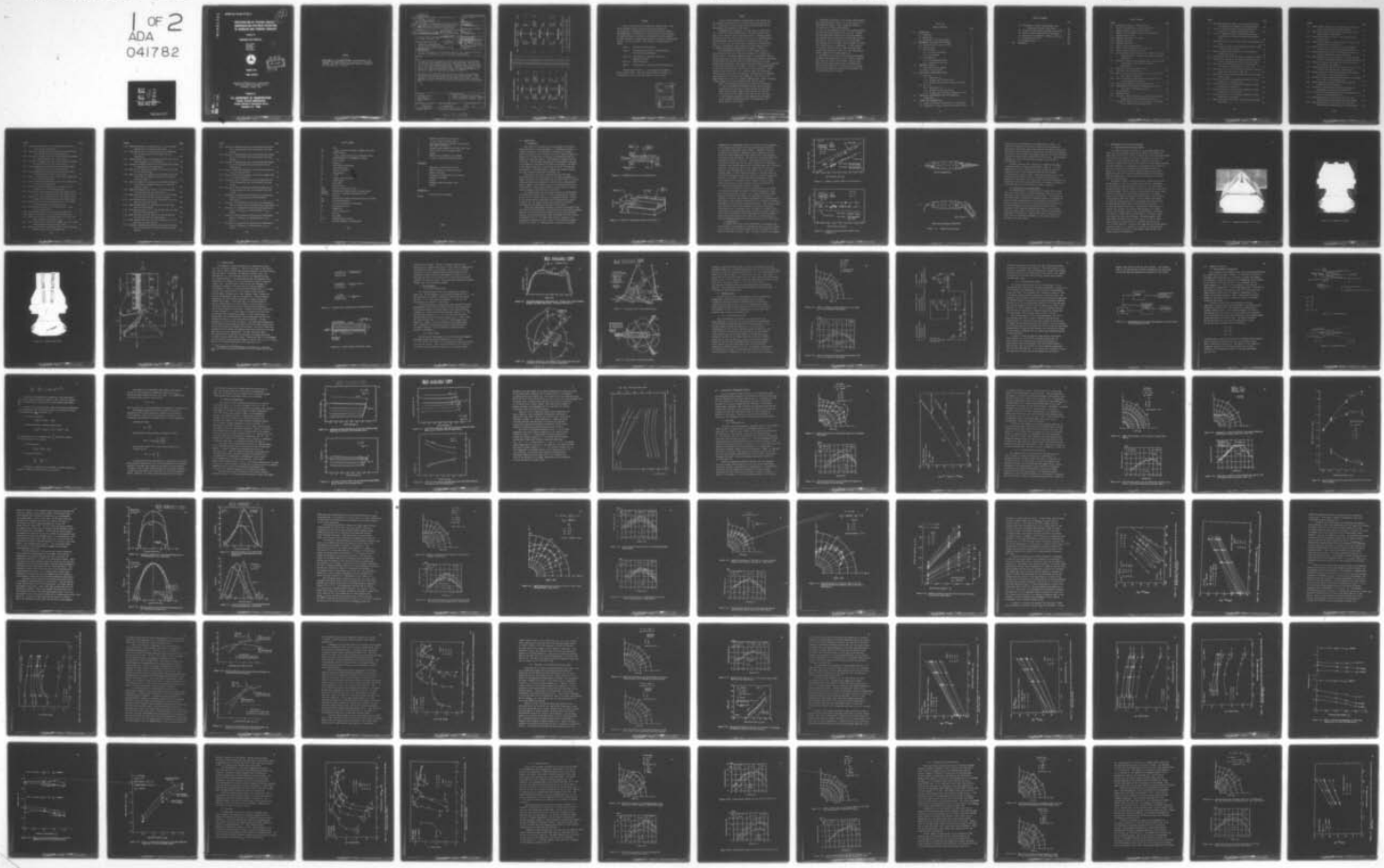

AD A041782

REPORT NO. FAA-RD-75-162,III

12

INVESTIGATION OF FEASIBLE NOZZLE CONFIGURATION FOR NOISE REDUCTION IN TURBOFAN AND TURBOJET AIRCRAFT

Volume III

SHROUDED SLOT NOZZLES

B.H. Goethert
J.R. Maus
W.A. Dunnill
M.C. Joshi
V.Veerasamy

DDC
RECEIVED
JUL 18 1977
C

MARCH 1977

FINAL REPORT

Document is available to the U.S. public through the National Technical Information Service, Springfield, Virginia 22161.

Prepared for

U.S. DEPARTMENT OF TRANSPORTATION
FEDERAL AVIATION ADMINISTRATION
Systems Research & Development Service
Washington, D.C. 20590

AD NO.
DDC FILE COPY

NOTICE

This document is disseminated under the sponsorship of the Department of Transportation in the interest of information exchange. The United States Government assumes no liability for its contents or use thereof.

A024926

Volume (18) (19)

Technical Report Documentation Page

1. Report No.	2. Government Accession No.	3. Recipient's Catalog No.
FAA-RD-75-162-III 3		(11)

4. Title and Subtitle (6)

Investigation of Feasible Nozzle Configurations for Noise Reduction in Turbofan and Turbojet Aircraft. III, Shrouded Slot Nozzle Configurations.

5. Report Date
March 1977

6. Performing Organization Code

8. Performing Organization Report No.
William

7. Author(s) (10)

B. H. Goethert, J. R. Maus, A. Dunnill, et. al.
M. C. Joshi
V. Veerasamy

9. Performing Organization Name and Address

The University of Tennessee Space Institute
Tullahoma, Tennessee 37388

10. Work Unit No. (TRAIS)

11. Contract or Grant No. (15)
DOT-FA72WA-3053

13. Type of Report and Period Covered (9)
Final Report,
August 1975-March 1977

(12) 116p.

12. Sponsoring Agency Name and Address

Department of Transportation
Federal Aviation Administration
Aircraft Safety and Noise Abatement Division
Washington, D. C.

14. Sponsoring Agency Code
ARD-550

15. Supplementary Notes

The first two volumes of this report are subtitled: Vol. 1 Summary and Selected Multinozzle Configurations; Vol. 2 Slot Nozzle Configurations.

16. Abstract

This report presents the results of a study of the acoustic and fluid dynamic characteristics of a shrouded slot nozzle. Experiments were carried out on a slot nozzle of aspect ratio 27 with an ejector shroud having a cross sectional area of four times the primary nozzle area. Parameters varied during the tests were, shroud length, shroud divergence ratio, and acoustical impedance of the shroud wall. Tests were conducted for primary flow Mach numbers from 0.5 to choking and stagnation temperatures from ambient to 1200° R.

The results of the study show that both the thrust and the noise attenuation characteristics of the ejector shroud improve with increasing length. Thrust increases of near 40% were obtained for the longest shroud tested. A noise reduction of 13 dB was obtained for the lined shroud with a near choked, high temperature primary jet. The corresponding thrust augmentation was approximately 20%.

17. Key Words	18. Distribution Statement
Aerodynamic Noise Aeroacoustics Noise Suppression V/STOL	Document is available to the public through the National Technical Information Service, Springfield, Virginia 22161.

19. Security Classif. (of this report)	20. Security Classif. (of this page)	21. No. of Pages	22. Price
UNCLASSIFIED	UNCLASSIFIED	125	

Form DOT F 1700.7 (8-72) Reproduction of completed page authorized

387 070

4B

METRIC CONVERSION FACTORS

Approximate Conversions to Metric Measures

Symbol	When You Know	Multiply by	To Find	Symbol
	LENGTH			
in	inches	*2.5	centimeters	cm
ft	feet	30	centimeters	cm
yd	yards	0.9	meters	m
mi	miles	1.6	kilometers	km
	AREA			
in^2	square inches	6.5	square centimeters	cm^2
ft^2	square feet	0.09	square meters	m^2
yd^2	square yards	0.8	square meters	m^2
mi^2	square miles	2.6	square kilometers	km^2
	acres	0.4	hectares	ha
	MASS (weight)			
oz	ounces	28	grams	g
lb	pounds	0.45	kilograms	kg
	short tons (2000 lb)	0.9	tonnes	t
	VOLUME			
tsp	teaspoons	5	milliliters	ml
Tbsp	tablespoons	15	milliliters	ml
fl oz	fluid ounces	30	milliliters	ml
c	cups	0.24	liters	l
pt	pints	0.47	liters	l
qt	quarts	0.95	liters	l
gal	gallons	3.8	liters	l
ft^3	cubic feet	0.03	cubic meters	m^3
yd^3	cubic yards	0.76	cubic meters	m^3
	TEMPERATURE (exact)			
°F	Fahrenheit temperature	5/9 (after subtracting 32)	Celsius temperature	°C

*1 in = 2.54 (exactly). For other exact conversions and more detailed tables, see NBS Misc. Publ. 286, Units of Weights and Measures, Price $2.25, SD Catalog No. C13.10:286.

Approximate Conversions from Metric Measures

Symbol	When You Know	Multiply by	To Find	Symbol
	LENGTH			
mm	millimeters	0.04	inches	in
cm	centimeters	0.4	inches	in
m	meters	3.3	feet	ft
m	meters	1.1	yards	yd
km	kilometers	0.6	miles	mi
	AREA			
cm^2	square centimeters	0.16	square inches	in^2
m^2	square meters	1.2	square yards	yd^2
km^2	square kilometers	0.4	square miles	mi^2
ha	hectares (10,000 m^2)	2.5	acres	
	MASS (weight)			
g	grams	0.035	ounces	oz
kg	kilograms	2.2	pounds	lb
t	tonnes (1000 kg)	1.1	short tons	
	VOLUME			
ml	milliliters	0.03	fluid ounces	fl oz
l	liters	2.1	pints	pt
l	liters	1.06	quarts	qt
l	liters	0.26	gallons	gal
m^3	cubic meters	35	cubic feet	ft^3
m^3	cubic meters	1.3	cubic yards	yd^3
	TEMPERATURE (exact)			
°C	Celsius temperature	9/5 (then add 32)	Fahrenheit temperature	°F

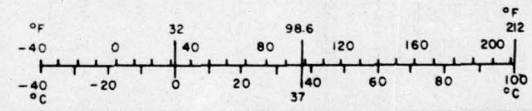

PREFACE

This is the third volume of Report No. FAA-RD-75-162. This report describes the work done and the results obtained by The University of Tennessee Space Institute under Contract Number DOT-FA72WA-3053. The objectives of the program were the development of feasible methods of reducing or redirecting the noise generated by high velocity jet streams exhausting from a variety of unconventional nozzles. The work statement of the contract is divided into five phases.

Phase I	Preliminary Investigations.
Phase II	Detailed Identification of Noise Generation and Transmission Mechanims.
Phase III	Investigation of Advanced Concepts for Reducing Jet Noise.
Phase IV	Task Integration.
Phase V	Investigation of Selected V/STOL Configurations.

The work done in Phases I - IV are reported in Volumes I and II of this report. This, the third volume of the report, is concerned with the work done under Phase V of the contract.

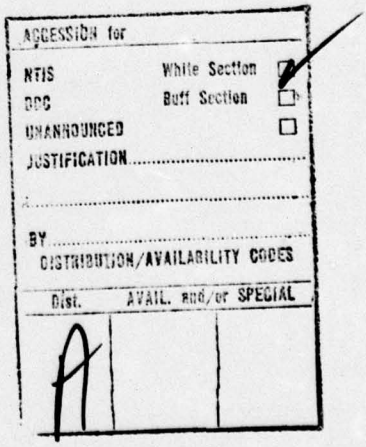

SUMMARY

In this research program a detailed study of the acoustic and fluid dynamic characteristics of a shrouded slot nozzle was carried out. A description of the work done and the results obtained in the investigation are presented in this report.

Experiments were carried out on a slot nozzle of aspect ratio w/h = 27 with an ejector shroud having a total base cross sectional area of four times the area of the primary nozzle. Parameters varied during the tests were shroud length, from 4.17 to 12.5 shroud heights; shroud divergence angle, giving ratios of shroud exit area to base area from 0.9 to 1.4; and the acoustical impedance of the shroud wall. Tests were conducted for various primary flow Mach numbers from 0.5 to choking and stagnation temperatures from ambient to 1200° R.

The aerodynamic performance of the nozzle-shroud system is characterized by the ratio of entrained secondary air to primary air and the thrust of the system compared to that of an unshrouded reference nozzle operating at the same stagnation pressure and stagnation temperature and delivering the same mass flow at the same pressure ratio as the primary unshrouded nozzle. The acoustic data taken during the tests consisted of overall sound pressure level (OASPL) contours in a plane perpendicular to the nozzle span (XZ plane) and contours in the nozzle plane. Sound pressure level spectra were taken at specific points in these planes. The noise output of the device is generally characterized by the maximum sound pressure level in the XZ plane ($OASPL_{max}$). This occurs at an angle between 30° and 50° to the primary flow direction. Noise reductions are with respect to the same reference nozzle used for thrust.

Some of the principal findings of this study are listed below:

1. Both the aerodynamic performance and the noise attenuation characteristics of the ejector shroud improve with increasing length over the range tested. Thrust increases of near 40% were obtained for the longest shroud under certain conditions.
2. The entrained secondary air flow measured for the longest shroud compared extremely well with a one-dimensional fully mixed analysis of the ejector.

PRECEDING PAGE BLANK-NOT FILMED

3. Aerodynamic performance of the ejector shroud improved with shroud divergence angle up to an area ratio of 1.2 and thereafter decayed. Noise attenuation generally decreased as the shroud walls diverged.

4. Use of noise attenuating liners in the shroud produced little further noise reduction for cold flow. However, for high temperature primary flow at high Mach numbers the lined shroud was significantly quieter than the hard wall shroud. This is primarily due to the increased noise generation by the higher velocity primary jet rather than a direct effect of temperature. A noise reduction of 13 dB was obtained from the lined shroud with near choked, high temperature primary jet. The corresponding thrust augmentation was approximately 20%.

5. The noise floor for the ejector system was determined by making sound measurements for flow through the shroud only, with the primary nozzle removed. The far field noise from the longest acoustically lined shroud with parallel walls was found to be within 5 dB of the noise floor for high temperature primary flow and within 2 dB of the noise floor for cold flow.

Volume III

TABLE OF CONTENTS

TABLE OF CONTENTS

LIST OF FIGURES

LIST OF SYMBOLS

A	Area
AR	$= A_s/A_p$, ratio of secondary to primary flow areas
c	Speed of Sound
CR	$= A_2/A_1$, shroud area ratio or contraction ratio
D_s	Shroud diameter for axisymmetric shrouds
F	Static thrust
f	Frequency
f_o	Characteristics frequency
h	Slot nozzle height
h_o	Specific total enthalpy
h_s	Shroud height
i	$= \sqrt{-1}$
K_m	$= \dot{m}_s/\dot{m}_p$, mass flow ratio
L	Shroud length
M	Mach number
$\dot{m}$	Mass flow rate
OASPL	Overall sound pressure level
$OASPL_{max}$	Maximum sound pressure level in flyover plane
$\Delta OASPL_{max}$	Reduction in maximum sound pressure level
P	Pressure
ΔP_v	Pressure drop between upstream and throat of venturi
ΔPWL	Sound power reduction
R	Acoustic resistance of shroud walls
SPL	Sound pressure level
T	Temperature
TR	$= F/F'$, thrust ratio
V	Velocity
w	Slot width
X,Y,Z	Coordinate axes of model
Z	Acoustic impedence of shroud walls

α	Absorption coefficient of the liner
γ	$= c_p/c_v$, ratio of specific heats
θ	Polar angle measured in XZ plane from the flow axis (Positive upwards)
ϕ	Aximuthal angle measured in YZ plane from Y axis
Λ_p	$= w/h$, aspect ratio of primary nozzle
ρ	Density
ρc	Characteristic impedence of the medium
τ	$= T_{op}/T_{os}$, stagnation temperature ratio

Subscripts

1	conditions at shroud inlet section
2	mean conditions at shroud exit section
a	ambient conditions
e	conditions at primary nozzle exit section
o	stagnation conditions
p	primary
s	secondary (unless otherwise noted)
v	Venturi

Superscripts

' (prime)	Reference nozzle conditions

1.0 INTRODUCTION.

1.1 Background.

This report is concerned with an investigation of the noise characteristics and thrust performance of a shrouded slot nozzle. A schematic diagram of a shrouded nozzle consisting of a primary nozzle that exhausts into a constant area duct is shown in Figure 1.1. External air is ingested by the ejector action and mixes with the primary air producing, ideally, a well-mixed flow stream at the end of the duct. The entrained secondary air flow provides an increase in the momentum of the exhaust jet causing an increase in the thrust of the system as compared to the primary jet alone. The duct may be diverged, or a diffuser added, to improve the pressure recovery and cause a greater entrainment of secondary air.

Acoustically, the ejector represents an effective noise suppression device for three reasons: (1) the large secondary flow causes a reduction in the mean shear near the nozzle exit, (2) the jet stream exiting from the shroud has a velocity that is substantially reduced compared to the primary jet and (3) the shroud walls act as a noise shield. Further noise reduction can be obtained by fitting acoustic lining to the inner wall of the shroud.

The primary impetus for the present work was the investigation by Goethert and Borchers (Ref. 1) in which experiments were carried out on a pair of circular nozzles in a rectangular shroud. A sketch of the shrouded nozzle system used in that investigation is shown in Figure 1.2; the symbols used in this figure are consistent with those used throughout the remainder of this report.

Sound power measurements were made by Goethert and Borchers using both hard wall and acoustically lined ejectors for various shroud lengths. Results for the hard wall ejector showed an increase in sound power reduction with increasing shroud length confirming the earlier results of Middleton (Ref. 2). The sound power reduction appeared to be approaching an asymptotic value of about 7 dB for hard-wall internal surfaces (no liners). A comparison with a theoretical calculation

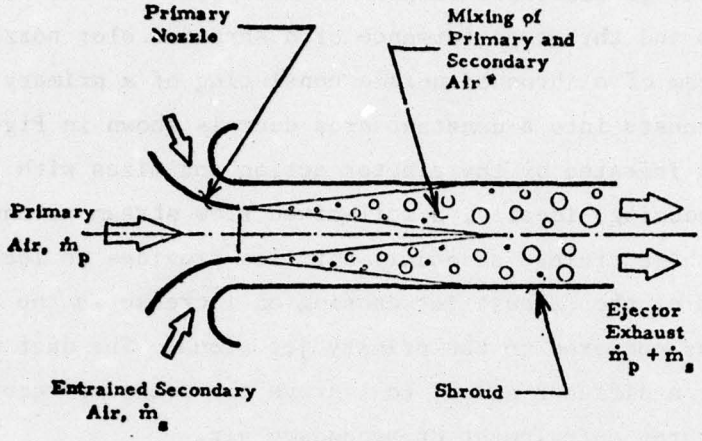

Figure 1.1. Configuration Sketch of Shrouded Nozzle.

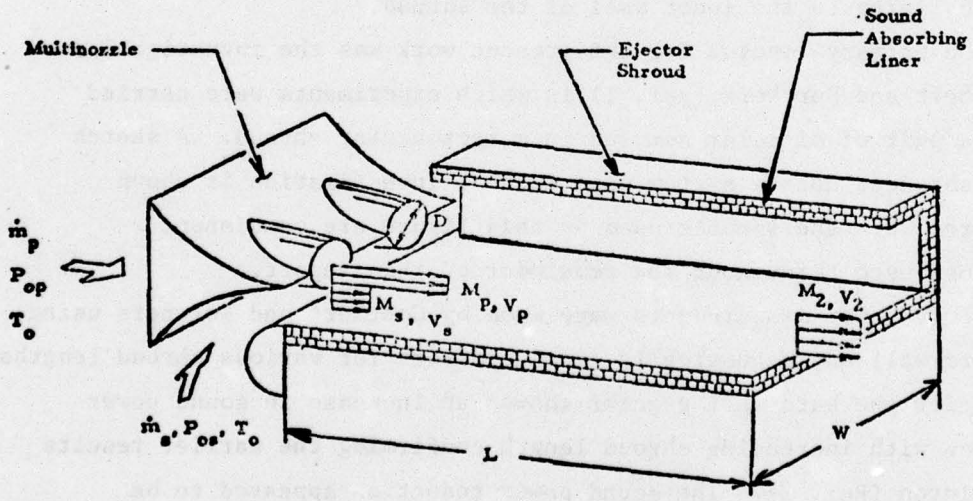

Figure 1.2. Sketch of Configuration Tested in Reference 1.

suggested that a substantial portion of the noise was being generated in the mixing region beneath the shroud and thus would be reduced by acoustically lining the ejector channel. Subsequent tests with a lined ejector produced a substantial further reduction in noise output but caused unexpectedly large internal flow losses impairing the thrust gain by the ejector. The results of this investigation are summarized in Figures 1.3 and 1.4. These figures show the noise reduction and thrust ratio of the ejector compared to an unshrouded reference nozzle plotted against ratio of secondary mass flow to primary mass flow. The data are shown for the longest ejector tested at a pressure ratio corresponding to a Mach number of 0.9. The large circular symbols in these figures correspond to conditions where the secondary flow stagnation pressure is equal to the static pressure at the exit of the shroud. These conditions would prevail in normal static operation of a shrouded nozzle. Figures 1.3 and 1.4 show clearly the increase in noise reduction caused by the addition of the liner and the accompanying decrease in thrust.

The results obtained by Goethert and Borchers were considered to be quite encouraging and worthy of further investigation. Based on the experience gained in these tests, a new experimental program, guided by theoretical calculations, was undertaken to attempt to optimize the acoustic and aerodynamic performance of a shrouded nozzle. Improvement in the aerodynamic performance of the system was obtained by redesigning the ejector with increased flexibility. Also a higher aspect ratio shroud was used to take advantage of the better directional characteristics of a high aspect ratio slot nozzle. In order to more fully explore the radiated sound field, acoustic tests were carried out in the free field rather than the reverberant room used in Reference 1. A more detailed description of the model used in this investigation and the experimental facilities are given in Section 2.0 of this report.

1.2 Application.

A shrouded nozzle such as was investigated in the present study is more likely to be employed as a powered lift device for STOL aircraft. Such a device would be deployed during take-off and landing and folded back into the wing for cruise. Figure 1.5 shows a sketch of an augmentor

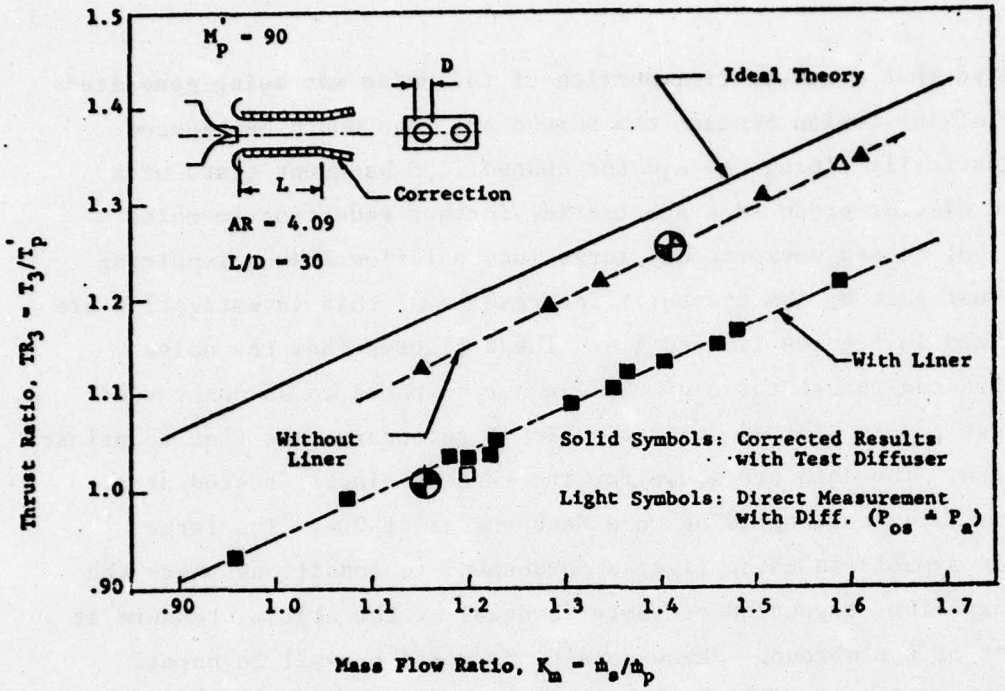

Figure 1.3. Summary of Thrust Results from Reference 1.

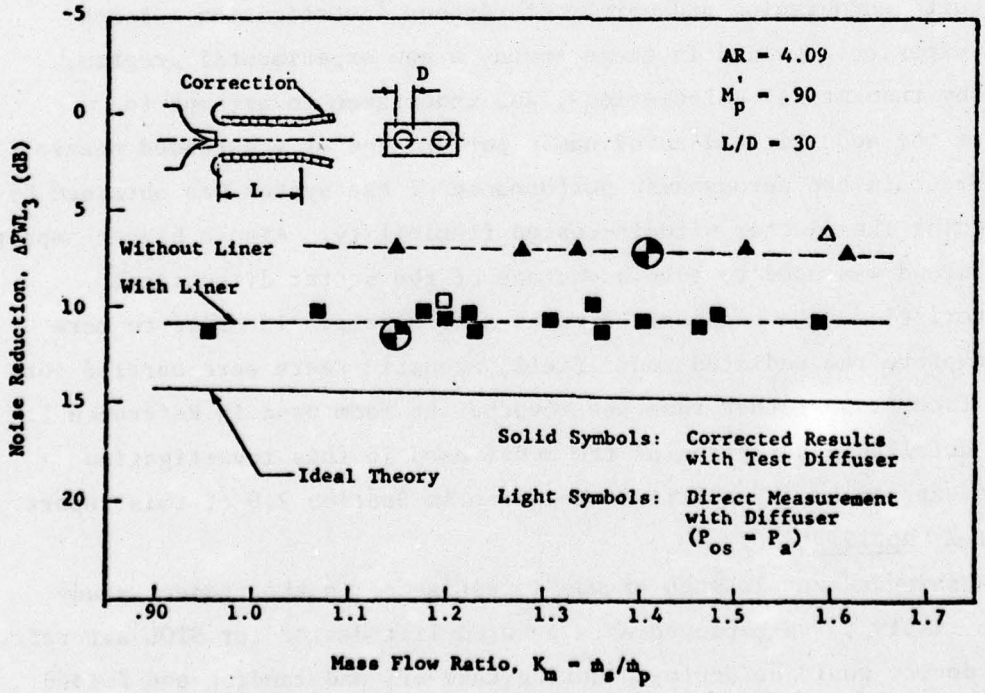

Figure 1.4. Summary of Noise Reduction Results from Reference 1.

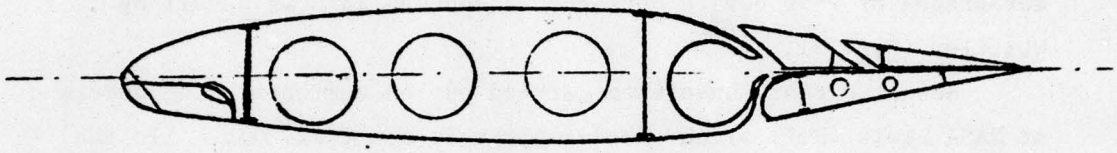

Cruise Configuration

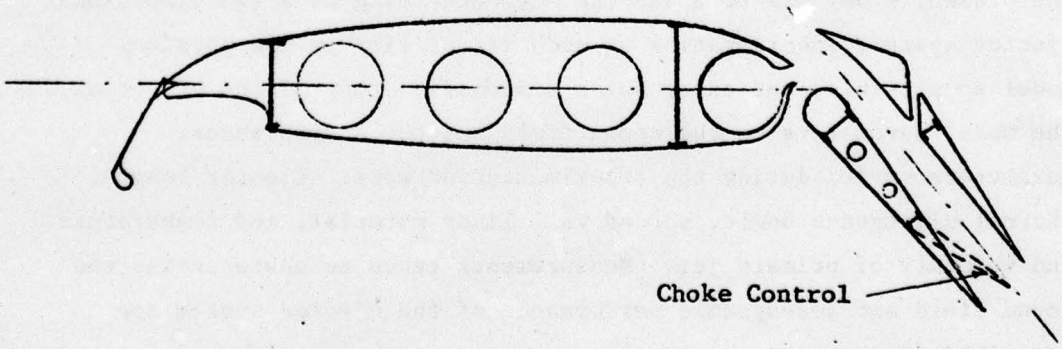

Take-off and Landing Configuration

Figure 1.5. Augmentor-Wing Section.

wing in a take-off configuration and folded away for cruise. In powered lift operation air from the turbofan is ducted through the wing section and exhaust from a nozzle through the augmentor wing shroud. The enhanced thrust generated by the ejector action more than compensates for the duct losses and make the augmentor wing one of the more attractive powered lift devices being considered for STOL aircraft. The aerodynamic advantages of this device have been discussed in some detail by Whittley (Ref. 3).

Acoustic tests have been carried out on augmentor wing models at NASA Lewis (Ref. 4) and Boeing Aircraft Co. (Ref. 5). In the experiments at Boeing a multirow lobe nozzle was used to shift the primary jet noise to high frequencies which are more amenable to attenuation by acoustic liners. This nozzle together with a lined shroud and screech shield produced a substantial noise reduction compared to a high aspect ratio slot nozzle. The Boeing estimates of the noise output for a full scale aircraft with four engines of 18,000 lbs. thrust each gave less than 95 PNdB at the 500 ft. sideline.

1.3 Objectives of the Present Study.

The shrouded nozzle is a geometrically flexible device in that there are a large number of geometric parameters which can be varied even after a basic configuration has been selected. The objective of the present study was to model the augmentor wing by a two dimensional ejector system, incorporating as much versatility in the physical model as possible, and carry out a systematic study of the effect of the model parameters on the sound field and the static thrust. Parameters varied during the experimentation were: Ejector length, channel divergence angle, shroud wall liner material, and temperature and velocity of primary jet. Measurements taken to characterize the sound field and aerodynamic performance of the ejector system are described in the next chapter.

2.0 EXPERIMENTAL FACILITIES AND PROCEDURES.

2.1 Selection and Description of Model.

For reasons discussed in Section 1.1 a rectangular geometry was chosen for both the primary nozzle and the shroud. The primary slot nozzle has an exit area of 2.4 in^2, an aspect ratio (slot width/slot height) of 26.67 with a slot height of 0.3 inch. The shroud duct has a basic height of 1.2 inches and the same width, 8 inches, as the nozzle. This gives a nominal area ratio for the ejector of 3 which seems reasonable for STOL applications. A photograph of the nozzle with the transition piece that attaches to the primary stilling chamber is given in Figure 2.1a. The nozzle is made of stainless steel and has smooth machined contours on the inside and machined surfaces on the outside with thin rounded lips. Nozzle sides are closed by plates that also hold the shroud in place.

The shroud is made in three sections each 5 inches long so that shroud lengths of 5, 10 and 15 inches can be achieved. Photographs of the shroud are shown in Figures 2.1b and 2.1c. The side plates facing the viewer have been removed to reveal the internal construction and flow passages. The first section of the shroud has a smooth, high contraction entrance for the secondary induced flow. The shroud walls can be diverged by rotating them about hinges on the side walls at the primary nozzle exit section. Care was taken in the design to avoid any diverging sections in the secondary flow inlet section. The aluminum wall panels shown in the shroud can be replaced by noise attenuating liner blocks. With parallel shroud walls (i.e., constant area channel) the internal shroud height is 1.2 inches and its width is always equal to the slot nozzle width. This gives a secondary to primary area ratio (AR) equal to 2.75 (after taking into account the nozzle lip thickness). Shroud divergence can be continuously varied from $A_2/A_1 = 0.9$ to $A_2/A_1 = 1.4$ for all three shroud lengths, A_2 being the area of the shroud exit and A_1 the area of shroud entrance. A sketch of the model with the 10 inch shroud is shown in Figure 2.2. Included in the figure are the geometrical model parameters and principal fluid dynamic quantities that were varied during the investigation.

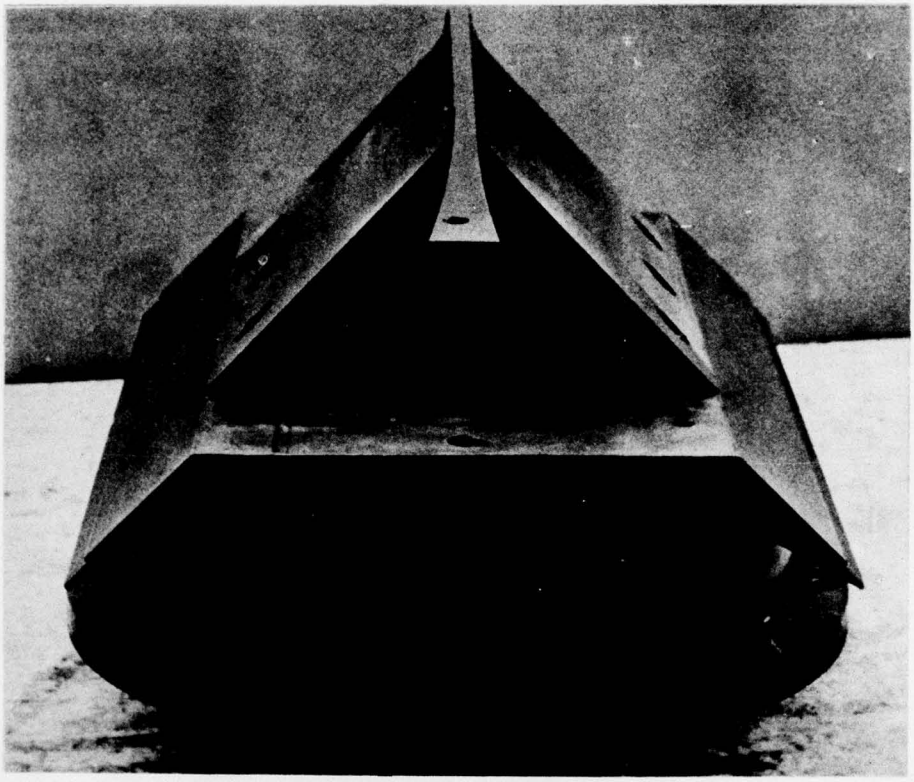

Figure 2.1a. Augmentor Wing Model, Slot Nozzle.

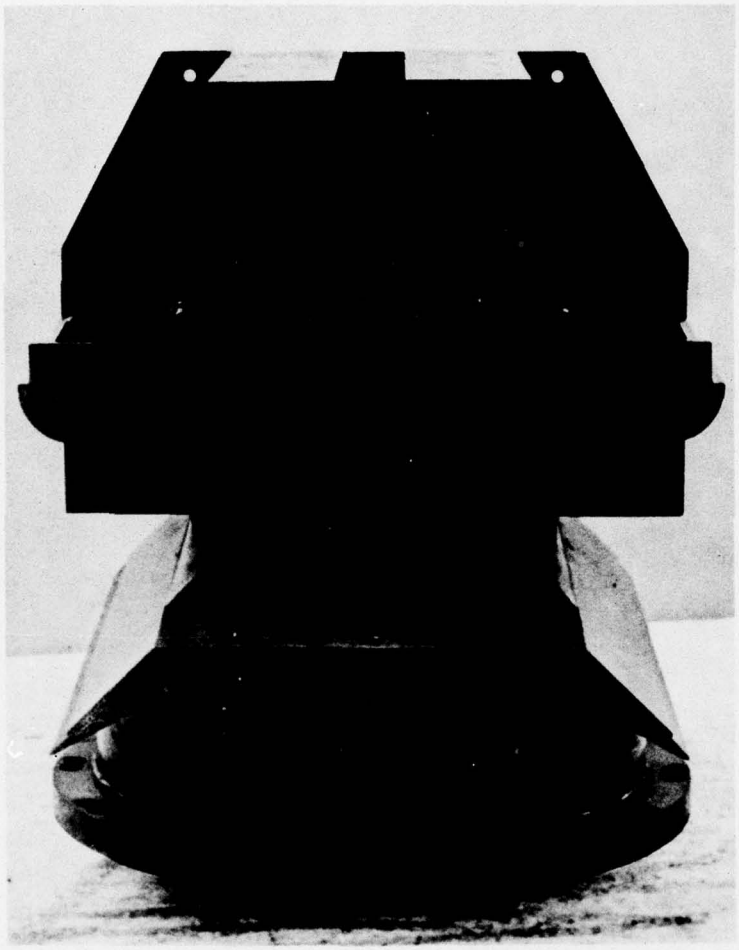

Figure 2.1b. Augmentor Wing Model.

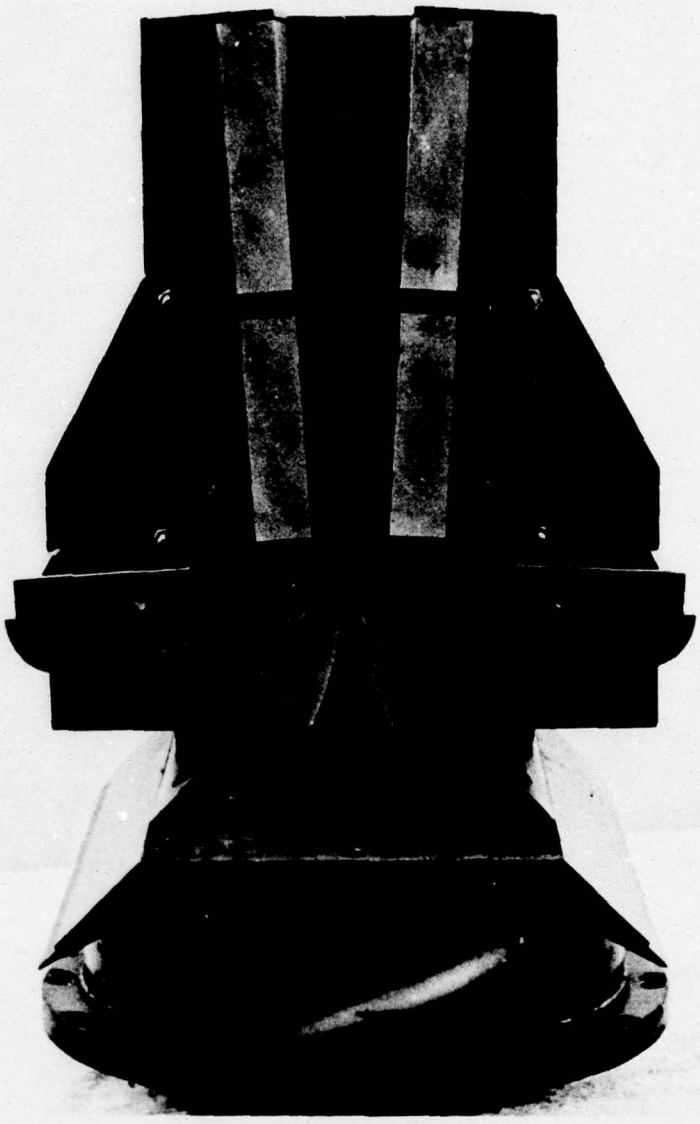

Figure 2.1c. Augmentor Wing Model.

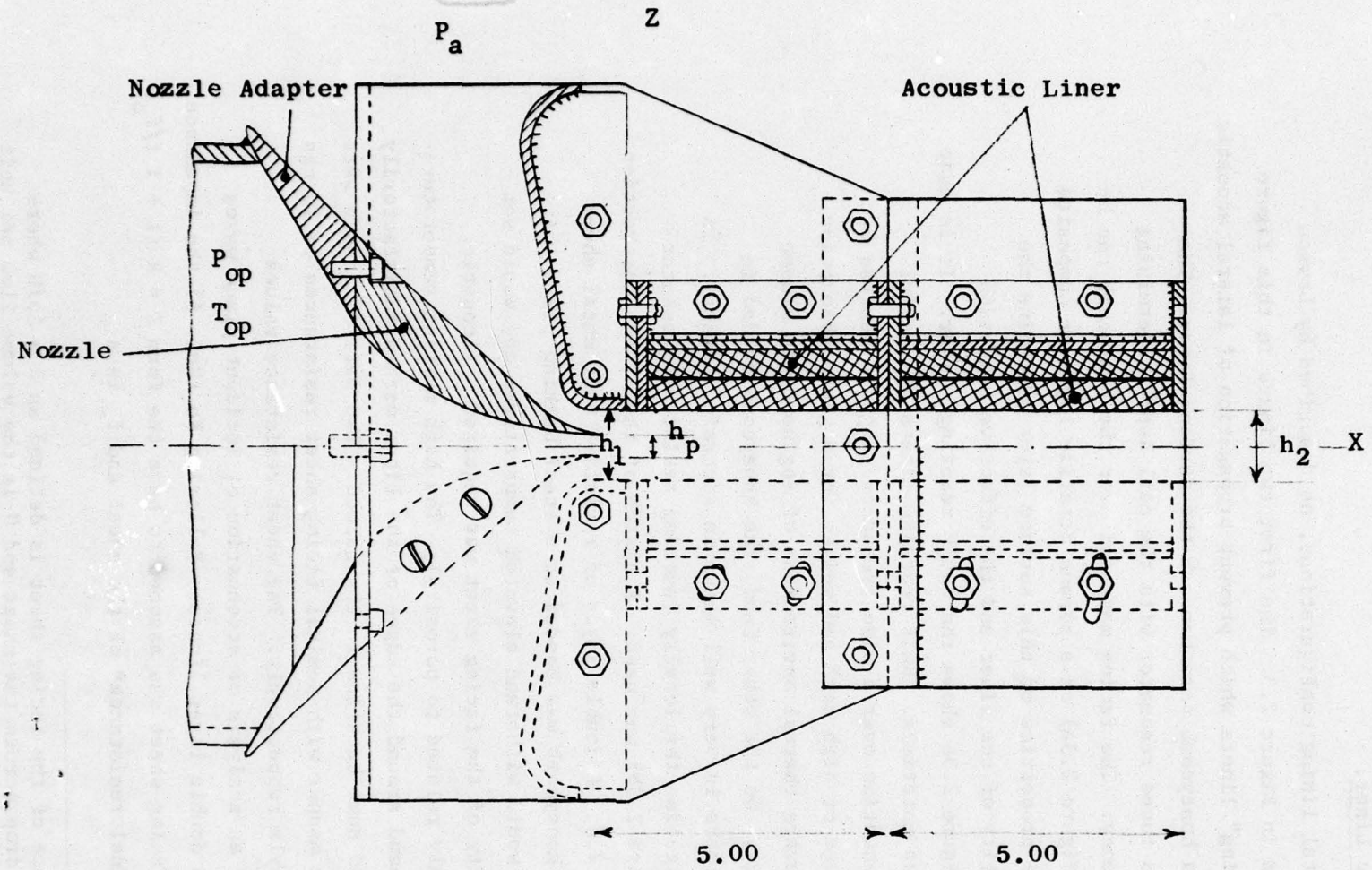

h_1 = 1.20in. h_2 = variable h_p = 0.30 in.

w = channel width= 8 in., $M_p' = f\left(\frac{P_{op}}{P_a}\right)$

Figure 2.2. Sketch of Ejector-Shroud Model.

2.2 Acoustic Liner.

The fundamental lining configurations, as described by Lowson (Ref. 16) are shown in Figure 2.3. The first two liners in this figure are "locally reacting" liners which prevent propagation of lateral acoustic waves by means of a honeycomb core beneath the surface layer. The honeycomb acts as a tuned resonator with the cell depth determining the resonant frequency. The facing material over the honeycomb can be perforated sheet (Figure 2.3a) or a porous metallic layer or composite (Figure 2.3b). The properties of this surface layer determine the attenuation capability of the liner and the effective bandwidth of attenuation. Figure 2.3c shows the "bulk reacting" liner. It is made entirely from porous materials. Bulk reacting liners are useful in cases where attenuation over a wide frequency range is desired but have the disadvantage of high cost and weight for a given absorption. Furthermore, the severe thermal environment of engine ducts almost prohibit their usage. On the other hand, the honeycomb needed in locally reacting liners is very well known in aircraft industry. In the present investigation the locally reacting resistive-resonator type of liner (Figure 2.3b) was used. A sketch of the liner construction is given in Figure 2.4. A double layer of resistive felt metal sheet on stainless steel honeycomb was bonded to a steel backing plate. A bonding agent that would withstand elevated temperatures and would not decrease the porosity of the facing sheet was required. (Acoustic resistance is closely related to porosity). The high melting temperature solder applied by hand around the edges of the liner worked satisfactorily but may have allowed some backflow in the shroud. Two sets of liners were constructed in this manner with nominal facing sheet resistances of 10 cgs Rayls and 30 cgs Rayls respectively. The sheet resistance values were selected after an analysis of attenuation of incident plane waves by single layer and double layer liners. Following Ko (Ref. 6) the impedance of the felt metal facing sheet was assumed to have the form $Z = R\,(1 + i\,f/f_o)$ where R is the nominal resistance* of the sheet and f_o is a

*The resistance of the facing sheet is defined as $R = \Delta p/U$ where Δp is the pressure drop across the sheet and U is the volume flow per unit area.

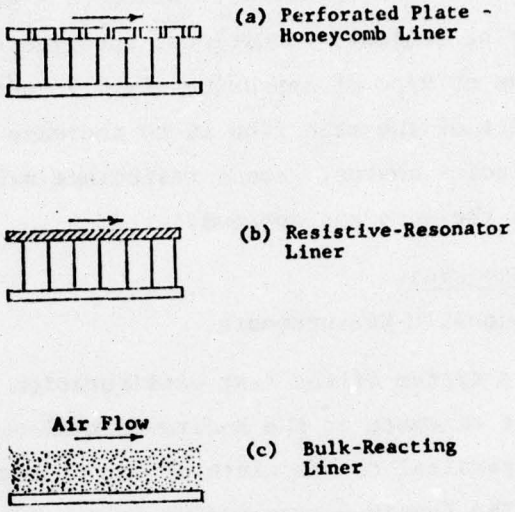

Figure 2.3. Typical Liner Configurations (From Reference 16).

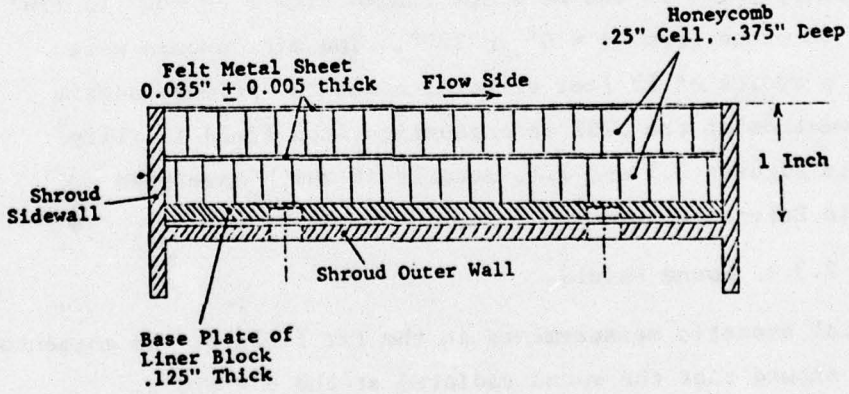

Figure 2.4. Sketch Showing Shroud Wall Lining.

characteristic frequency. Figure 2.5 shows the results of the calculation for a double layer liner for three values of dimensionless resistance $R/\rho c$ and for f_o = 15,000 Hz. Since ρc = 41.6 in Rayls (cgs units) for air at standard conditions, the liners selected correspond to values of $R/\rho c$ of approximately 0.25 and 0.75. It is known that one effect of the mean flow is to increase the effective resistance of the facing sheets. Hence resistance values were selected somewhat lower than the apparent optimum.

2.3 Test Procedures.

2.3.1 Acoustic Measurements.

The coordinate system of the test configuration is shown in Figure 2.6. The jet exhausts in the X-direction along the axis $\theta = 0°$. The Y-direction is parallel to the width of the slot nozzle along the axis $\phi = 0°$. The Z-axis corresponding to $\theta = 90°$, $\phi = 90°$ lies parallel to the height of the nozzle.

The acoustic data taken during these tests consisted of overall sound pressure level directivity plots in the XZ and YZ planes and the frequency spectra at selected points in these planes as shown in Figure 2.6. These selected points included values of $\theta = \pm 30°$, $\pm 60°$ and $+90°$ and values of $\phi = 0°$, $+25°$, $+45°$, $+65°$ and $+90°$. The directivity plots in the XZ plane ranged from $\theta = -60°$ to $+90°$ and in the YZ plane from $\phi = 0°$ to $180°$. The microphones were located at a radius of 13 feet centered about the primary nozzle exit. Schematics of the UTSI aeroacoustics free field facility are shown in Figures 2.7 and 2.8, details of which have been described in Reference 1.

2.3.2 Sound Shield.

Initial acoustic measurements in the far field of the augmentor wing model showed that the sound radiated at the $\theta = +90°$, $\phi = +90°$ position (See Figure 2.6) contained noise which was radiated from the ejector inlet. Since it was the purpose of this study to investigate the noise reduction potential of the ejector geometry

BEST AVAILABLE COPY

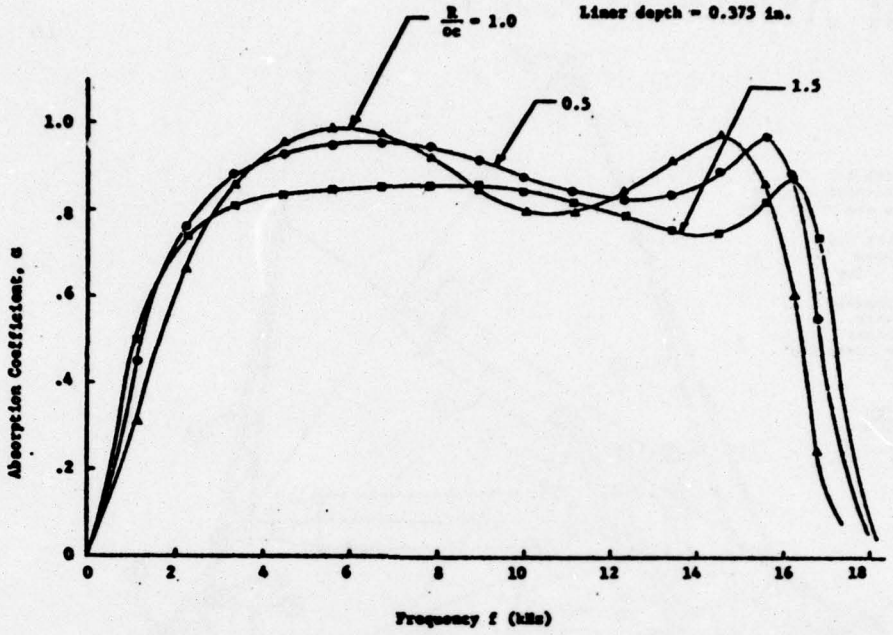

Figure 2.5. Calculated Absorbtion Coefficient for a Double Layer Liner Assuming Normally Incident Plane Waves, (following Reference 6).

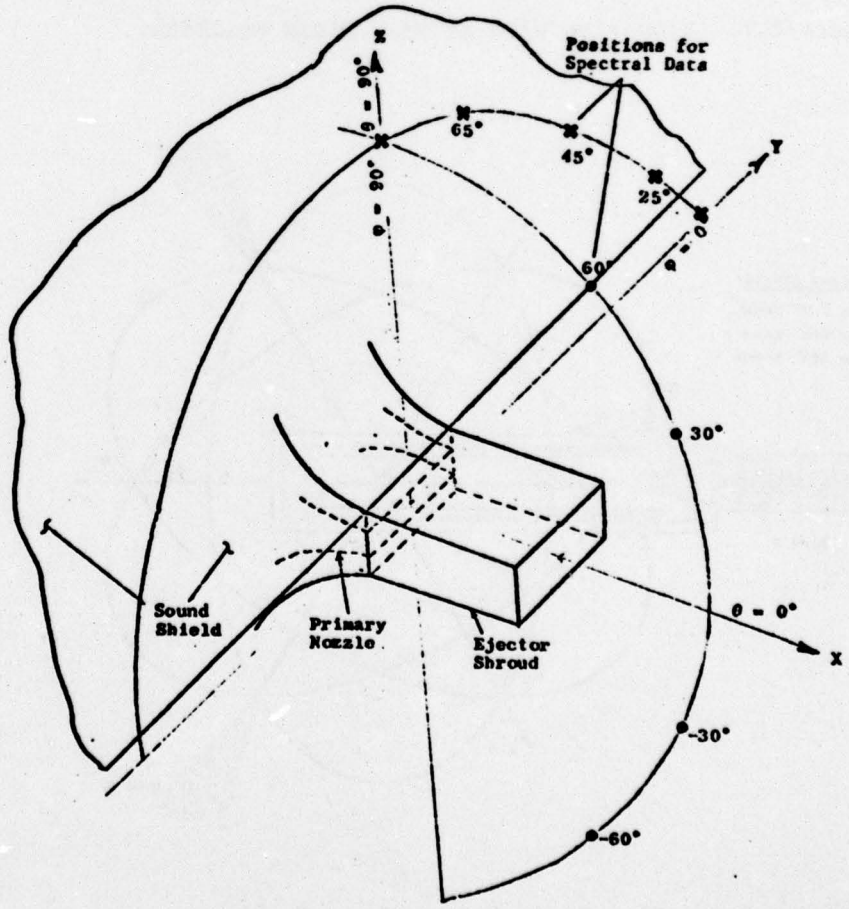

Figure 2.6. Coordinate System for the Augmentor Wing Indicating Planes and Positions in the Planes for Acoustic Measurement.

BEST AVAILABLE COPY

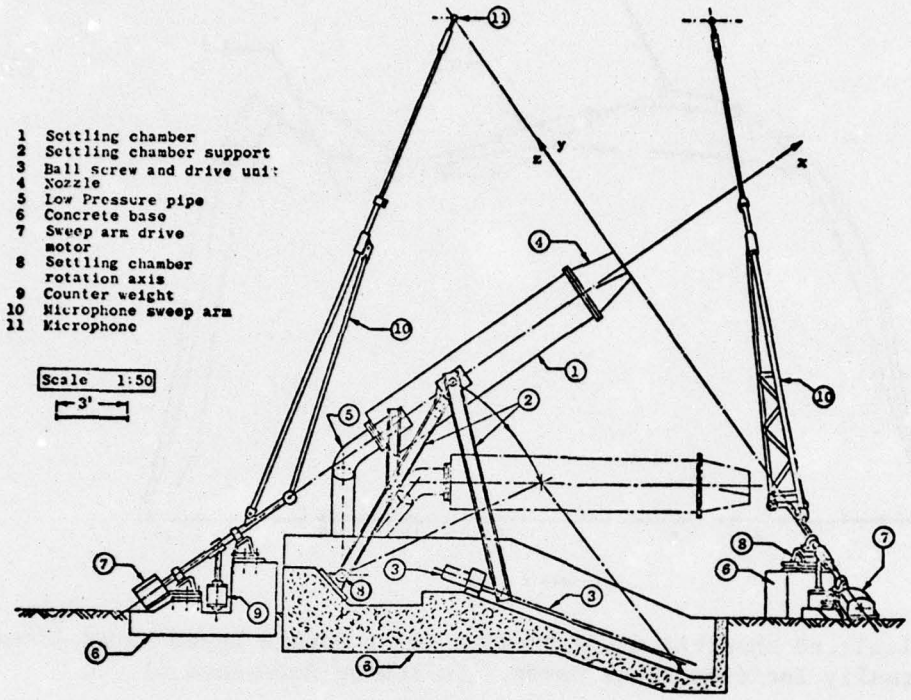

Figure 2.7. Elevation View of Free Field Facility.

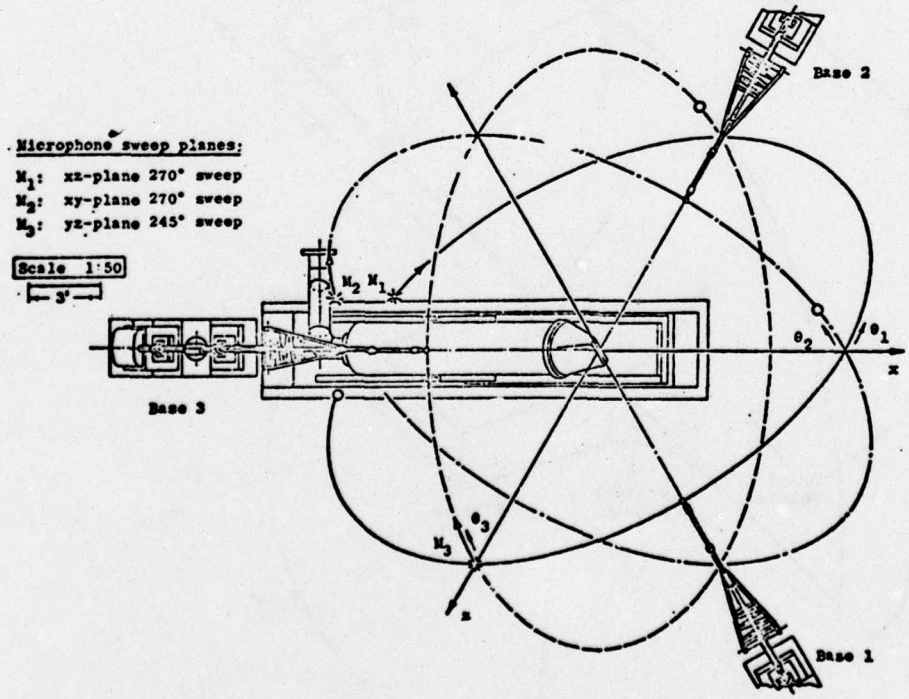

Figure 2.8. Plan View of Free Field Facility.

exclusive of any sound radiated from the inlet a sound shield was mounted as shown in Figure 2.6. The shield was made of 8 ft x 4 ft x 1/2 in. thick plywood with 4 inch thick foam glued on both sides. The shield was mounted on the model so as to make an angle of $\theta \approx +120°$ to the jet axis. This set-up blocked the inlet noise but did not affect the sound radiating from the ejector exhaust to the $\theta = +90°$ position. Comparative data showing the effect of the sound shield are given in Figures 2.9. Ejector inlet noise was also observed by Middleton (Ref. 2) in his experiments on axisymmetric ejectors. It was effectively suppressed by means of an intake box made of plywood and poly-urethane foam.

2.4 Instrumentation.

In order to gain a better understanding of the noise generating mechanisms of jets the fluid flow parameters must be measured. Consequently the UTSI aeroacoustic instrumentation is comprised of a fluid flow measuring system as well as a sound measuring system. These systems are used to obtain and record data from three different test chambers at UTSI. In this investigation, the free field test stand was used to obtain all pertinent data.

2.4.1 Flow Measuring System.

Using one-dimensional, isentropic flow relations the bulk flow conditions at the nozzle exit can be obtained from measurements of the atmospheric barometric pressure and from measurements of the stilling chamber pressure and temperature. For a given model configuration the fluid dynamic quantities (shown in Figure 2.2) that could be directly varied in the tests include the stilling chamber total pressure (P_{op}) and stilling chamber total temperature (T_{op}). As shown in Figure 2.10, the control valve (point 3) and the heater (point 10) are used to control P_{op} and T_{op} in the stilling chamber. During the tests the Mach number M_p' based on the stilling chamber total pressure (P_{op}) and exit pressure equal to the atmospheric pressure (P_a) was varied from 0.5 to 0.9. To determine experimentally the primary mass flow ($\dot{m}_p$) a venturi meter was installed in the main flow line (point 6 of Figure 2.10. The total pressure (P_{ov}) upstream of

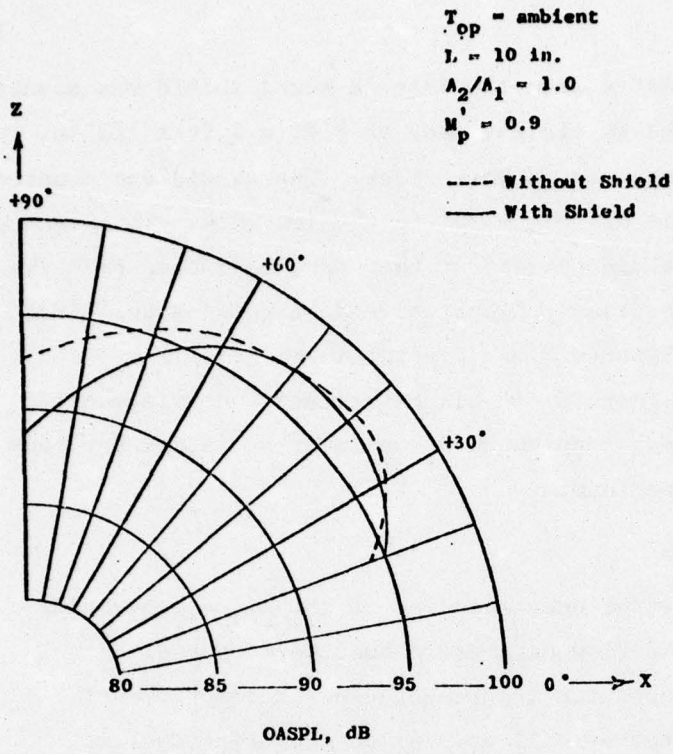

Figure 2.9a. Effect of Shield on OASPL Directivity in XZ Plane for 10 Inch Augmentor Wing Model.

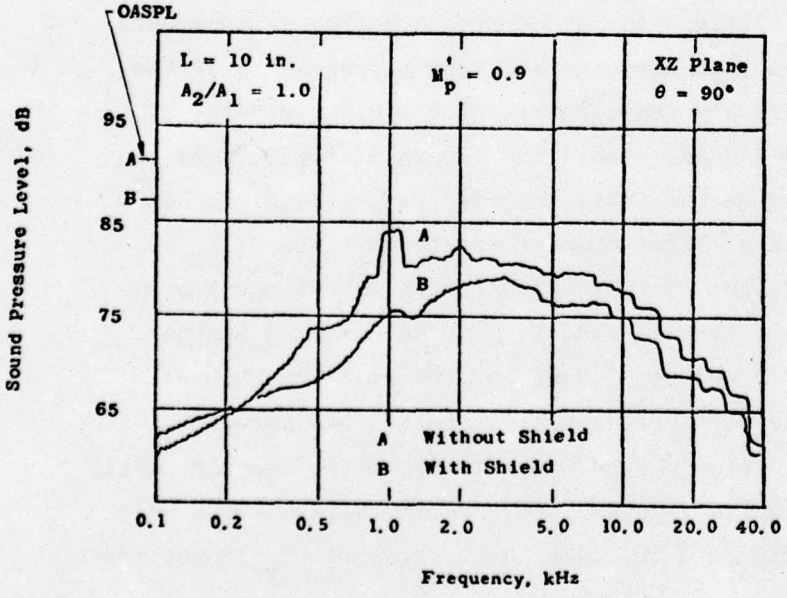

Figure 2.9b. Effect of Shield on Sound Pressure Spectrum at 90° for 10 Inch Augmentor Wing Model.

1. Air Storage Tank
2. High Pressure Pipe - 3"
3. Control Valve
4. Rupture Diaphram
5. Low Pressure Pipe - 8"
6. Mass Flow Meter
7. Reverberation Room
8. Fluid Dynamics Test Chamber
9. Control Panel
10. Heater
11. Stilling Chamber
12. Microphone Sweep Arm Pads

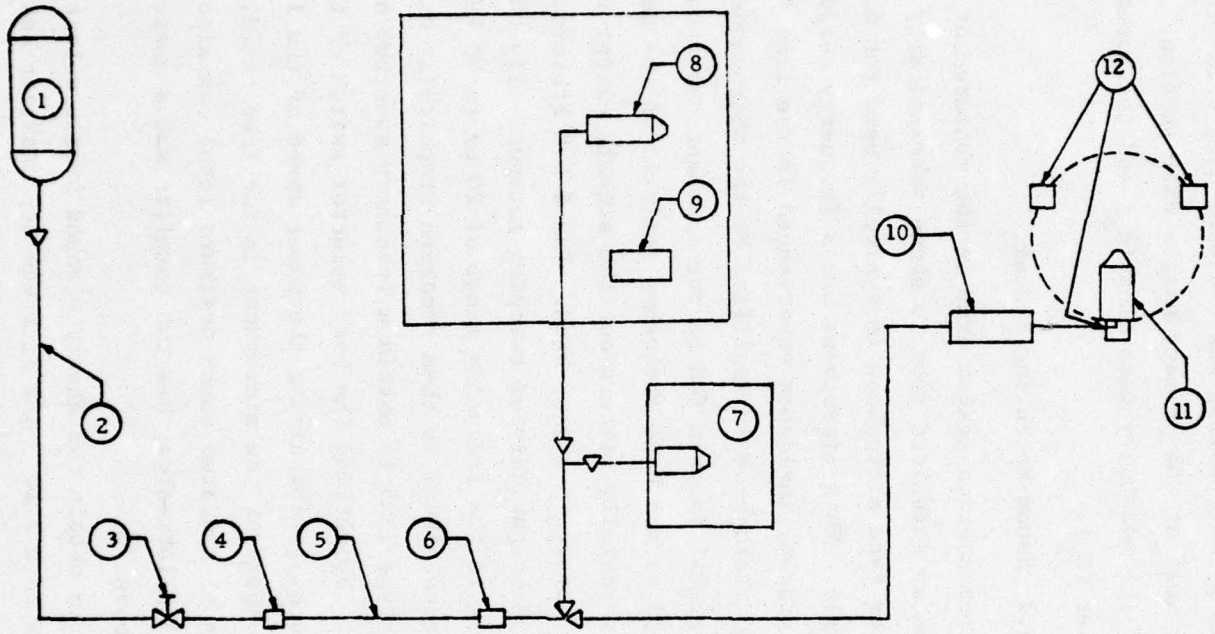

Figure 2.10. Aeroacoustics Laboratory's Air Supply System.

the venturi throat and the pressure drop (ΔP_v) between the upstream and throat of the venturi were measured. The static pressure (P_e) at the exit of the primary nozzle was measured by a pressure tap provided in the ejector wall at the primary nozzle exit section. This enabled calculation of the secondary mass flow ($\dot{m}_s$) and the actual primary flow Mach number (M_p).

2.4.2 Sound Measuring System.

The instrumentation system used in the measurement of the sound generated by turbulent jets is shown schematically in Figure 2.11. A 1/4" condenser type microphone is typically used for measurements in the free field. This microphone has a frequency response of 30 Hz to 40 kHz for grazing incidence experienced in the free field. The signal from the microphone is amplified by the microphone pre-amplifier. The amplified signal is then fed to the constant percentage bandwidth analyzer for 1/3 octave band frequency analysis of the measured noise. The analyzer essentially filters out the signals except those in the particular 1/3 octave frequency band. The B & K Frequency Analyzer Type 2112 has the capability of sweeping automatically through the 1/3 octave bands in the frequency range of 20 Hz to 40 kHz.

The filtered signal is then recorded graphically on the B & K Level Recorder Type 2305 to obtain a frequency spectrum of the radiated sound. By setting the band selector switch of the analyzer to "Linear" and by synchronizing the paper speed of the level recorder with the sweep speed of the microphone in the free field, the directional characteristics of radiated sound pressure level can also be recorded. The aeroacoustics labroatory has two complete sound measuring systems as described above.

In order to obtain the absolute sound pressure level values (with reference to 2×10^{-5} N/m^2), frequency analyzer and the level recorder are calibrated before each test by means of a General Radio Sound Level Calibrator Type 1562-A which produces a sound pressure level at 114 dB at any of the following frequencies: 125, 250, 500, 1000, 2000 Hz. It can also be seen in Figure 2.11 that the measured data (signal from the microphone) can be stored on

magnetic tape, using the tape for later analysis. The frequency limit of the tape recorder is 20 kHz; consequently the tape system is used only when the frequencies of interest are under 20 kHz.

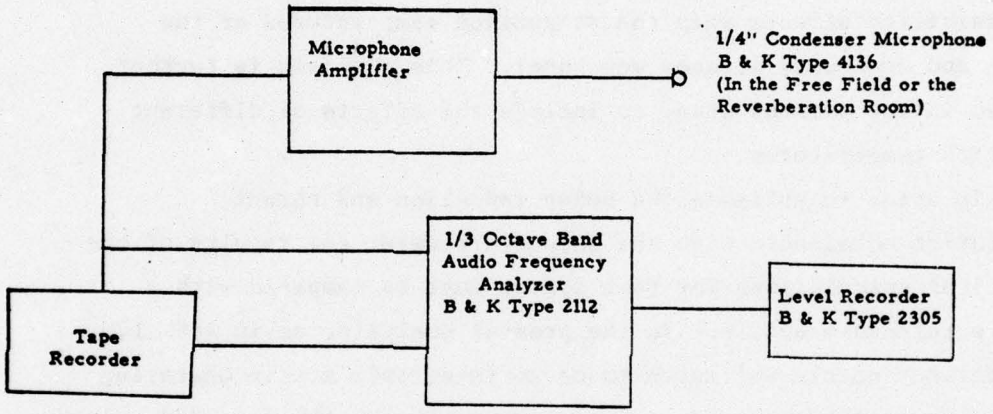

Figure 2.11. Instrumentation for Acoustic Measurements in the Free Field and the Reverberation Room.

3.0 THEORETICAL ANALYSIS.

3.1 Basic Equations and Approach.

Fluid dynamically the augmentor wing can be modelled satisfactorily by a simple ejector as shown in Figure 3.1. The ejector consists of a primary nozzle exhausting into a constant or variable area shroud. It is possible to apply the equations of one-dimensional fluid mechanics to the ejector to calculate the rate of air entrainment and the thrust augmentation. One of the first analyses of this type was performed by von Karman (Ref. 7) for incompressible flow. This work has been extended by Goethert and Borchers (Ref. 1) to take into account compressibility effects when the stagnation temperatures of the primary and secondary streams are equal. This analysis is further extended in the present study to include the effects of different stagnation temperatures.

In order to estimate the noise reduction and thrust augmentation obtainable with the shrouded nozzle, the results of the theoretical calculations for that system must be compared with a suitable reference nozzle. In the present analysis, as in Ref. 1, the reference nozzle was taken to be an isentropic nozzle operating at the same stagnation pressure and temperature as the shrouded primary nozzle and passing the same mass flow. The physical variables for the reference nozzle are typically indicated by a prime and thus the above conditions may be expressed by

$$P_{op} = P'_{op}$$
$$T_{op} = T'_{op}$$
$$\dot{m}_p = \dot{m}'_p$$

To satisfy these conditions the area of the reference nozzle generally must be slightly different from the area of the primary nozzle. This is illustrated in Figure 3.2. The equality of the stagnation pressures, assuming that both systems exhaust into the same atmosphere can be expressed in terms of a reference Mach number, M'_p, such that

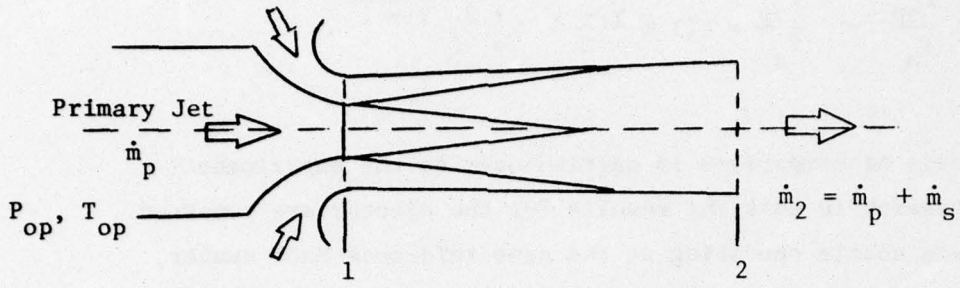

A_p = Primary Nozzle Area

A_s = Secondary Flow Area at Station 1

$P_{op} = P'_{op}$

$T_{op} = T'_{op}$

$\dot{m}_p = \dot{m}'_p$

$T_{os} = T_2 = T_a$

Figure 3.1. Shrouded Nozzle

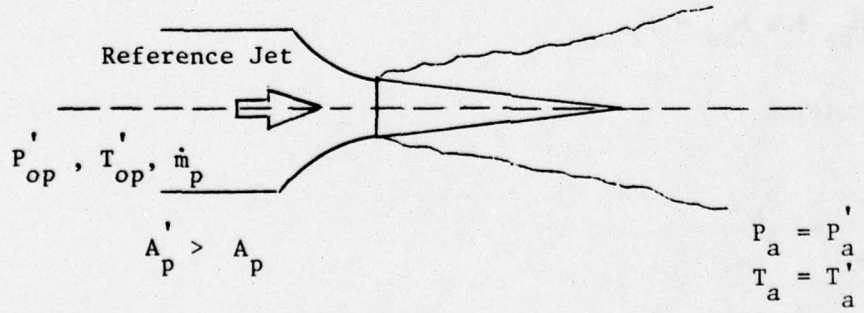

Figure 3.2. Reference Nozzle.

$$\frac{P_{op}}{P_a} = \frac{P'_{op}}{P_a} = \left(1 + \frac{\gamma - 1}{2} M_p'^2\right)^{\frac{\gamma}{\gamma - 1}}$$

This basis of comparison is carried over to the experimental part of the research in that the results for the ejector are compared with a reference nozzle operating at the same reference Mach number, M_p'.

In order to calculate the noise reduction and thrust augmentation for the shrouded nozzle, flow variables must be determined to satisfy the following equations (see Figure 3.1):

a) Continuity Equation

$$\rho_p A_p V_p + \rho_s A_s V_s = \rho_2 A_2 V_2$$

b) Momentum Equation (parallel shroud walls)

$$\rho_p A_p V_p^2 + \rho_s A_s V_s^2 + P_1 A_1 = \rho_2 A_2 V_2^2 + P_2 A_2$$

For non-parallel walls an additional term $\int_1^2 PdA$ must be added to the left hand side of the equation.

c) Energy Equation

$$\dot{m}_p h_{op} + \dot{m}_s h_{os} = \dot{m}_2 h_{o2}$$

d) Pressure Condition

$$\frac{P_2}{P_{os}} = \frac{P_a}{P_{os}} = 1$$

In addition, isentropic flow is assumed to prevail between the stagnation chambers and the nozzle exit at station 1.

The geometry of the shrouded nozzle system is specified by the ratio of the secondary to primary flow areas, $AR = A_s/A_p$, and by the shroud contraction ratio, $CR = A_2/A_1$. It is assumed that the primary nozzle lip has no area so that

$$A_1 = A_s + A_p$$

This is correct for the station immediately downstream of the nozzle lip.

The algebraic manipulations used to prepare the system of equations for an iterative solution are similar to those carried out in Reference 1 and will not be presented. The results of the theoretical calculations are expressed in terms of three parameters:

the mass flow ratio

$$K_m = \frac{\dot{m}_s}{\dot{m}_p}$$

the sound power reduction based on Lighthill's V^8-Law

$$\Delta PWL = 10 \log_{10} \frac{A'_p}{A_2} \left[\frac{V'_p}{V_2}\right]^8$$

and the static thrust ratio of the ejector system to the reference nozzle

$$TR = (1 + K_m) \frac{V_2}{V'_p}$$

It should be noted that the theoretical expression for the sound power reduction assumes that all of the noise generated by the turbulent mixing of the primary and secondary flow streams is absorbed beneath the shroud. Thus the ΔPWL values obtained from the analysis represent maximum values that would only be obtained for a perfectly absorbing shroud. Similarly, the thrust calculation assumes that the shroud

is sufficiently long so that complete mixing occurs and does not take into account losses due to viscosity or flow separation. Thus, the calculations are for an ideal ejector and provide optimal values against which experimental results can be compared.

3.2 Results of Calculations.

Some results of the one dimensional analysis for a constant area shroud ($A_2/A_1 = 1$) are given in Figures 3.3 to 3.7. The first three figures (3.3 to 3.5) represent the variation with reference Mach number of the mass flow ratio (K_m), the thrust augmentation ratio (TR) and the noise reduction (ΔPWL) for two temperature ratios (τ) and several secondary to primary area ratios (AR). The mass flow ratio is seen to be a very weak function of the reference Mach number - it decreases slightly at high Mach numbers. It is, however, strongly dependent on the area ratio AR. By increasing the secondary flow area, A_s (i.e., using a larger shroud) the induced flow can be considerably increased. Figure 3.3 shows that the secondary flow rate ($\dot{m}_s$) is 3 to 4 times as much as the primary mass flow ($\dot{m}_p$) for an ejector system with AR = 12. The mass flow ratio is further increased by increasing the temperature ratio (τ). The higher value is mainly due to decrease in $\dot{m}_p$ at same M_p' (a consequence of high jet temperature - or low density) at about the same $\dot{m}_s$.

The thrust ratio, like the mass flow ratio, is weakly dependent on the operating pressure ratio of the nozzle (or the reference Mach number). It again increases with increasing area ratio, AR (see Figure 3.4). Since the shroud exit velocity V_2 decreases with increasing shroud area, and since the thrust ratio depends on V_2, the augmentation in thrust due to increasing AR is not as great as the augmentation in the mass flow induction. Still with a simple ejector system of AR = 3.0 and τ = 2.0, thrust augmentation of the order of 30% can be ideally achieved. The decrease in thrust ratio with increasing temperature ratio is due to the increase in the reference jet velocity (and a consequent increase in the reference jet thrust).

The ideal noise reduction potential of the ejector system is depicted in Figure 3.5. The sound power reduction is, again, only weakly

BEST AVAILABLE COPY

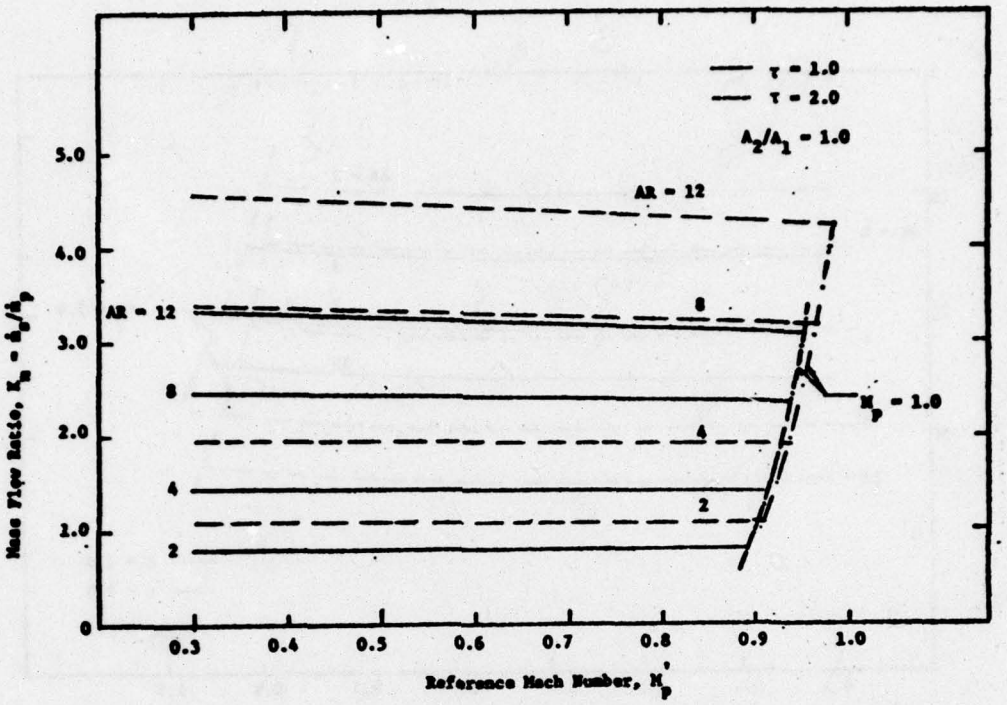

Figure 3.3. Variation of Mass Flow Ratio, K_m with the Reference Mach Number M_p' for Constant Area Shrouded Nozzle.

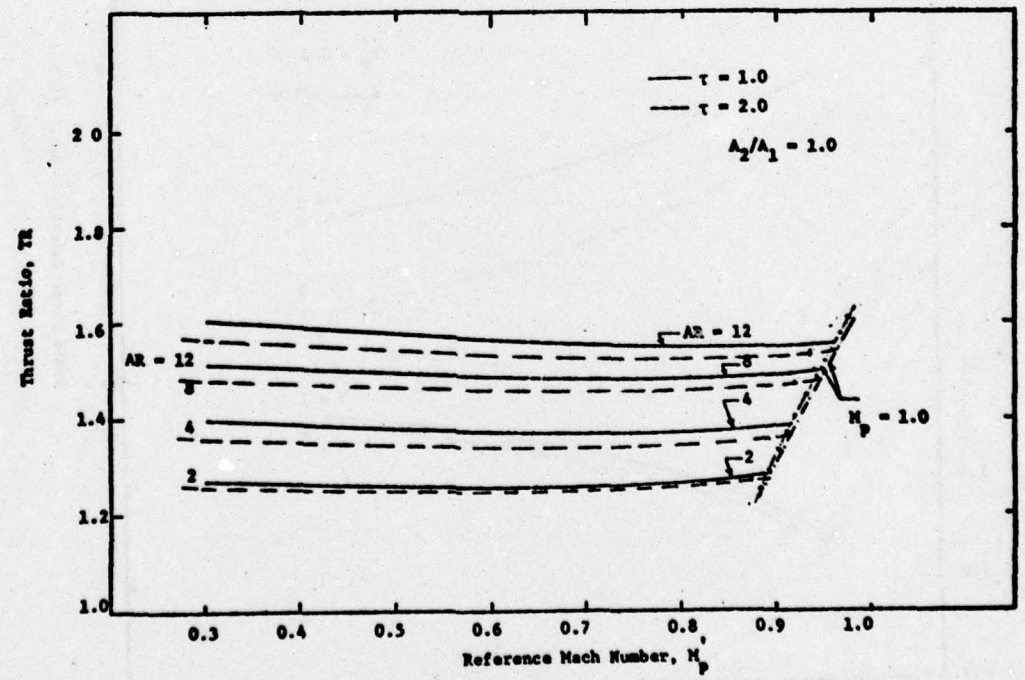

Figure 3.4. Variation of Thrust Ratio, TR with Reference Mach Number M_p' for Constant Area Shrouded Nozzle.

BEST AVAILABLE COPY

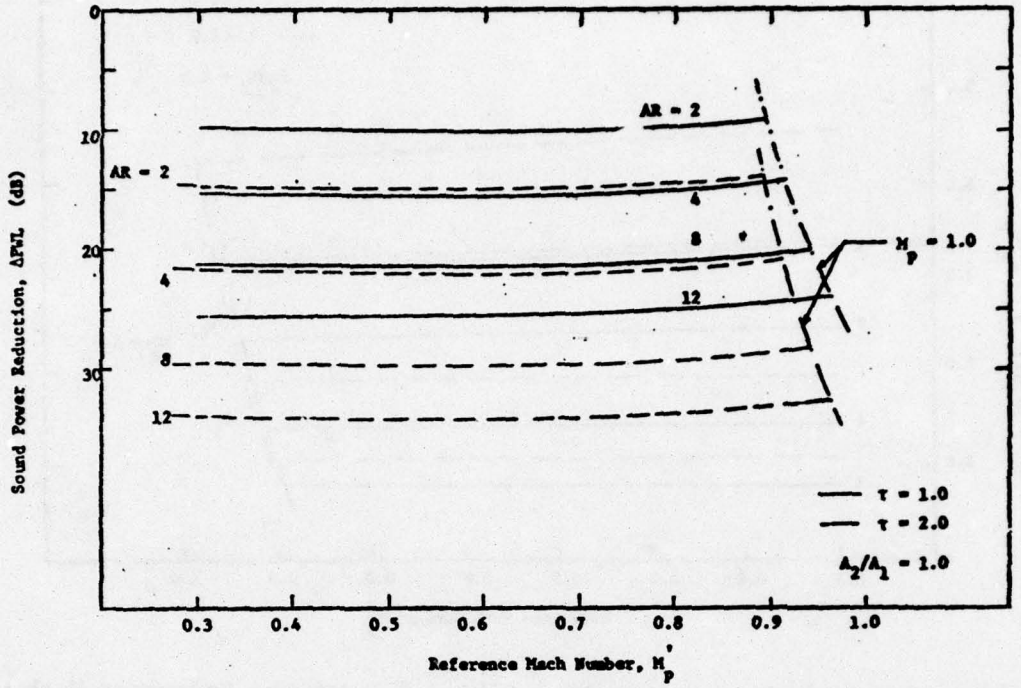

Figure 3.5. Sound Power Reduction, ΔPWL as a Function of Reference Mach Number M_p' for Constant Area Shrouded Nozzle.

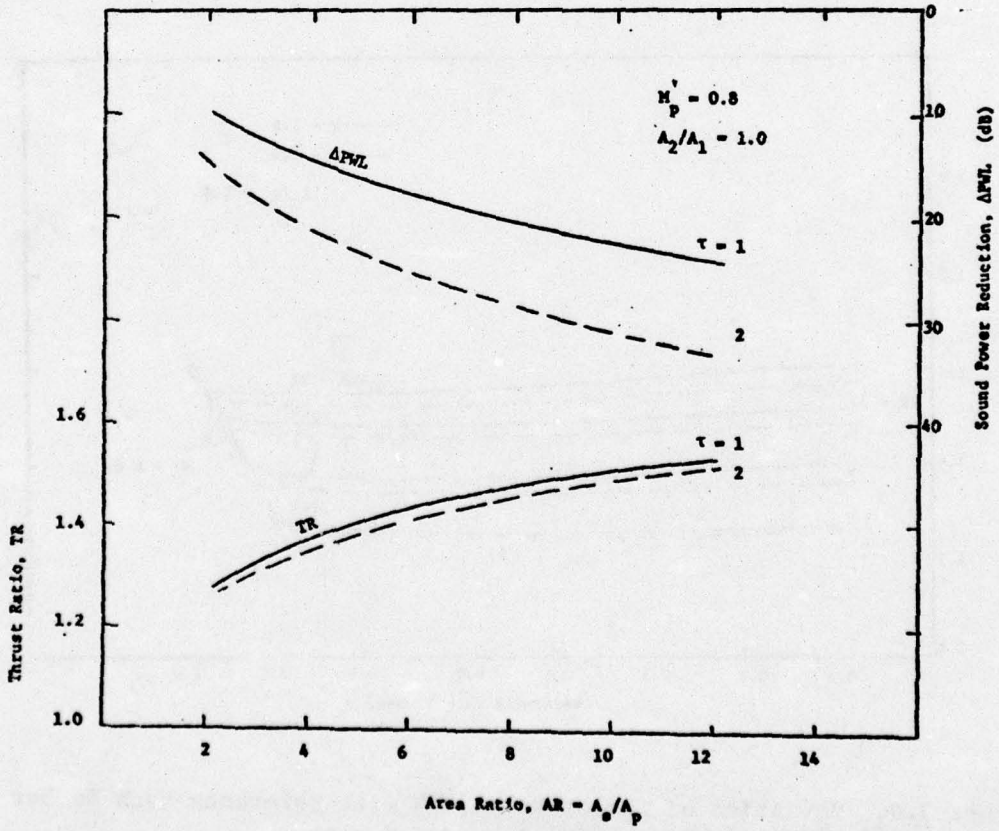

Figure 3.6. Effect of Area Ratio on Thrust Ratio and Sound Power Reduction for Constant Area Shrouded Nozzle.

dependent on the Mach number but strongly determined by the area ratio (AR). The increased noise attenuation due to increase in AR is a consequence of reduced shroud exit velocity (V_2). Noise generated by high temperature jets should ideally be better attenuated by the ejector system (as shown in Figure 3.5). The figure shows a possible noise reduction of 19 dB for an area ratio of 3.0 and hot flow. Recall, however, that these noise attenuation figures are based on the assumption of total absorption of internal noise which cannot in practice be achieved.

Figures 3.4 and 3.5 show that higher thrust augmentation and noise attenuation can be achieved by increasing the secondary to primary area ratio (AR) of the ejector system and this is explicitly displayed in Figure 3.6. Larger shrouds (i.e., higher AR) bring with them additional external drag, and installation problems. For practical applications therefore the smallest ejector system capable of attaining the desired performance must be chosen.

The effect of stagnation temperature ratio (τ) on the thrust augmentation and noise reduction capability of the ejector system is shown in Figure 3.7. Interestingly the thrust augmentation (though not strongly dependent on τ) is maximum when the primary and secondary streams have identical stagnation temperature (i.e., at $\tau = 1$). At lower values of τ, that is $\tau < 1.01$, the reduced thrust augmentation is mainly due to the reduction in the mass flow ratio (K_m) while at higher values of τ, $\tau > 1.0$, as noted in Figure 3.4, it is a consequence of increased velocity of the reference nozzle. The noise reduction, on the other hand, increases continuously with increasing temperature ratio chiefly due to the increased noise level of the reference jet at higher temperatures and the assumption of total absorption of internal noise.

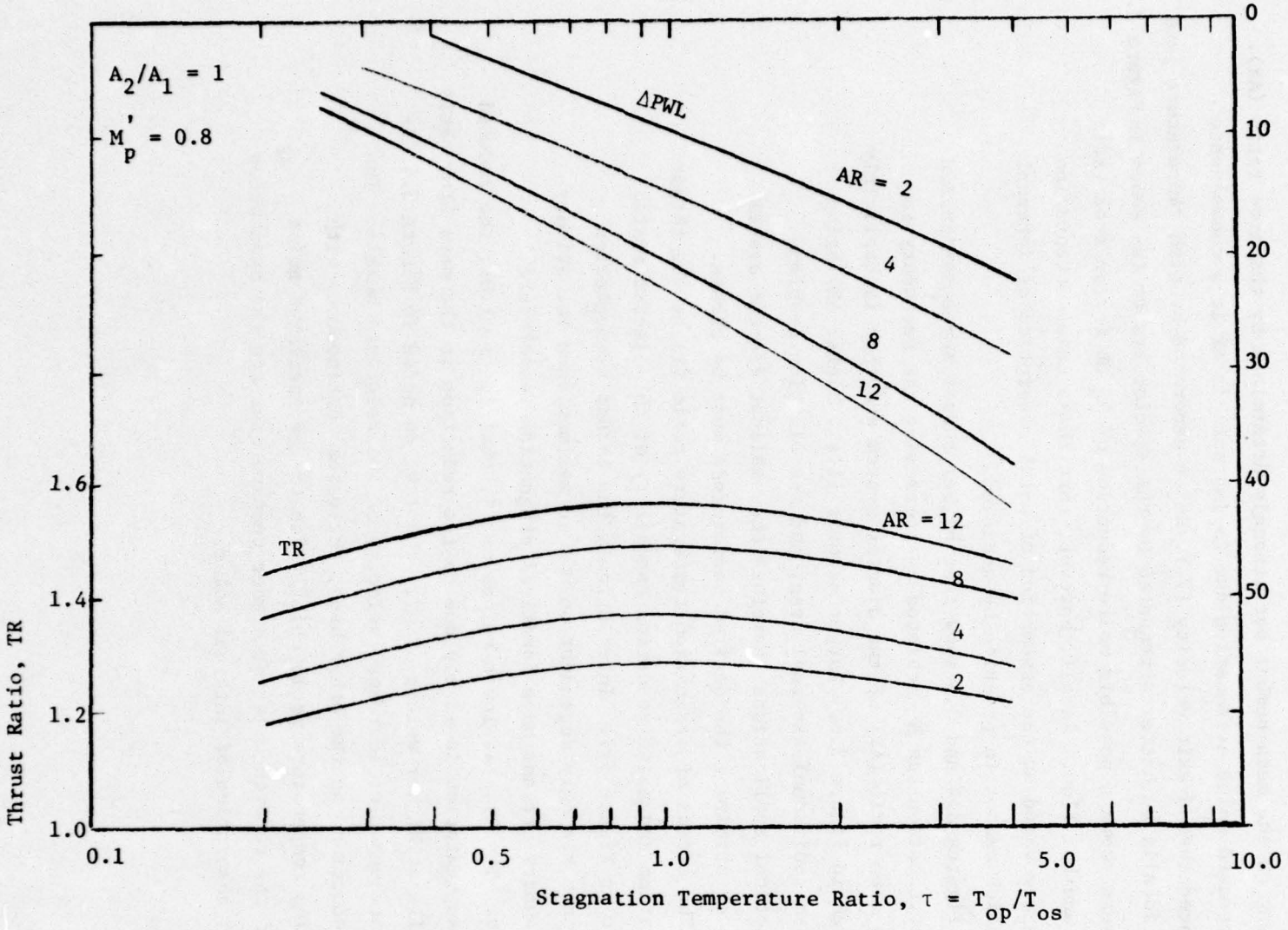

Figure 3.7 Effect of Temperature Ratio on Thrust Ratio and Sound Power Reduction, ΔPWL for Constant Area Shrouded Nozzle.

4.0 DISCUSSION OF EXPERIMENTAL RESULTS.

It is the purpose of this section to record observations from the measurements made according to the procedure outlined in Section 2.0. Data are presented under two major subsections: i) cold primary jet and ii) hot primary jet. The noise reduction and thrust augmentation potential of the ejector system and their dependence on the ejector shroud length, divergence, wall resistance and operating conditions are evaluated for each case. The performance characteristics of the nozzle without the shroud must obviously be known in order to assess the benefits of the ejector. The basic nozzle data will therefore be presented at the beginning of each of the above mentioned subsections.

4.1 Cold Jets.

4.1.1 Unshrouded Jets.

The noise directivity patterns of the basic nozzle in the XZ plane shown in Figure 4.1 support the well established concepts of jet noise (Ref. 8). There is clear evidence of the convective amplification and refraction of noise causing a peak level in the plane around $\theta = 30°$ from the flow axis. The increase in the difference between the peak noise level and the noise level at $\theta = 90°$ with increasing jet exit velocity indicate increased convective effects with jet velocity. (The difference increases from about 5 dB at $M_p = 0.5$ to about 10 dB at $M_p = 0.9$). Another characteristic of jet noise indicated by the present data concerns the frequency content of the radiated noise. Figure 4.2 indicates that while the low pitch noise dominates at smaller angles to the flow axis, the high frequency components have a fairly uniform contribution throughout the plane. This is in agreement with Ribner's theory of jet noise (Ref. 9).

Based on dimensional reasoning, Lighthill (Ref. 10) estimated the total acoustic power output of a jet to vary as the eighth power of the jet velocity. Sound power level measurements (in a reverberation room) were not made during this investigation and hence a direct correlation with jet velocity is not possible. However as shown in Figure 4.3 the OASPL at $\theta = 90°$ and the maximum OASPL in the XZ plane

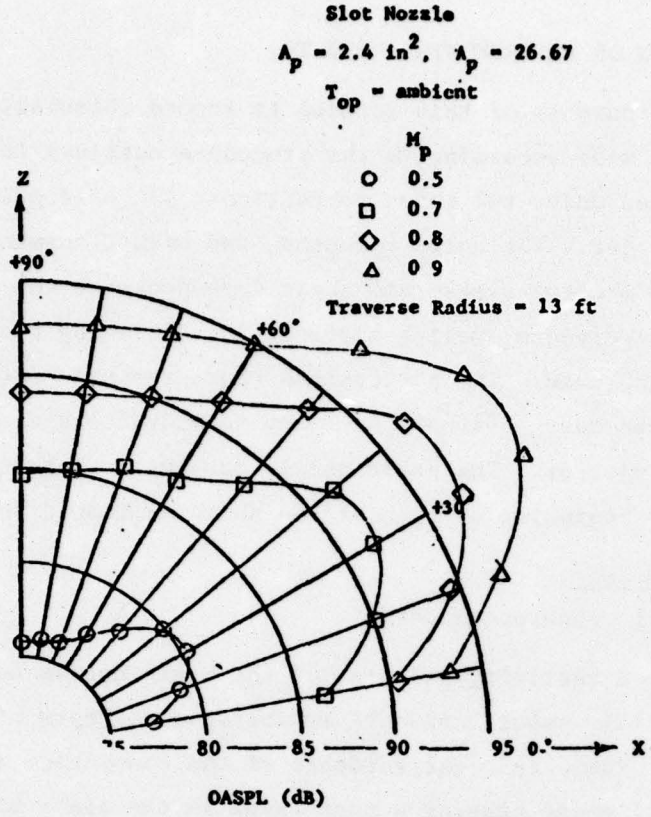

Figure 4.1. OASPL Directivities in the Flyover Plane of the Primary Slot Nozzle.

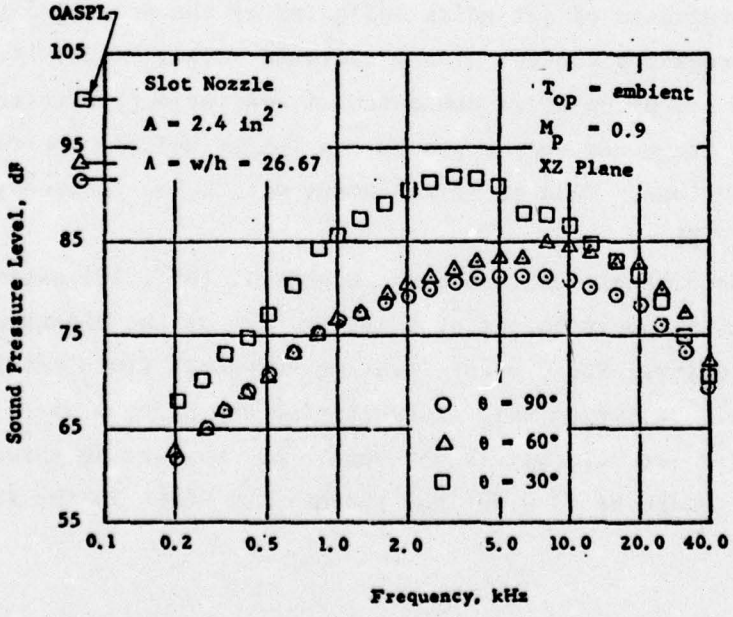

Figure 4.2. Sound Pressure Spectra of the Primary Slot Nozzle at Three Positions in the XZ Plane.

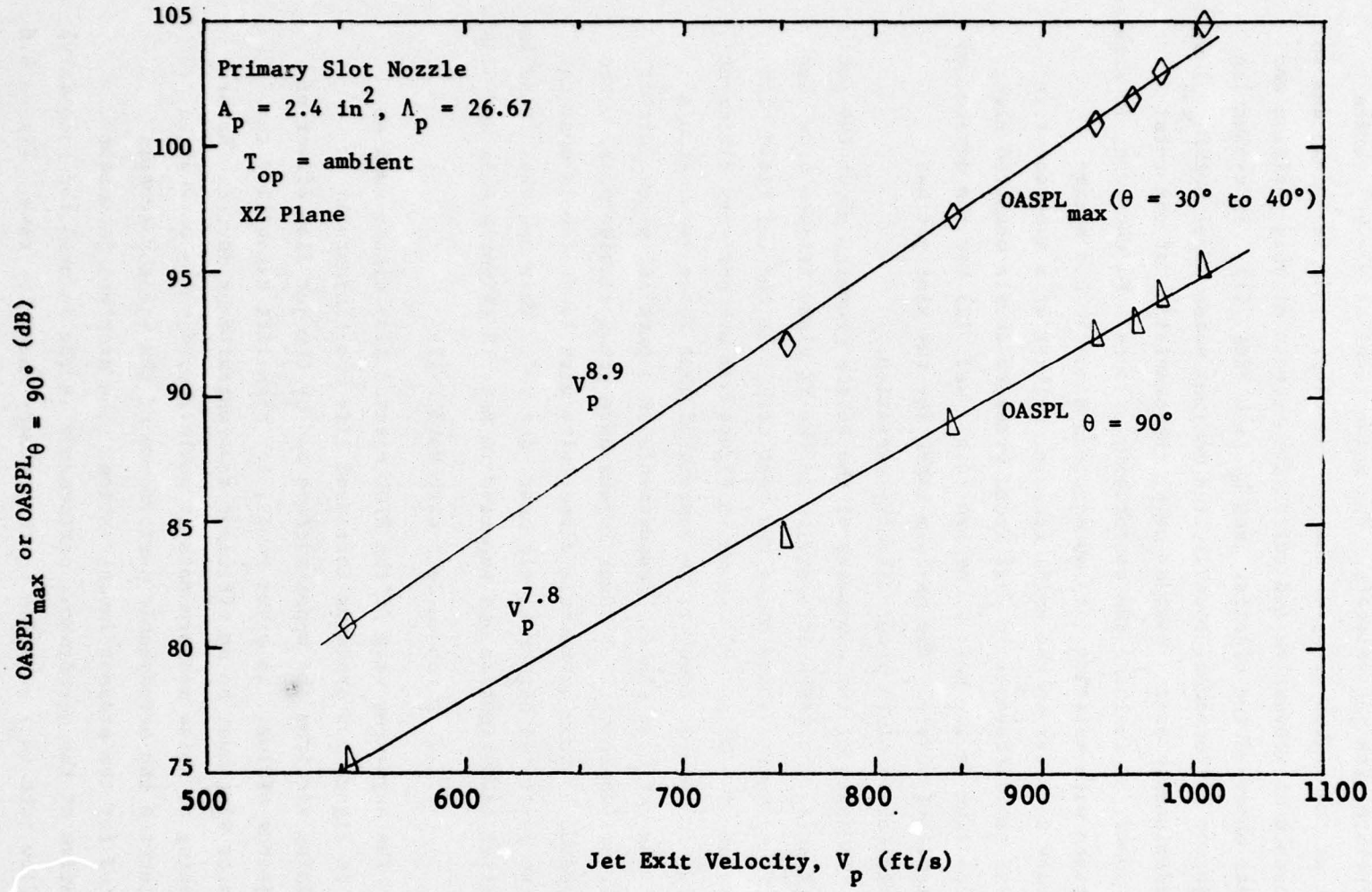

Figure 4.3. OASPL Variations with Jet Velocity in the XZ Plane of Primary Slot Nozzle.

do correlate with jet velocity. The noise level at $\theta = 90°$ varies almost as the eighth power of the jet velocity. This is mainly due to the absence of convective and refractive effects at this position and has been observed for circular jets by Lush (Ref. 11). In evaluating the ejector performance, however, the maximum noise level ($OASPL_{max}$) will be predominantly used. Besides being representative of the total sound power, it includes the directivity effects. Furthermore, it enables comparison with existing data on ejectors since it has become customary to refer to the noise reducing ability of a suppressor in terms of the difference in peak sound pressure levels measured along the same line (e.g., Ref. 2) or arc (e.g., Ref. 12) for the device and an unmodified nozzle. The maximum OASPL for the slot jet has approximately a ninth power velocity variation.

In spite of the asymmetry of the nozzle geometry about the jet axis (X axis) the OASPL directivity in the YZ plane (Figure 4.4a) has a fairly symmetric shape along the test circle in the far field. The spectra at $\phi = 0°$ and 90° shown in Figure 4.4b are not very different either. It should, however, be remembered that these measurements are in the jet exit plane. Measurements in a parallel plane further downstream (where the jet shear layers have grown considerably) would be expected to show asymmetric directivity with lower levels near the sideline point and higher levels near $\phi = 90°$. This has been found in an earlier investigation and reported in Ref. 13 (Figures 4.5a and 4.5b).

4.1.2 Shrouded Jets with Hard Walls.

The augmentor wing or the STOL ejector flap system such as shown in Figure 1.5 produces increased lift coefficients by entraining air from the upper surface and by the jet flap effect of the ejector efflux. In other words, for high lift capability the augmentor wing must be an efficient mass entrainment device. Before proceeding to noise measurements it would therefore be worthwhile to determine the aerodynamic performance of the ejector systems selected for the present investigation. The simplest parameter indicative of the aerodynamic performance is the induced (or secondary) mass flow rate ($\dot{m}_s$) relative to the primary mass flow rate. Figure 4.6

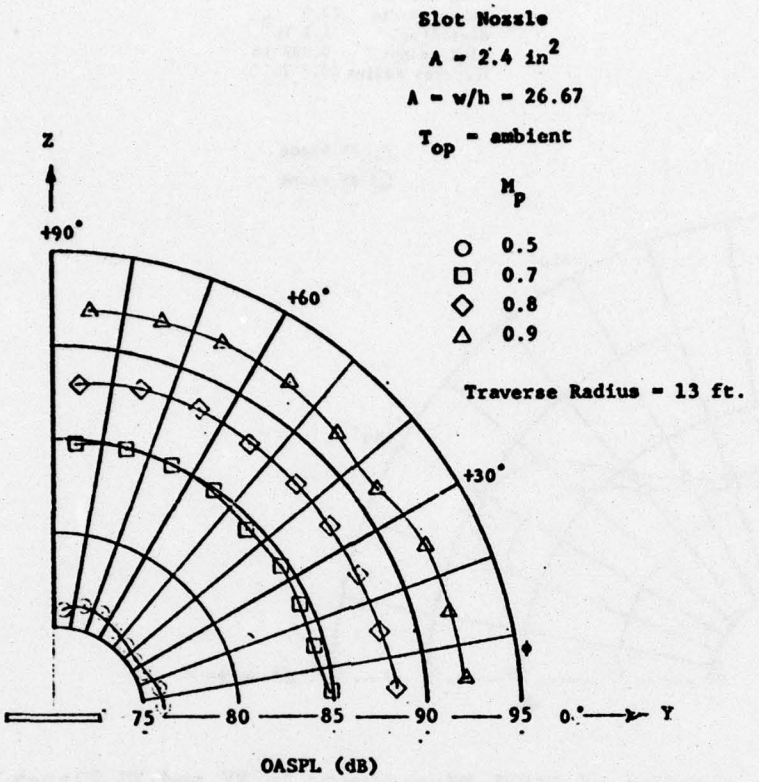

Figure 4.4a. OASPL Directivities in the YZ Plane of Primary Slot Nozzle.

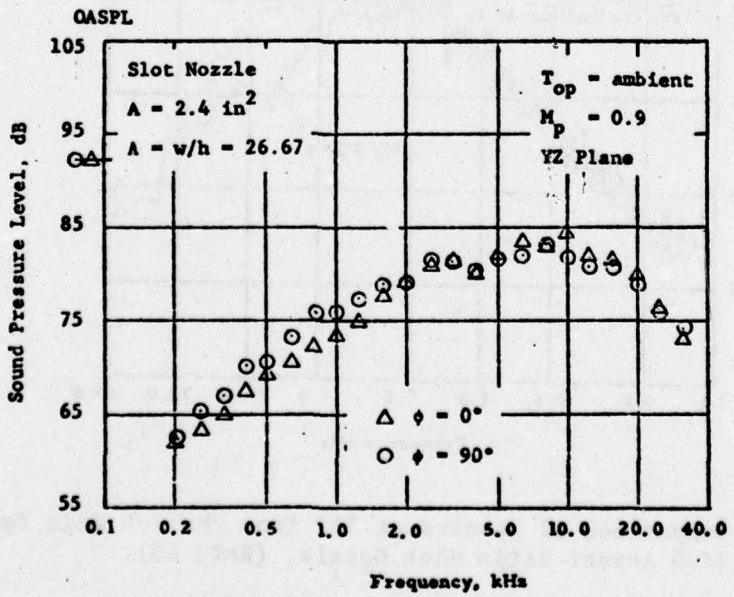

Figure 4.4b. Sound Pressure Spectra of the Primary Slot Nozzle at the Flyover and Sideline Positions in the Exit Plane.

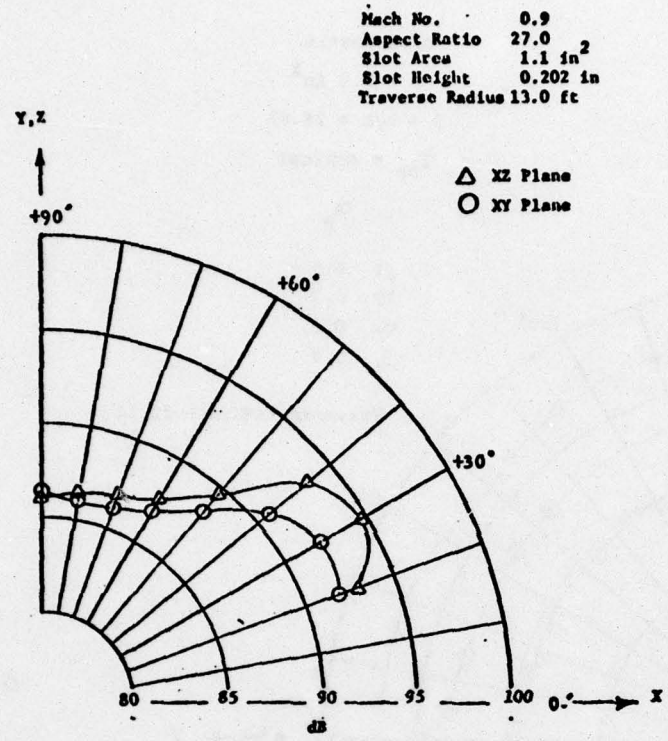

Figure 4.5a. Comparison of OASPL Directivity in XY and XZ Planes for Slot Nozzle of Aspect Ratio 27.0. (Ref. 13).

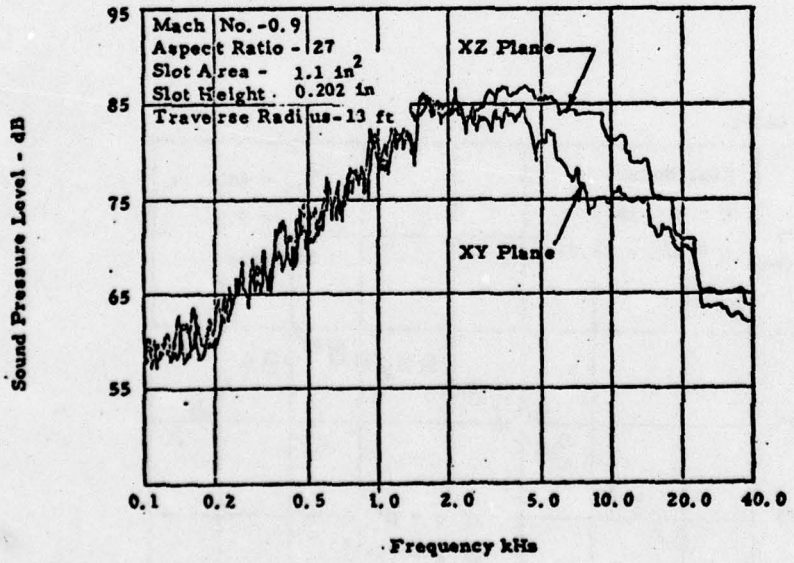

Figure 4.5b. Comparison of Spectra at 30° from the Jet Axis for the 27.0 Aspect Ratio Slot Nozzle, (Ref. 13).

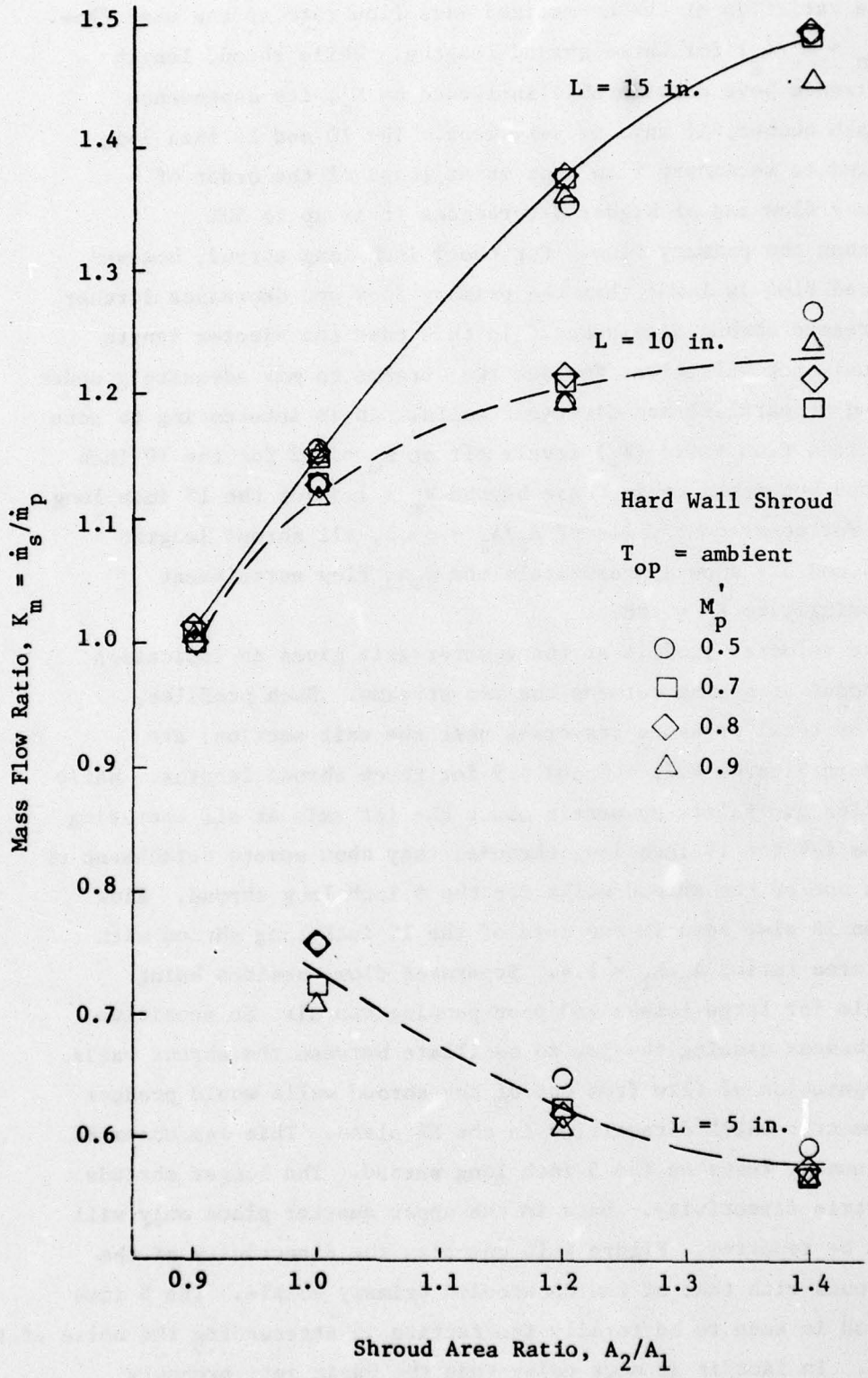

Figure 4.6. Mass Flow Ratio Variation with Shroud Area Ratio for Three Shroud Lengths.

shows the variation of the normalized mass flow rate or the mass flow ratio ($K_m = \dot{m}_s/\dot{m}_p$) for three shroud lengths. While shroud length and divergence have considerable influence on K_m, its dependence on jet Mach number, if any, is very weak. The 10 and 15 inch long shrouds induce secondary flow that is at least of the order of the primary flow and at higher divergences it is up to 50% greater than the primary flow. For the 5 inch long shroud, however, the induced flow is lower than the primary flow and decreases further with increased shroud divergence. In this case the ejector length is obviously not sufficient for the two streams to mix adequately under the shroud at parallel and divergent walls. It is interesting to note that the mass flow ratio (K_m) levels off at $K_m = 1.2$ for the 10 inch long shroud but seems to increase beyond $K_m = 1.5$ for the 15 inch long shroud. For convergent walls of $A_2/A_1 = \sim.8$, all shroud lengths (15", 10" and 5") show approximately the same flow entrainment correspondingly to $K_m = .88$.

The velocity profile at the ejector exit gives an indication of the amount of mixing between the two streams. Such profiles, obtained by total pressure traverses near the exit section, are presented in Figures 4.7, 4.8 and 4.9 for three shroud lengths. While the profiles are fairly symmetric about the jet axis at all operating conditions for the 15 inch long shrouds, they show severe detachment of flow from one of the shroud walls for the 5 inch long shroud. Flow separation is also seen in the case of the 10 inch long shroud with a shroud area ratio, $A_2/A_1 = 1.4$. Separated flow, besides being responsible for large losses and poor pumping can also be sensitive to disturbances causing the jet to oscillate between the shroud walls.

Separation of flow from one of the shroud walls would produce a non-symmetric OASPL directivity in the XZ plane. This was observed in the acoustic tests on the 5 inch long shroud. The longer shrouds had symmetric directivity. Data in the upper quarter plane only will therefore be reported. Figure 4.10 compares the directivity of the three shrouds with that of the unshrouded primary nozzle. The 5 inch long shroud is seen to be totally ineffective in attenuating the noise of the basic jet. In fact it is more noisy than the basic jet; probably due to the separated flow and added inlet noise due to poor pumping.

BEST AVAILABLE COPY

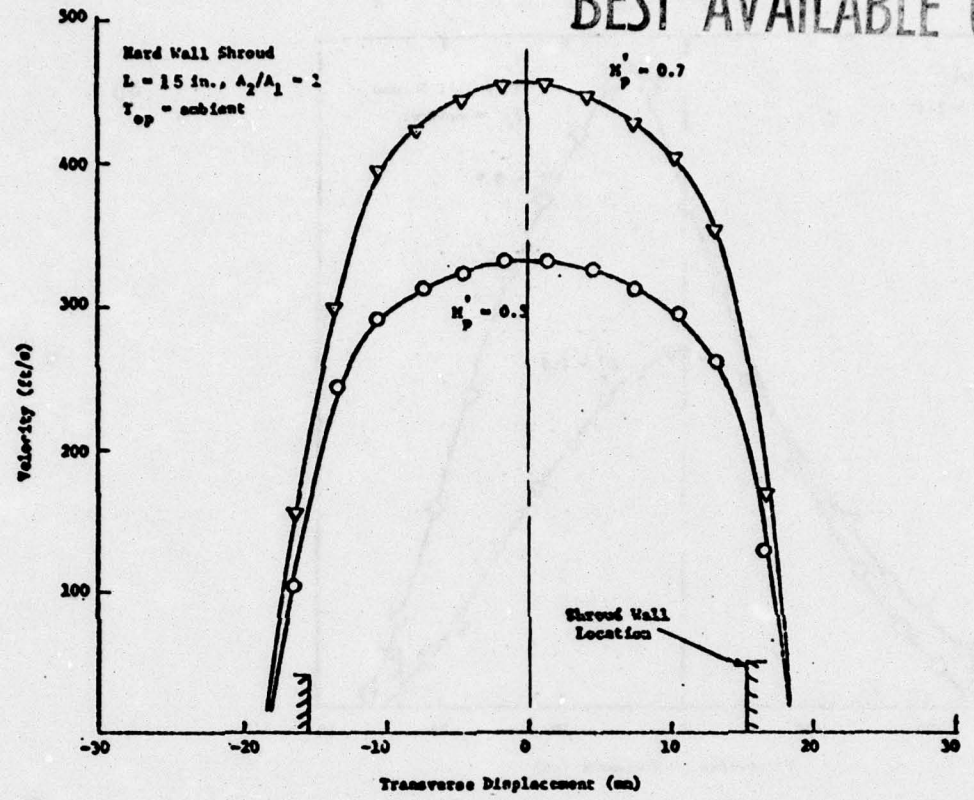

Figure 4.7a. Velocity Profiles for 15 inch Shroud Measured 0.75 inch Downstream of the Shroud Exit.

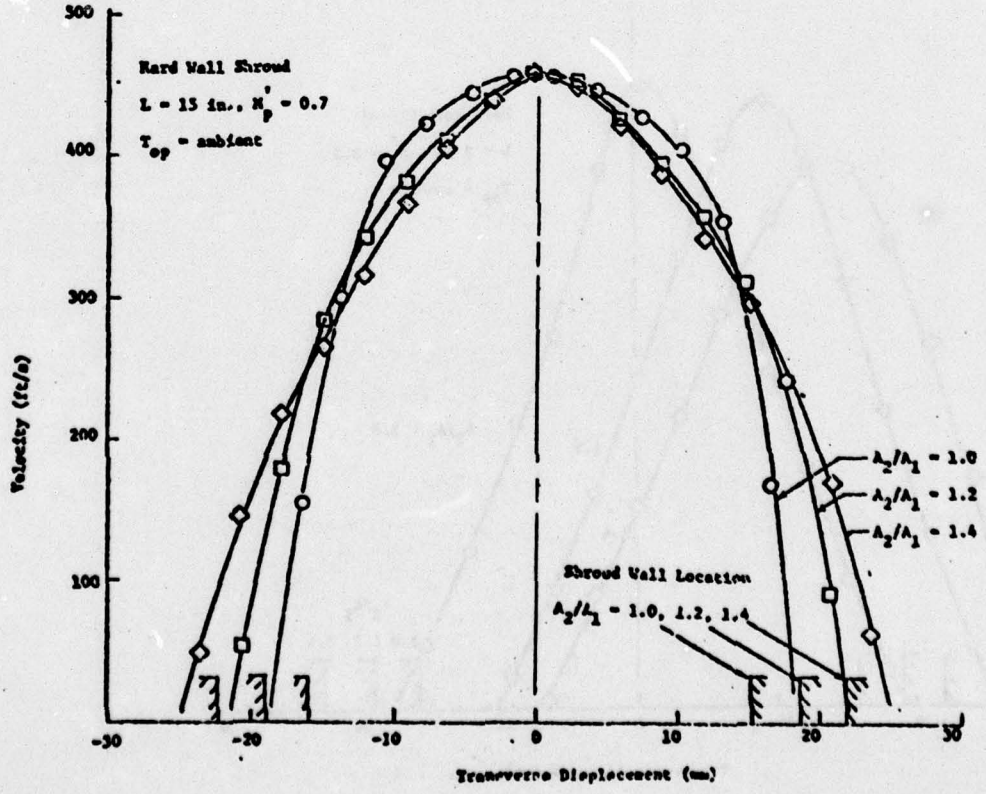

Figure 4.7b. Velocity Profiles for 15 inch Shroud Measured 0.75 inch Downstream of Shroud Exit.

BEST AVAILABLE COPY

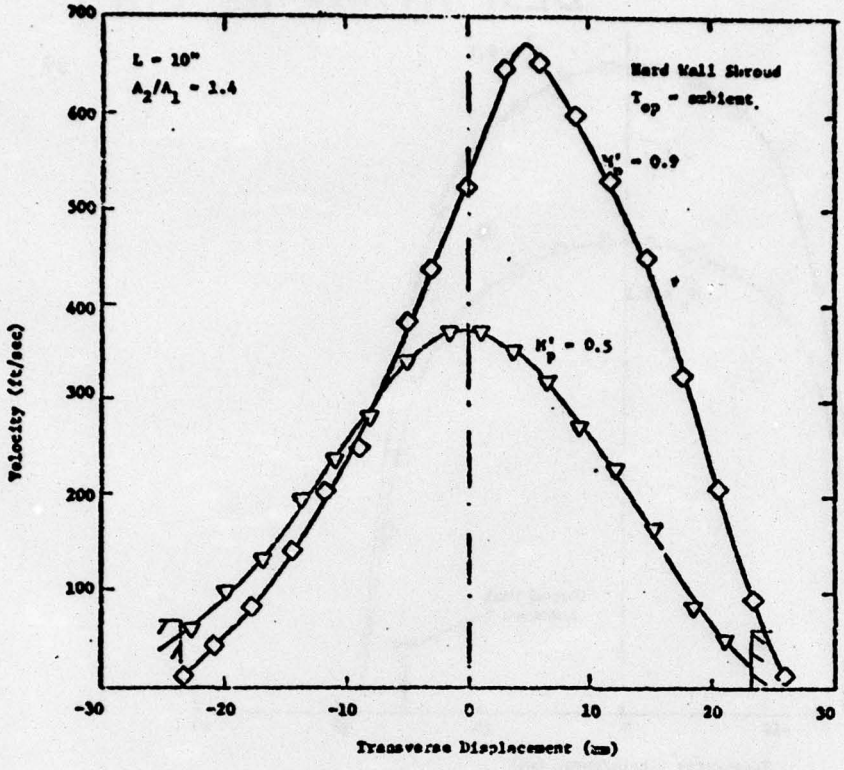

Figure 4.8. Velocity Profiles for 10 inch Shroud Measured 0.75 inch Downstream of the Shroud Exit.

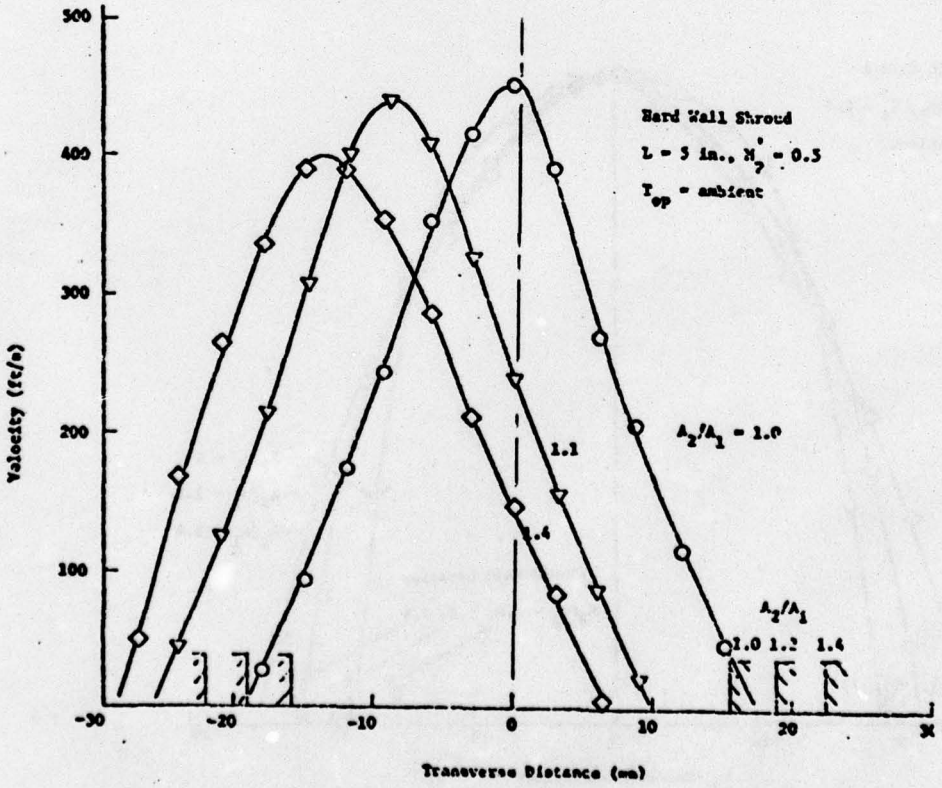

Figure 4.9. Velocity Profiles for 5 inch Shrouds Measured 0.75 inch Downstream of Shroud Exit.

These tests have already shown that the ejector system with the 5 inch long shroud has a poor potential for noise reduction or thrust augmentation. At this stage in the test series it was decided to stop further testing on the 5 inch long shroud.

The directivity patterns of Figure 4.10 clearly show the noise reduction ability of the 10 and 15 inch long shrouds. While the reduction due to the 10 inch long shroud is mainly around the peak radiation direction, the 15 inch shroud has lower sound pressure levels throughout the plane. These reductions, as can be seen in Figure 4.11 are mainly due to reductions in components above 1000 Hz.

The effects of operating pressure ratio and shroud divergence ratio (A_2/A_1) on the OASPL directivity and spectra for the 10 and 15 inch long shrouds are presented in Figures 4.12 through 4.17. The directivities for the 15 inch shroud peak around 45° in contrast to the peak at 35° for the unshrouded jet. In Figure 4.12 the difference between the maximum OASPL and the OASPL at $\theta = 90°$ does not seem to change with increase in the primary jet velocity. The convective effect for the shroud exhaust jet is reduced by the lower shroud jet velocity and the presence of the shroud would tend to eliminate the directionality of the primary jet sources. All the spectral components are seen to increase uniformly (Figure 4.13) with increasing jet velocity. The spectral comparison of Figure 4.14 indicates the dominance of low frequency noise at small angles to the jet axis. The directional radiation of various frequency components from the shrouded jet is however different from that of an unshrouded jet (cf. Figure 4.2).

With increasing shroud divergence ratio (A_2/A_1) the noise level throughout the flyover plane is seen to increase for the 10 and 15 inch shrouds mainly through an increase near the peak frequency components (Figures 4.15 to 4.17). The induced mass flow ($\dot{m}_s$) and the ejector exit area do go up at higher shroud divergence ratio (A_2/A_1). But the shroud exit velocity (V_2) decreases considerably as shown in Figure 4.18. A plot (Figure 4.19) of the maximum overall sound pressure level ($OASPL_{max}$) versus the shroud exit velocity (V_2) in fact shows that the data for different shroud divergence ratios (A_2/A_1) are widely separated and would not fall on one curve even if the $OASPL_{max}$ values were

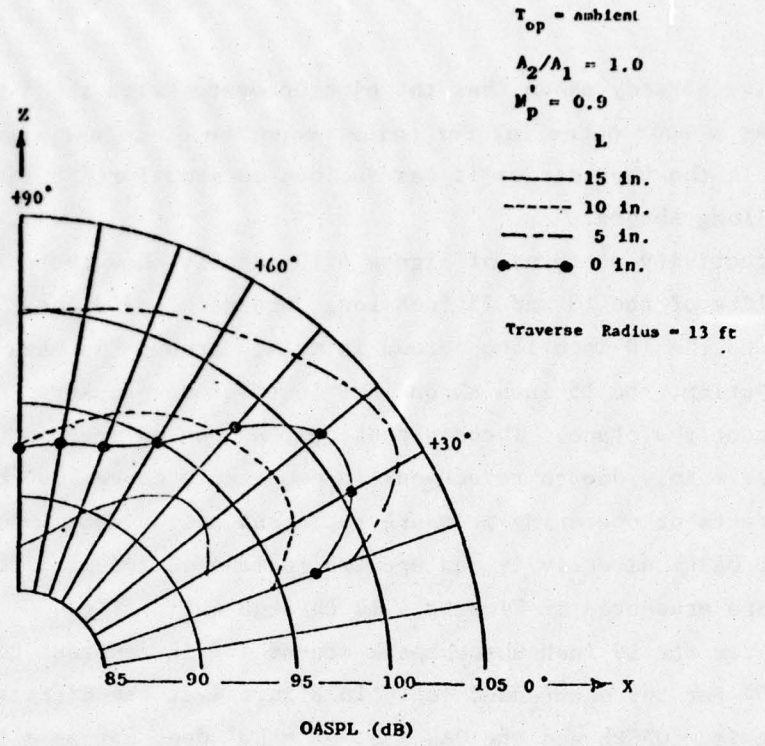

Figure 4.10. OASPL Directivities in XZ Plane for Three Ejector Lengths. (Hard Walls).

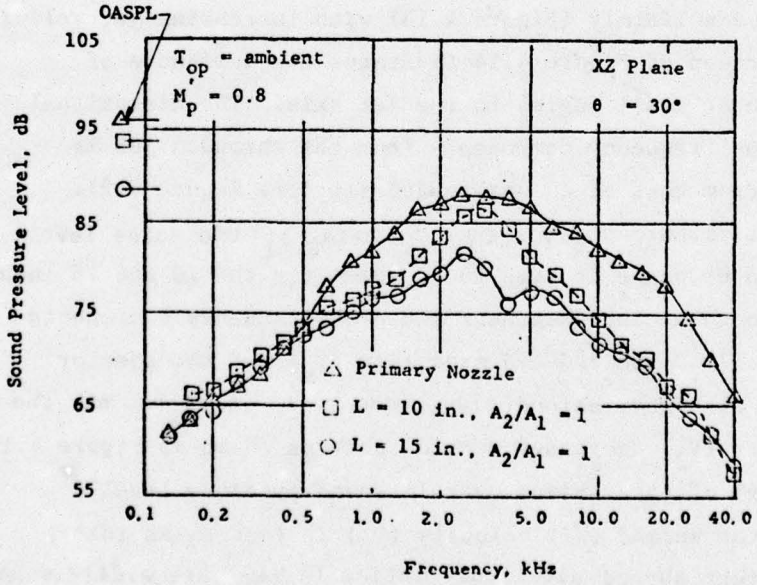

Figure 4.11. Sound Pressure Spectra for the Primary Nozzle and the 10 and 15 Inch Shrouded Nozzle. (Hard Walls).

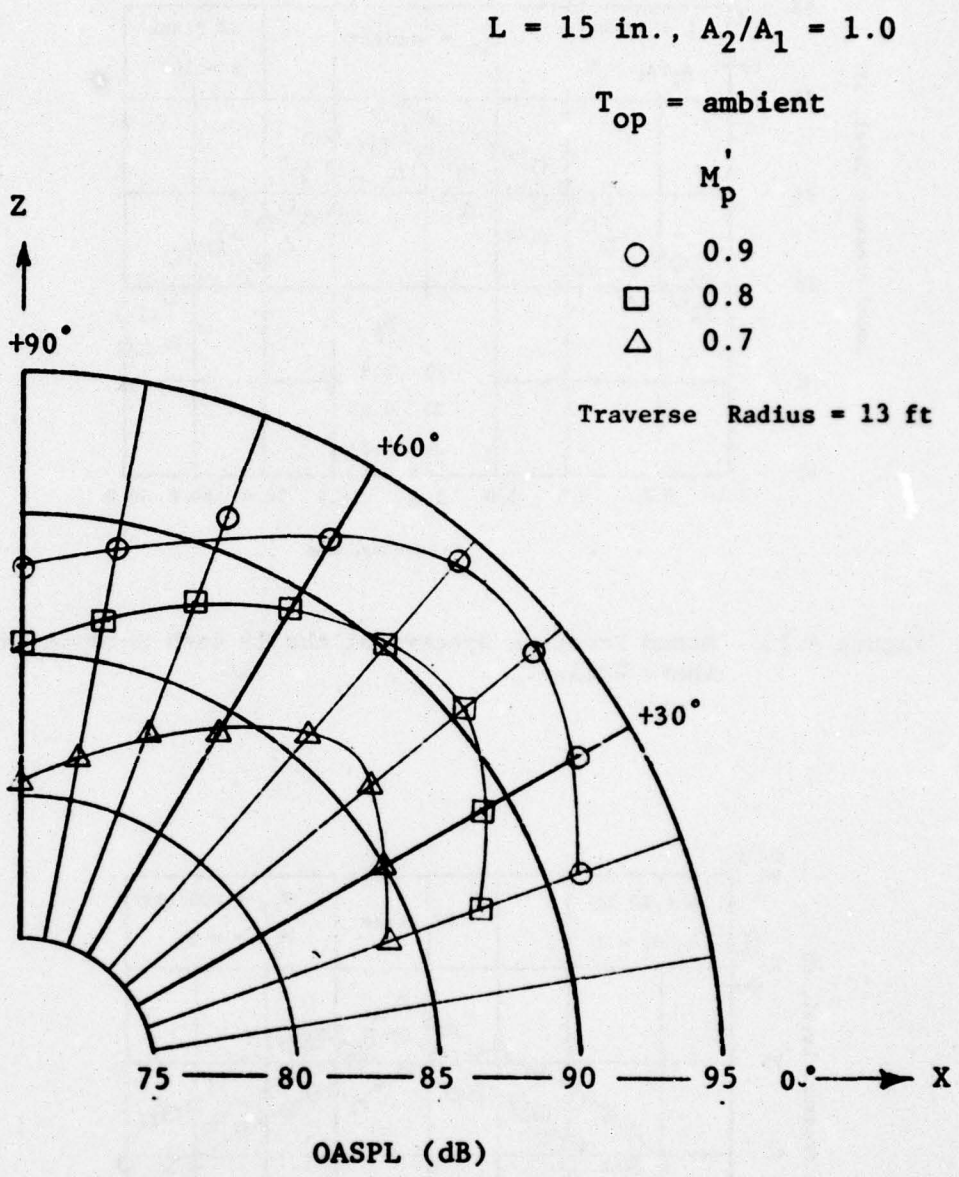

Figure 4.12. OASPL Directivities in the Flyover Plane of the 15 Inch Shrouded Nozzle. (Hard Walls).

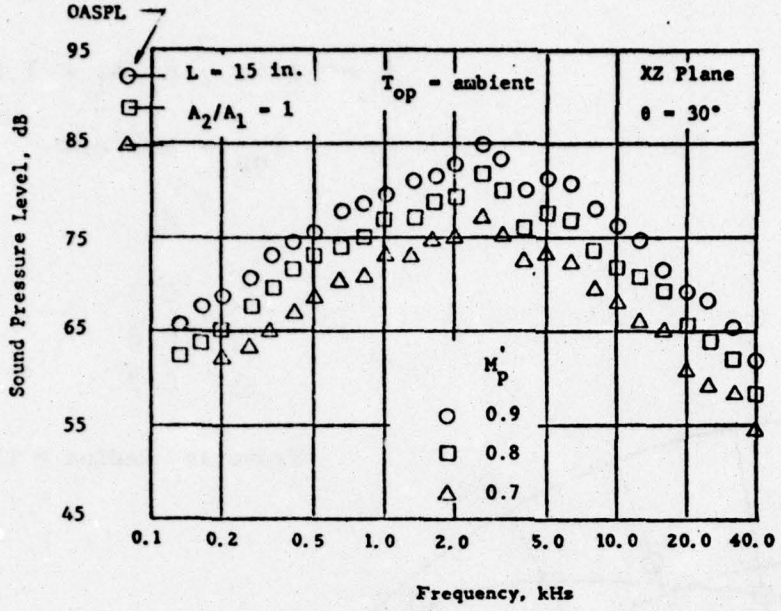

Figure 4.13. Sound Pressure Spectra of the 15 Inch Shrouded Nozzle. (Hard Walls).

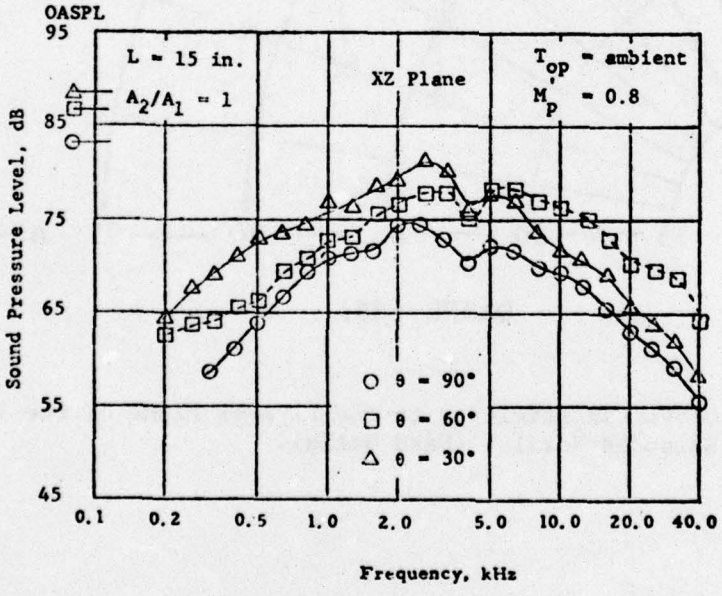

Figure 4.14. Sound Pressure Spectra at Three Positions for the 15 Inch Shrouded Nozzle. (Hard Walls).

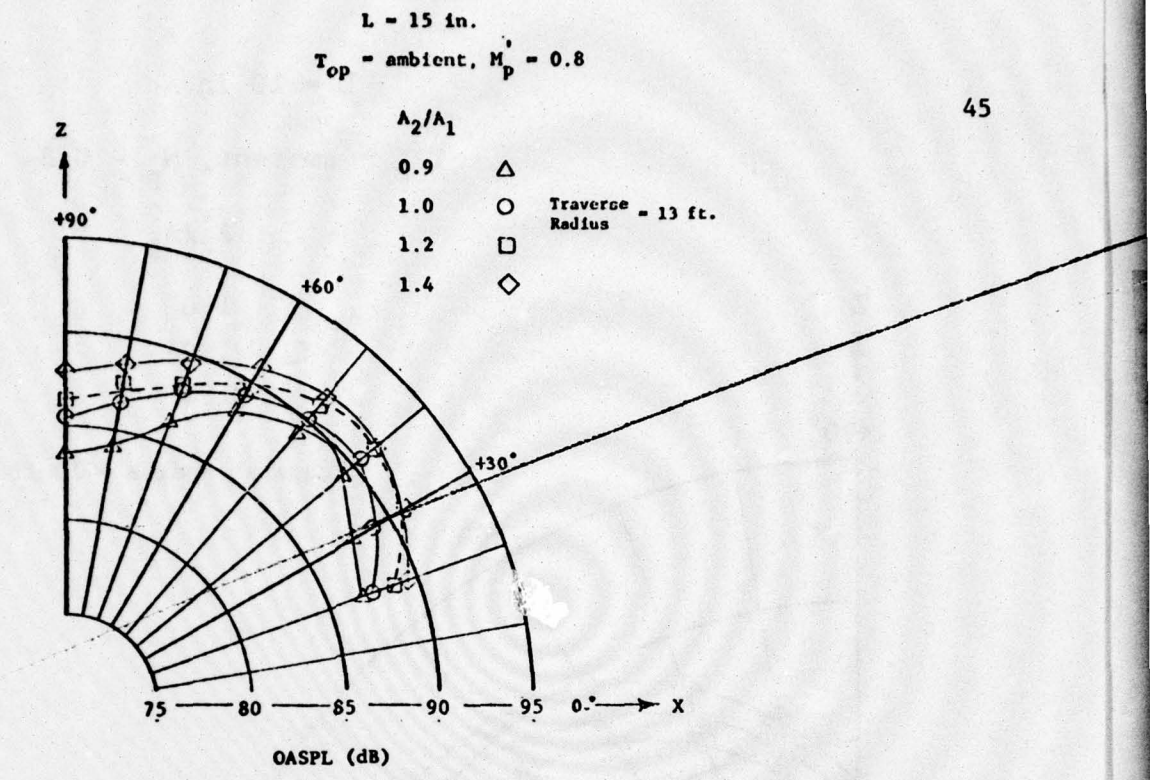

Figure 4.15. OASPL Directivities in XZ Plane for 15 Inch Shrouded Nozzles with Different Area Ratios. (Hard Walls).

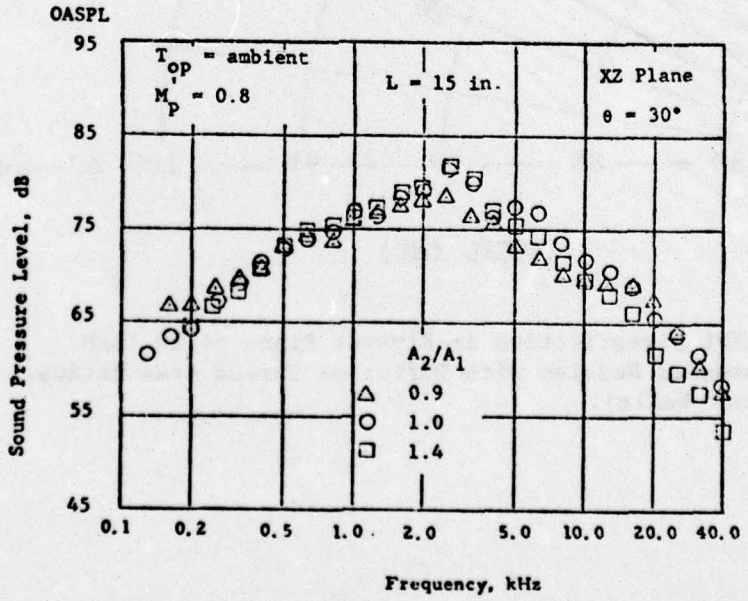

Figure 4.16. Sound Pressure Spectra for 15 Inch Shrouded Nozzles with Different Shroud Area Ratios (Hard Walls).

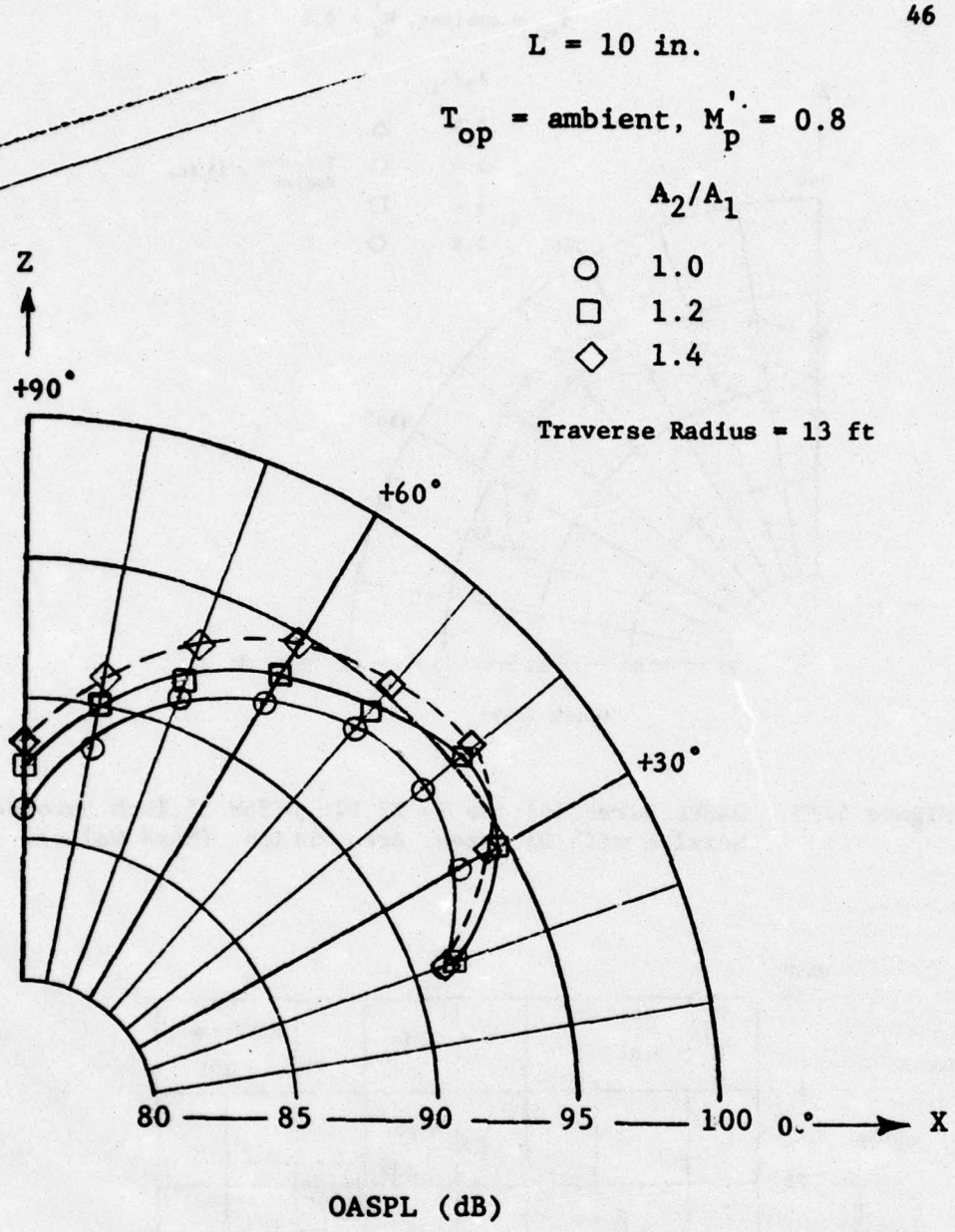

Figure 4.17. OASPL Directivities in Flyover Plane of 10 Inch Shrouded Nozzles with Different Shroud Area Ratios. (Hard Walls).

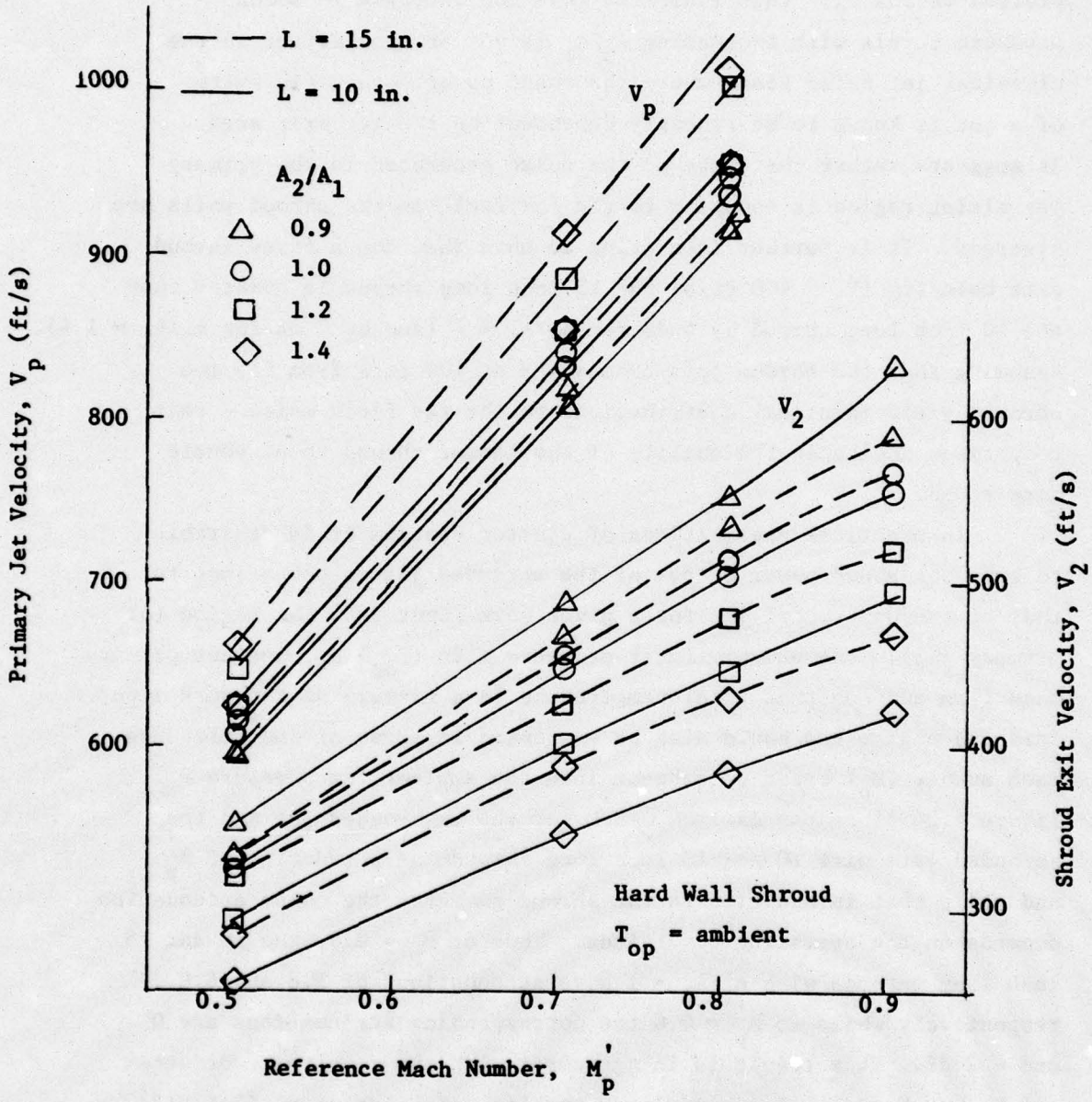

Figure 4.18. Primary Jet Velocity and Shroud Exit Velocity Variation with Reference Mach Number.

scaled for a constant value of A_2/A_1. In other words, the data would not give a single unique curve if $OASPL_{max}$-10 $\log_{10}$ (A_2/A_1) is plotted versus V_2. This indicates that the increase in sound pressure levels with increasing A_2/A_1 is not an area effect in the classical jet noise sense where the sound power output (in watts) of a jet is known to be linearly dependent on the jet exit area. It suggests rather that more of the noise generated in the primary jet mixing region is escaping to the far field as the shroud walls are diverged. It is further intersting to note that for a fixed shroud exit velocity (V_2 = 400 ft/s) the 15 inch long shroud is quieter than the 10 inch long shroud by 5 dB for A_2/A_1 = 1 (and by 7 dB for A_2/A_1 = 1.4). Assuming that the shroud jets exhausting at 400 ft/s from the two shrouds yield identical contributions to the far field noise - this comparison indicates the ability of the longer shroud to attenuate more sound.

In practical applications of ejector systems it is desirable to know the sound power output of the shrouded jet in comparison to that of the unshrouded jet for a given work input into the engine (or primary jet). The primary total pressure rise (P_{op}) at constant primary mass flow and constant total temperature is a measure of the work input into the engine and could also be expressed in terms of the reference Mach number (M_p') based on exhaust into the ambient (at pressure P_a). Figure 4.20 plots the maximum OASPL for the unshrouded jet and the shrouded jets with 10 and 15 inch long shrouds as a function of M_p' and shows that in addition to the shroud geometry the noise attenuation depends on the operating conditions. Thus at M_p' = 0.9, the 10 and 15 inch long shrouds with A_2/A_1 = 1 give attenuations of 3.8 and 6.9 dB respectively while at M_p' = 0.6 the corresponding attenuations are 0 and 4.2 dB. This result is in agreement with the results of Greatrex and Brown (Ref. 14) for suppressor nozzles and Coles et al (Ref. 12) for ejectors but in contrast to the results of Middleton (Ref. 2) who obtained a constant attenuation for axisymmetric ejector systems (independent of the operating pressure ratio).

In Figure 4.6, however, the pressure ratio was found to have little influence on the mass flow ratio (K_m) of the ejector. It also

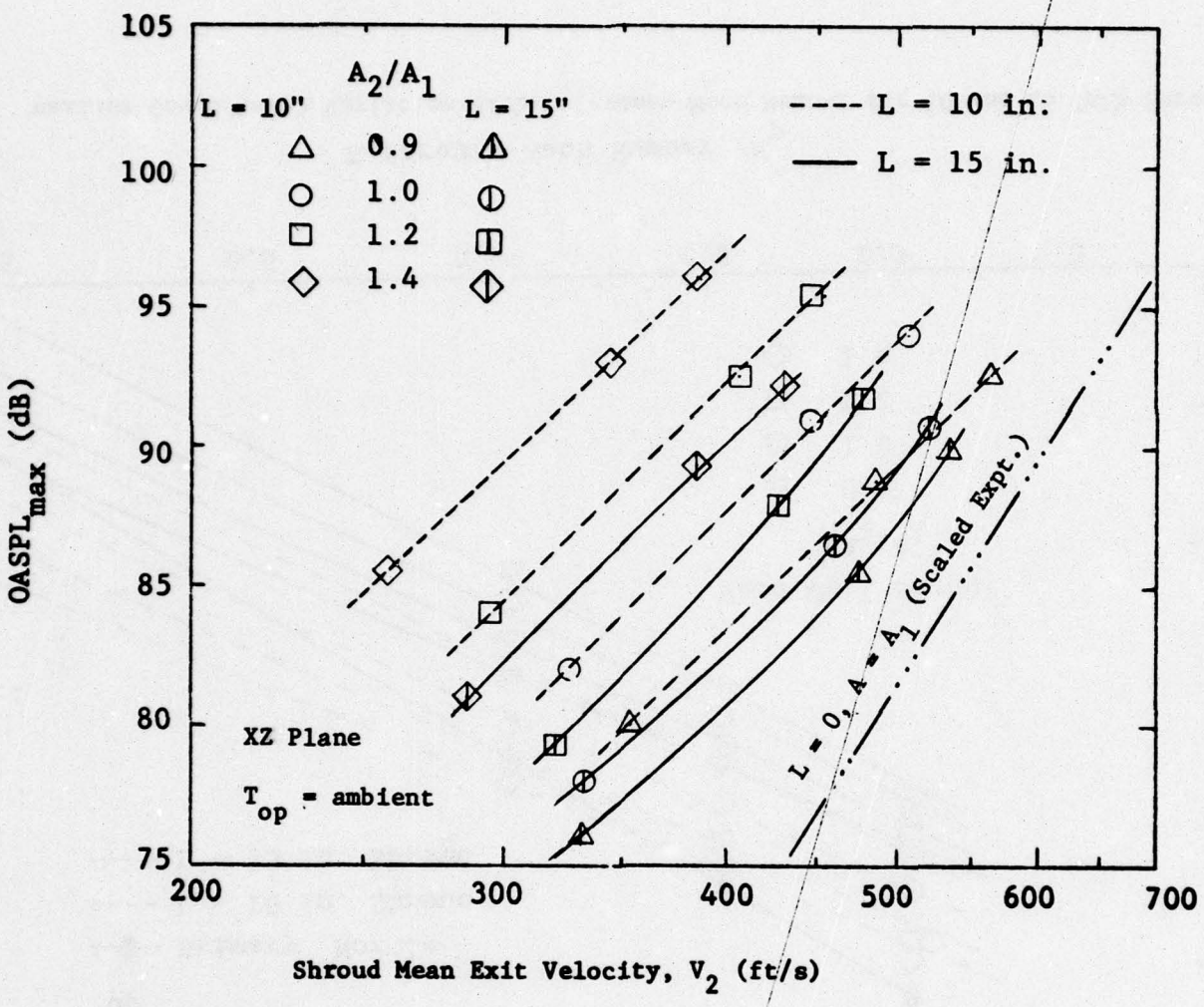

Figure 4.19. Maximum Sound Level Variation with Shroud Exit Velocity for 10 and 15 Inch Shrouded Nozzle, (Hard Walls).

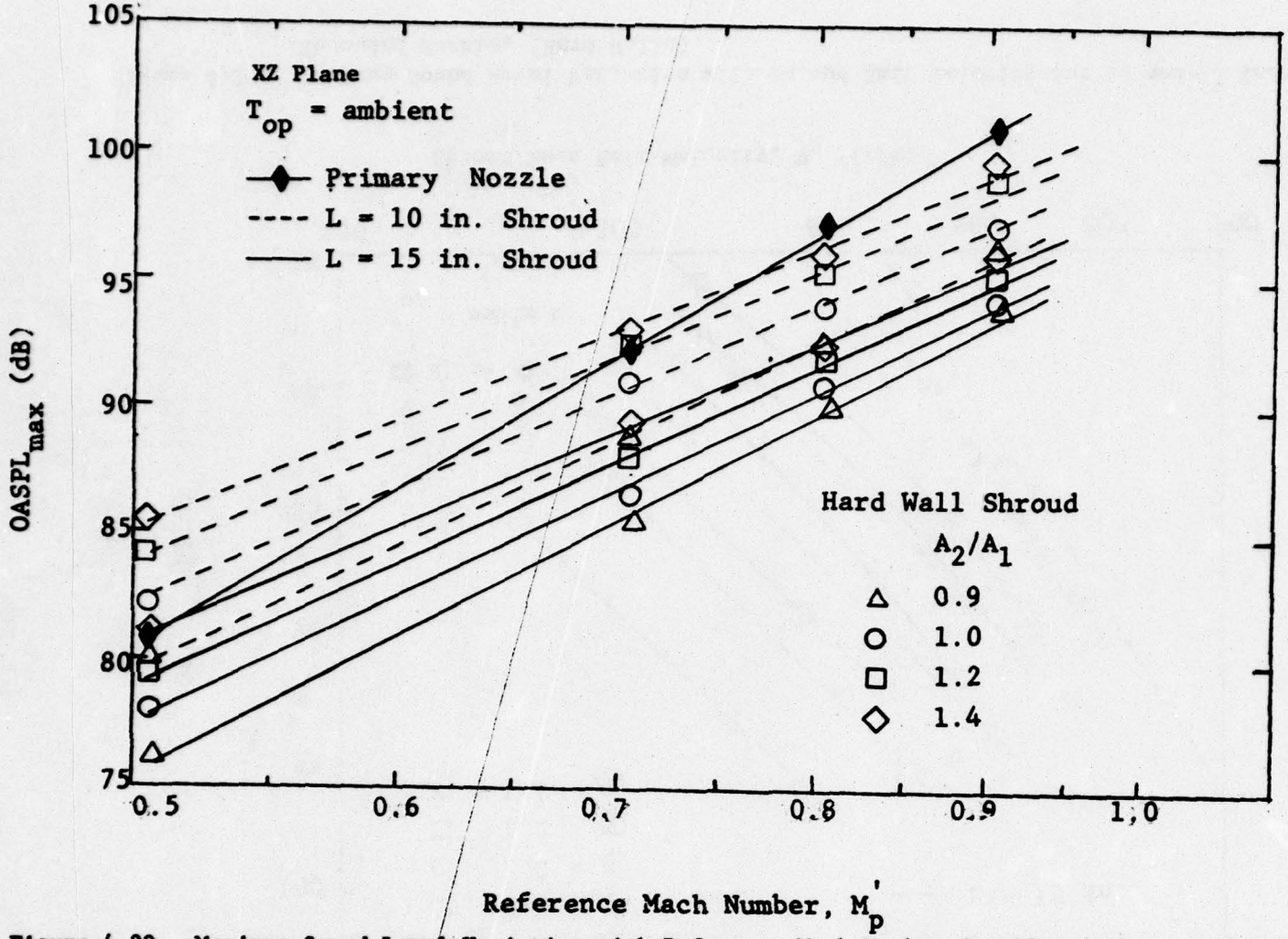

Figure 4.20. Maximum Sound Level Variation with Reference Mach Number for 10 and 15 Inch Shrouded Nozzle.

showed the pumping effectiveness to improve with the shroud area ratio (A_2/A_1). This gain is, however, accompanied by lower noise attenuation as shown in Figure 4.20.

A parameter which characterizes the aerodynamic performance of ejector systems is the thrust augmentation ratio (or simply thrust ratio). The static thrust (F) of the ejector system is given by the flux of momentum across the exit plane of the shroud. To achieve this thrust the primary nozzle ejects mass out of the stilling chamber (total pressure = P_{op}) into the shroud at a rate $\dot{m}_p$. If this mass were expanded isentropically from the chamber pressure (P_{op}) to ambient pressure (P_a) by a nozzle, the thrust produced will be F' (= $F_{isentropic}$). F' represents the maximum thrust that could be produced by an unshrouded nozzle at the given conditions. The ratio F/F' is thus a measure of the thrust augmentation of the ejector system over that of the ideal unshrouded nozzle. This ratio will be referred to as the thrust ratio (TR) of the ejector. The nozzle producing the thrust F' is called the reference nozzle. It was shown in Section 3.0 that the the thrust ratio (TR) can be expressed as $TR = (1 + K_m)\, V_2/V_p'$, where V_2 is the shroud exit velocity and V_p' is the exit velocity of the reference nozzle.

Thrust ratio calculated using the above formula and experimental results for the 10 and 15 inch long shrouds are plotted in Figure 4.21. One important result in this figure is the attainment of maximum thrust for shroud divergence ratio equal to 1.2 for the 15 inch long shroud as compared to the maximum at $A_2/A_1 = 1$ for the 10 inch long shroud. The mass flow ratio (K_m) is known to increase (from Figure 4.6) with A_2/A_1 for the 15 inch long shroud at a rate considerably faster than that for the 10 inch long shroud. The increase continues up to $A_2/A_1 = 1.4$ for the 15 inch long shroud whereas for the 10 inch shroud K_m reaches a maximum value of approximately 1.2 at $A_2/A_1 = 1.2$. Consequently, with increasing shroud divergence ratio (A_2/A_1) the shroud exit velocity (V_2) decreases considerably more for the 10 inch shroud than the 15 inch shroud. The two opposing effects of decreasing shroud exit velocity (V_2) and increasing mass flow ratio (K_m) due to increasing A_2/A_1 produces the variation of thrust ratio shown in Figure 4.21.

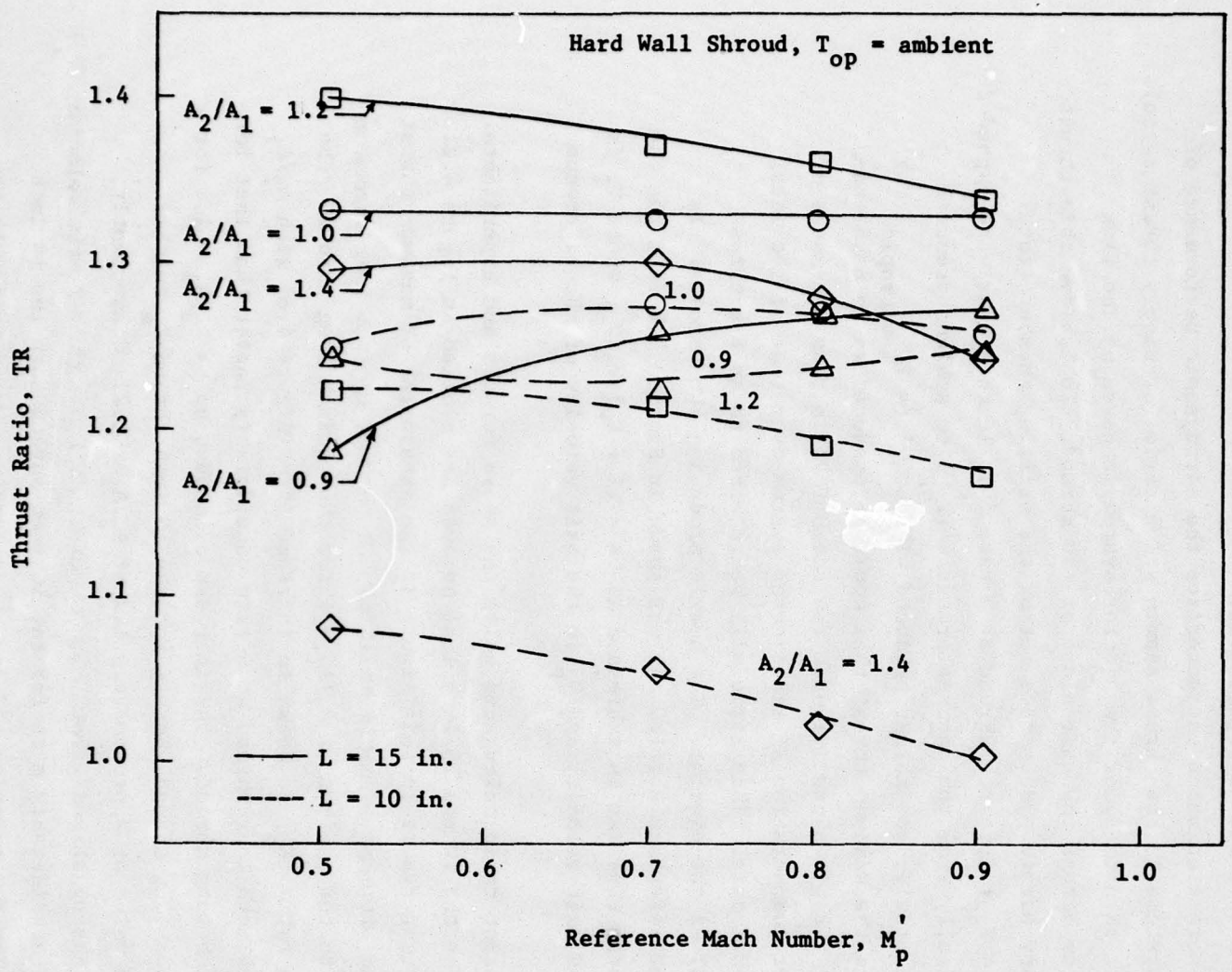

Figure 4.21. Variation of Thrust Augmentation with Reference Mach Number for 10 and 15 Inch Shrouded Nozzle.

It should be noted that the thrust augmentation of the ejector systems used here is very impressive - 20 to 40 percent for the 15 inch long shroud and 4 to 30 percent for the 10 inch long shroud.

Figure 4.22 presents a comparison of the present data with those of Reid (Ref. 15) and Goethert and Borchers' investigation of shrouded multinozzles (Ref. 1). Reid's data are for a circular ejector of secondary to primary area ratio equal to 2.9 and for $M_p' = 0.85$ whereas the data of Ref. 1 are for a dual circular nozzle surrounded by a rectangular shroud, the secondary to primary area ratio and M_p' being 4.09 and 0.9 respectively. For comparison purposes the shroud lengths are non-dimensionalized by shroud diameter (D_s) or shroud height (h_s). Data of the present investigation are directly comparable to those of Reid as presented in Figure 4.22 since the secondary to primary area ratios are almost the same in both cases. Comparison shows that with the present ejector system the maximum thrust augmentation is 33% compared to the 18% augmentation achieved by Reid. The ejector system of Ref. 1 did achieve thrust augmentation of about 30% but its secondary to primary area ratio was 4.09 as compared to 3.0 of the present system. A slot nozzle ejector system with area ratio equal to 4.09 can be expected to further augment the thrust.

In evaluating Figure 4.22 with respect to the effect of primary nozzle geometry on the shroud length required for maximum thrust augmentation, it should be kept in mind that the data are normalized by the shroud height or diameter. In general, increased perimeter of mixing between the primary and secondary streams and the corresponding reduction in the core length of the primary slot jet would require shrouds of shorter length in order to achieve a given thrust augmentation. This effect was observed in Ref. 1; the shrouded dual nozzle with a mixing perimeter equal to $\sqrt{2}$ times that for a shrouded single nozzle of equal area and a core length equal to $1/\sqrt{2}$ times that of the single nozzle was shown to achieve the maximum thrust augmentation with a shroud that was only $1/\sqrt{2}$ times as long as the shroud for maximum thrust augmentation with single nozzle. The slot nozzle used in the present investigation has a mixing perimeter that is $\sqrt{\text{aspect ratio}/\pi}$ times the mixing perimeter

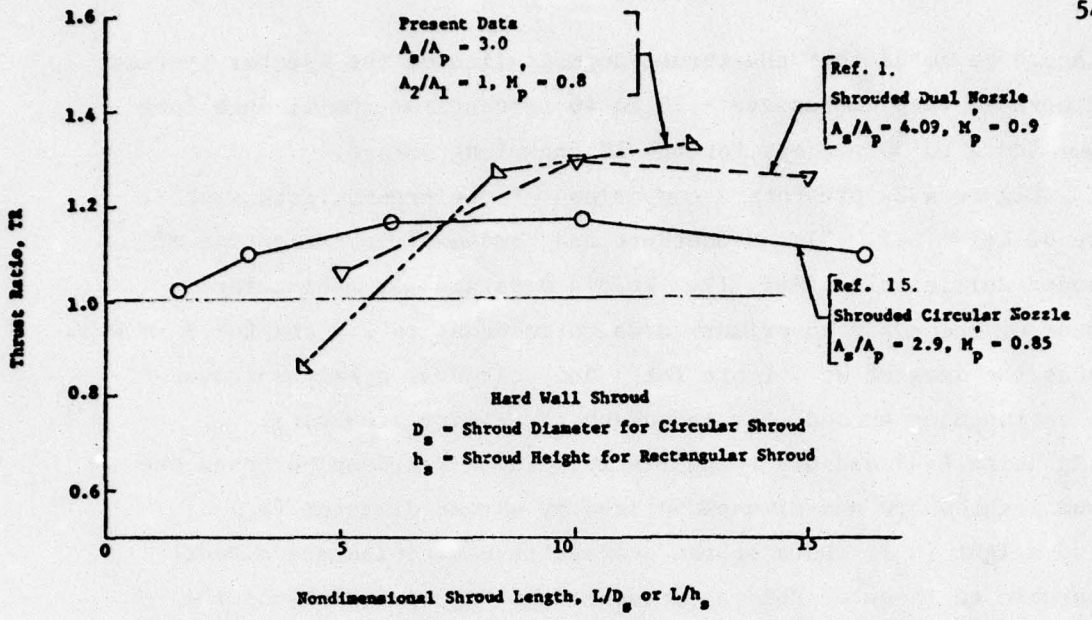

Figure 4.22. Thrust Augmentation Variation with Shroud Length and Comparison with Existing Data.

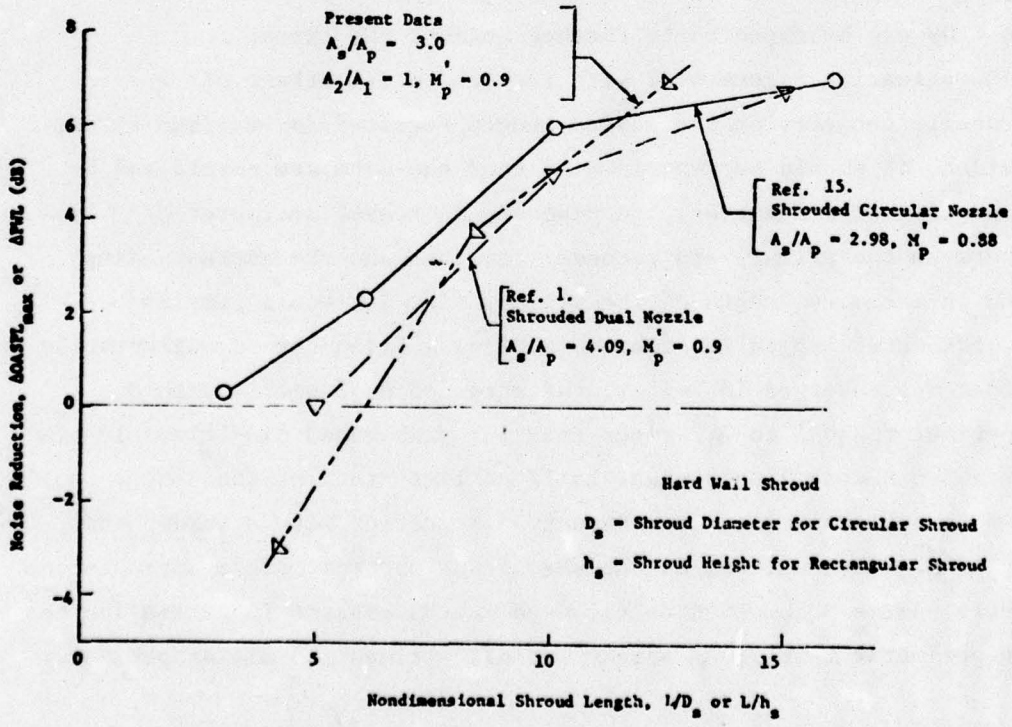

Figure 4.23. Variation of Noise Reduction with Shroud Length and Comparison with Existing Data, (Hard Wall).

of an equivalent circular nozzle and would therefore be expected to require a relatively shorter shroud to attain a given thrust augmentation.

A comparison of the acoustic data of the present ejector systems with those of Middleton (Ref. 2) for a circular shroud-nozzle system and of Goethert and Borchers (Ref. 1) for dual circular nozzle and rectangular shroud system is presented in Figure 4.23. The noise reduction in each case is seen to increase with increasing shroud length. Within the range of shroud lengths and hard walls used in the investigations a maximum noise reduction of 7 dB was achieved. The trends indicate that with further increase in the shroud length, a further additional noise attenuation for the shrouded slot nozzle system may be possible.

Since noise reduction and thrust augmentation are the most important quantities characterizing the performance of an ejector system it would be interesting to examine the variation of one with respect to the other. This is done in Figure 4.24 for both the 10 and 15 inch long shrouds operating at different pressure ratios and shroud divergence ratios. The 15 inch shrouds are clearly superior in thrust augmentation as well as noise reduction capability. The 15 inch shroud with shroud area divergence ratio equal to 1.2 produces maximum thrust augmentation at all operating pressures. The noise reduction, however, was measured to be a maximum when the shroud area ratio (A_2/A_1) was equal to 0.9 and might further increase as the area ratio decreases. For any given shroud geometry, the noise reduction increases with increasing reference Mach number. The thrust augmentation remains constant or decreases only slightly (5%) with increasing nozzle pressure ratio. The ejector system thus seems to be more efficient at higher operating pressure ratios. This should be particularly noted for the 10 inch shroud which is successful in attenuating the noise only at higher reference Mach number.

In Figure 4.24 the thrust ratio of the shrouded nozzle is given as its thrust relative to that of the reference nozzle (defined earlier). However, the noise reduction is shown relative to the primary nozzle operating at the same pressure ratio (P_{op}/P_a), but exhausting a

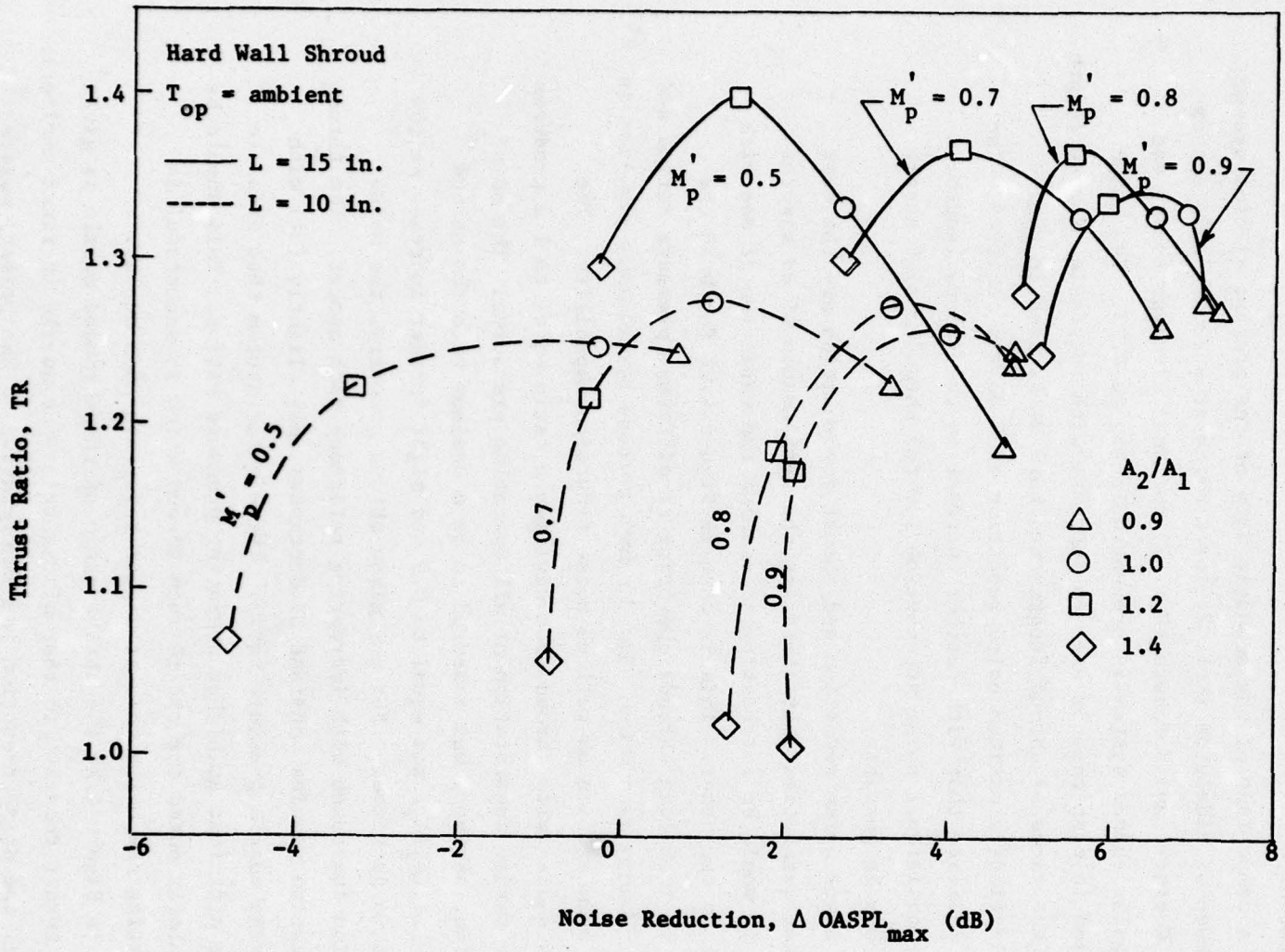

Figure 4.24. Variation of Thrust Augmentation with Noise Reduction for 10 and 15 Inch Shrouded Nozzles.

slightly smaller mass flow at a lower velocity. Thus, the reference nozzle exhausting the same mass flow as the shrouded primary nozzle is slightly larger in area and consequently noisier and therefore the noise reductions of Figure 4.24 are slightly conservative. This additional noise of the reference nozzle due to the area correction depends on the shroud geometry (L, A_2/A_1) and the operating condition (M_p') but has been found in the present investigation to be always less than 0.5 dB. Thus the actual noise reductions are somewhat larger than those of Figure 4.24 by less than 0.5 dB.

4.1.3 Shrouded Jets with Noise Attenuating Liners.

Noise levels of the ejector systems have been seen (Figure 4.19) to be considerably higher than that anticipated from simple jet exhausting from the shroud exit with equivalent velocity and area, suggesting that the noise measured was to a large extent that of the primary jet discharging and mixing within the shroud. This difference was shown in Figure 4.33 of Ref. 1 to be mainly due to a difference of about 10 to 17 dB in the high frequencies, f > 2000 Hz. The high frequency content of the internal ejector noise suggests the use of acoustically lined shroud which can be an effective attenuator in this frequency domain. Construction of the liners used in the present investigation has been described in Section 2. The acoustic performance of the lined shrouds will be presented in terms of the OASPL directivities, spectra, $OASPL_{max}$, etc. and compared with the corresponding data for the unlined (hard wall) shrouds.

Figures 4.25 and 4.26 show the OASPL directivities of the lined shrouds for the 15 and 10 inch long shrouds respectively. With the longer shroud the use of acoustic lining is seen to reduce the noise level throughout the plane by about 2 dB below that of the unlined shroud-nozzle system at the selected test conditions. Shroud lining, however, has no effect on the noise levels of the 10 inch long shroud. The 2 dB reduction with the longer shroud is due to reductions in components above 2000 Hz as shown in Figure 4.27. Figure 4.28 shows a comparison of the lined and unlined ejectors as a function of shroud exit velocity. Also shown on this figure are data taken for the 15 inch

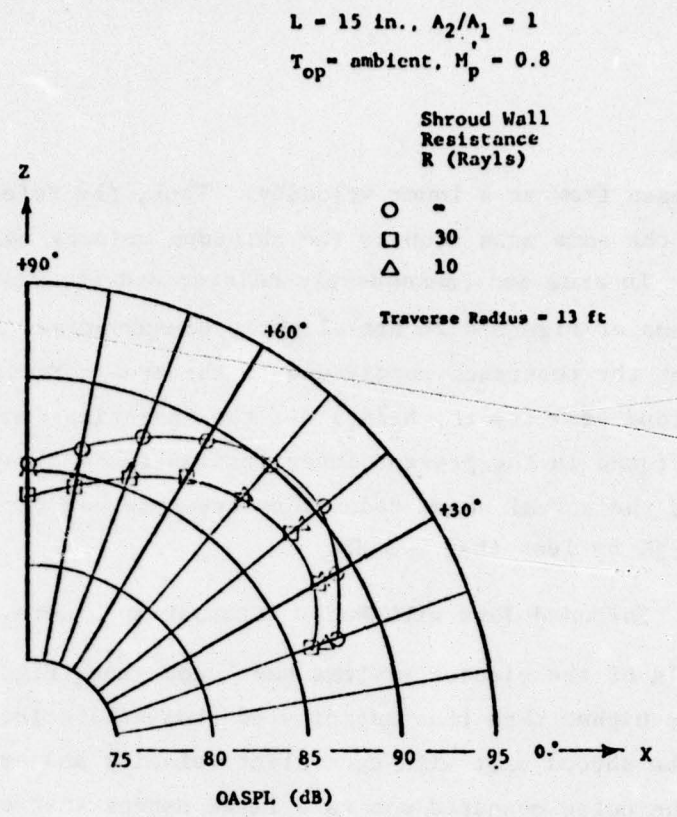

Figure 4.25. OASPL Directivities in the Flyover Plane of 15 Inch Shrouded Nozzles with Hardwall and Lined Shrouds.

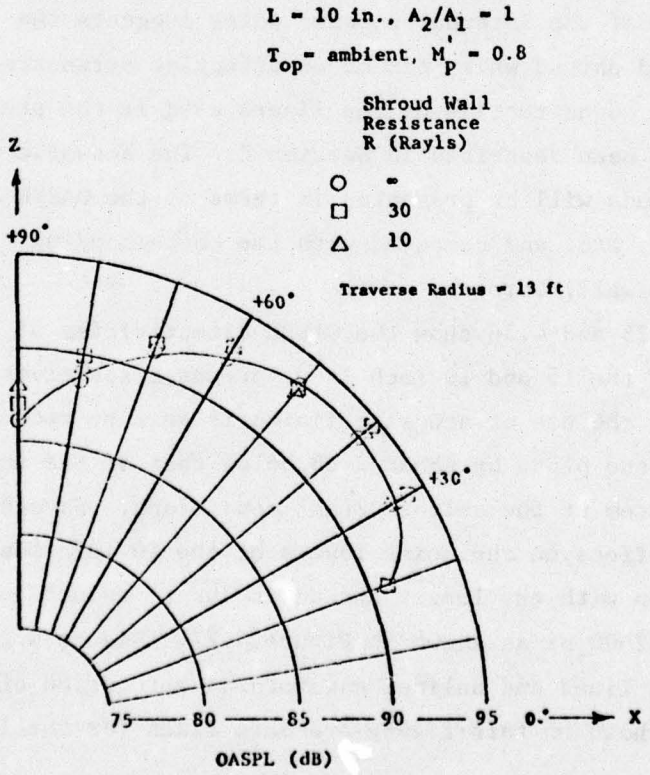

Figure 4.26. OASPL Directivities in the Flyover Plane of 10 inch Shrouded Nozzles with Hard Wall and Lined Shrouds.

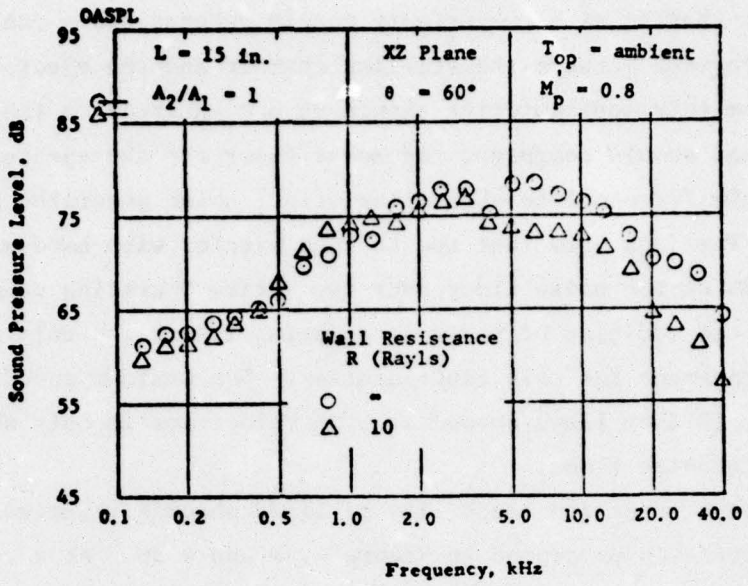

Figure 4.27. Sound Pressure Spectra of 15 Inch Shrouded Nozzle with Hard Wall and Lined Shrouds.

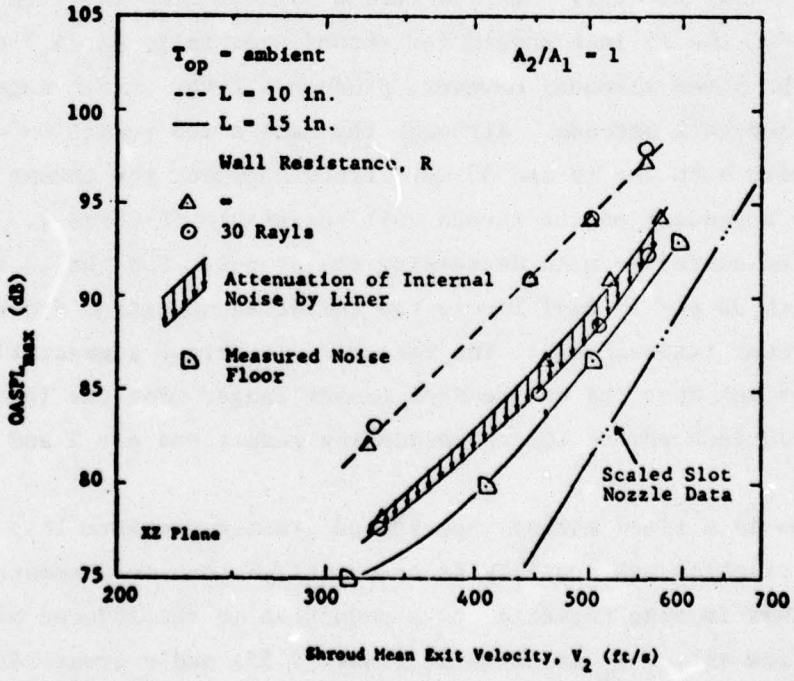

Figure 4.28. Variation of Maximum Sound Level with Shroud Exit Velocity for Hard Wall and Lined Shrouded Nozzles.

shroud alone; that is with the primary nozzle removed and a contoured transition provided between the stilling chamber and the ejector shroud. The noise from this configuration should be due entirely to the shroud exhaust jet and should represent the noise floor for the ejector system, attainable only for complete absorption of all noise generated beneath the shroud. The data show that the 15 inch ejector with hard walls is within 5 dB of the noise floor over the entire operating range. Consequently the addition of noise attenuating liners can only produce a modest improvement for this configuration. The maximum sound pressure level for the 15 inch lined shroud at high velocities is only about 1 dB above the noise floor.

The noise reduction capability of lined shrouds relative to the unshrouded nozzle is presented in Figure 4.29 and 4.30. At a reference Mach number (M_p') equal to 0.9 the noise reduction with the 15 inch long shroud is seen to increase to 9.2 dB compared to the 7 dB reduction with the unlined shroud (Figure 4.20).

The thrust ratio variations for the lined shrouds are shown in Figures 4.31 and 4.32. Maximum thrust augmentation is again achieved with the 15 inch shroud for shroud area ratio (A_2/A_1) equal to 1.2. The lined shrouds, however, produce a lower thrust augmentation than the hard wall shrouds. Although the same noise reduction was obtained with both the 10 and 30 Rayl lined shrouds, the thrust augmentation is clearly dependent on the shroud wall resistance (Figures 4.33 and 4.34) - augmentation decreases with decreasing resistance. For the 15 inch shrouds with 30 and 10 Rayl liners the thrust augmentation drops 5 and 10 percent respectively. The reduction in thrust augmentation is fairly constant over the entire Mach number range. For the less efficient 10 inch shroud the corresponding reductions are 2 and 4 percent only.

Flow in a lined shroud experiences greater pressure loss (due to increased friction and possibly secondary flow) than in a smooth unlined shroud. This is also reflected as a reduction in the induced mass flow (or mass flow ratio, K_m as shown in Figure 4.35) and correspondingly lower values for the thrust augmentation. Imperfections in liner construction could cause backflow within the liner cavities thereby impairing the air

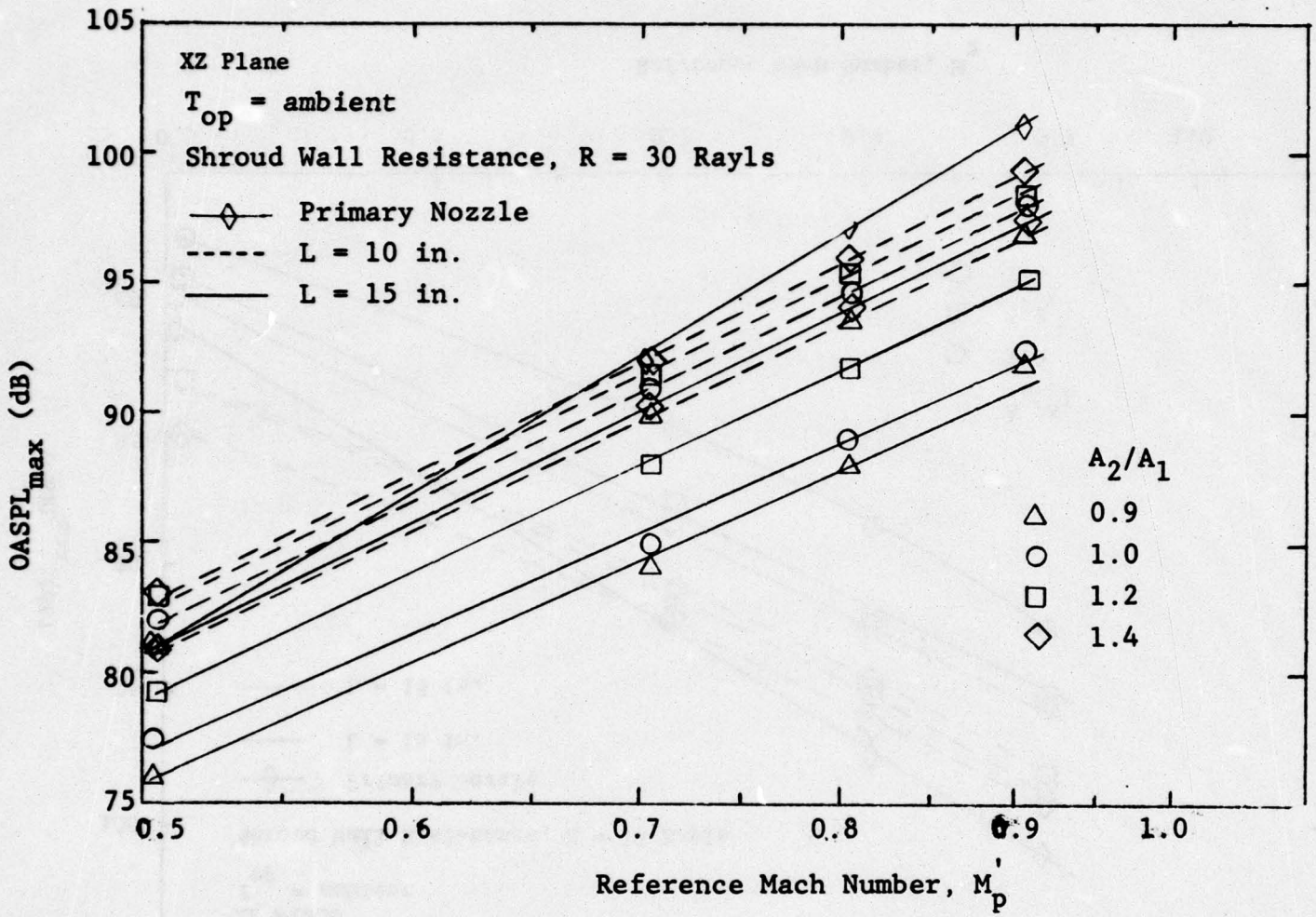

Figure 4.29. Variation of Maximum Sound Level with Reference Mach Number for Shrouded Nozzles with 30 Rayl Liners.

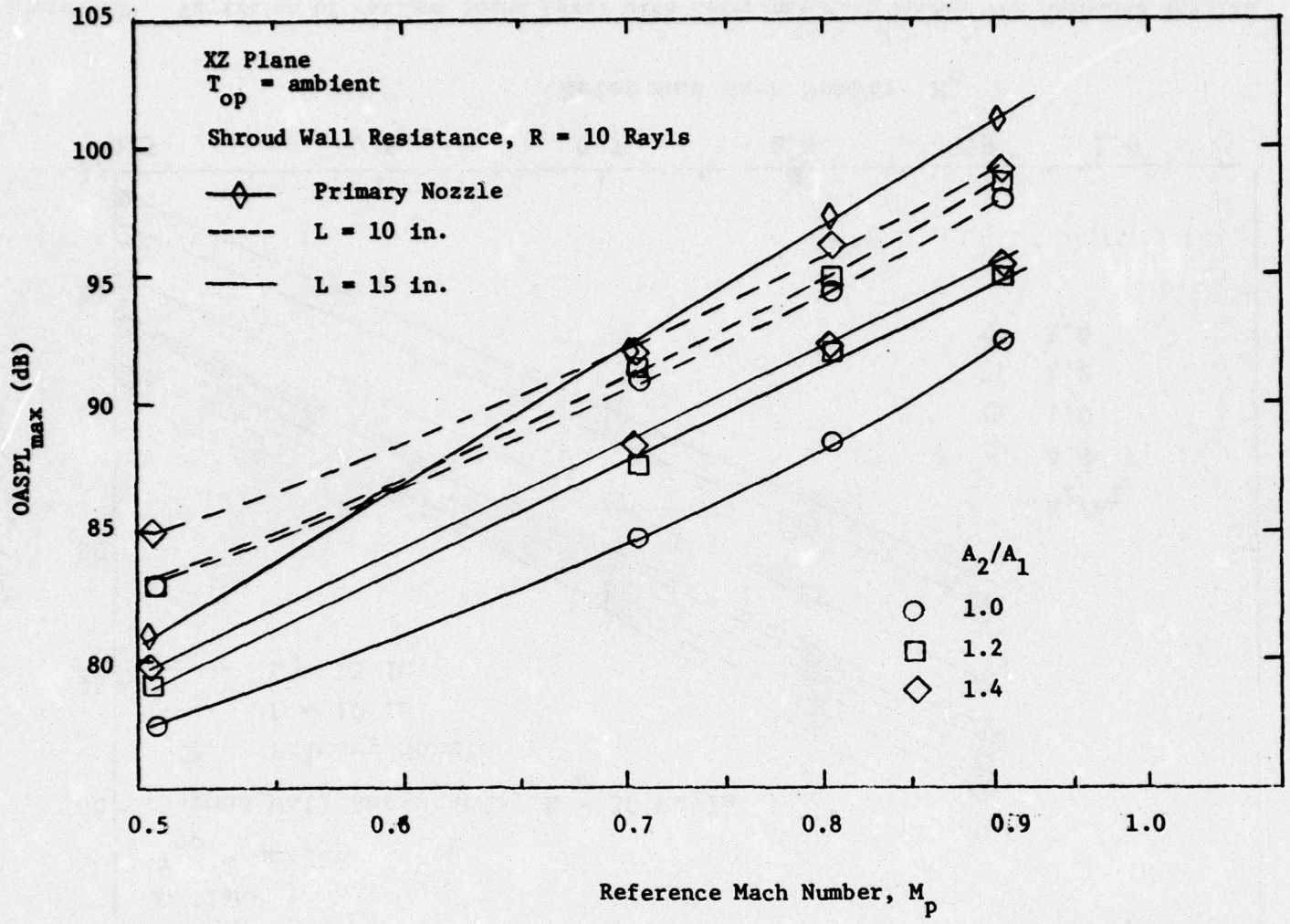

Figure 4.30. Variation of Maximum Sound Level with Reference Mach Number for Shrouded Nozzles with 10 Rayl Liners.

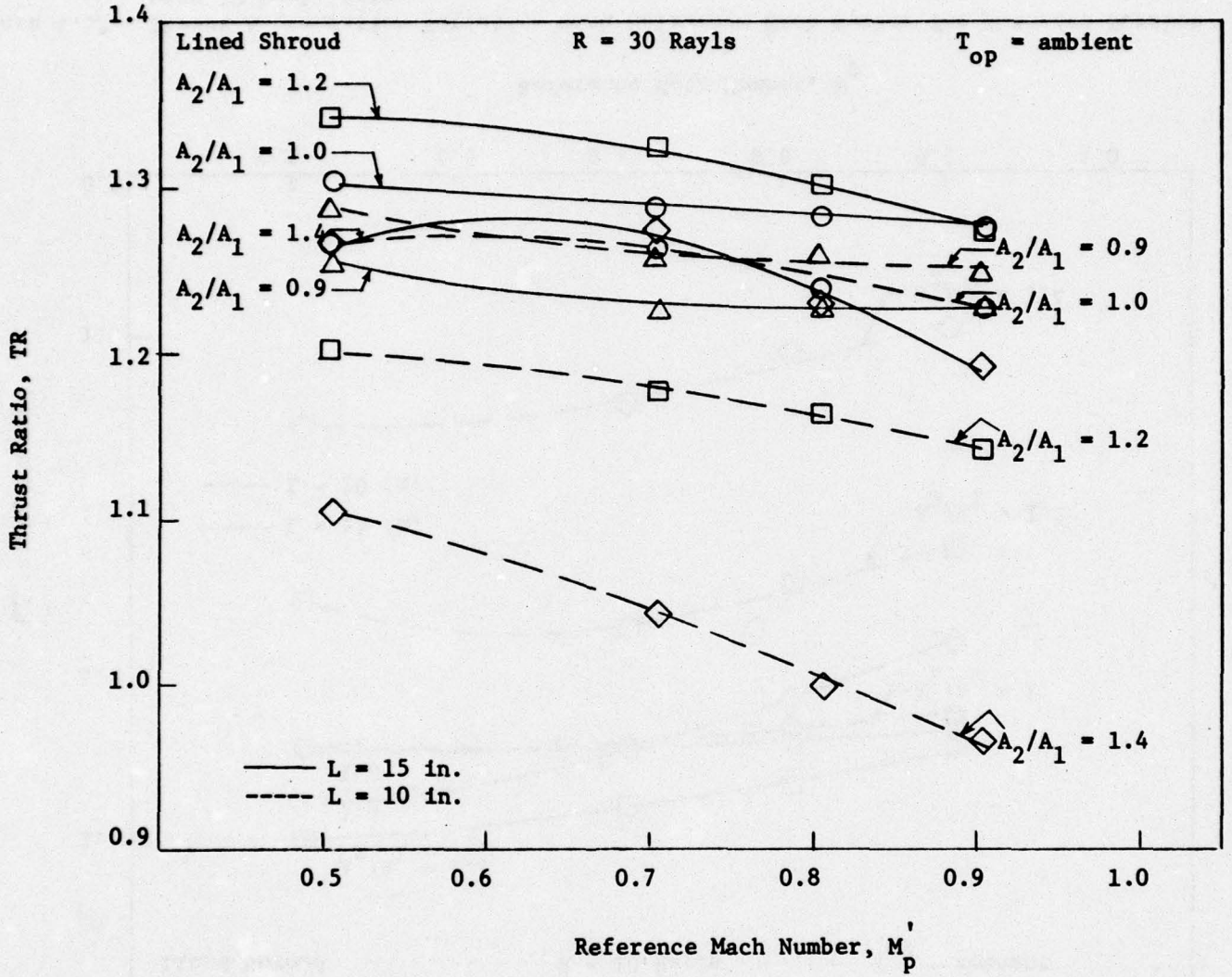

Figure 4.31. Thrust Augmentation Variation with Reference Mach Number for Shrouded Nozzles with 30 Rayl Liners.

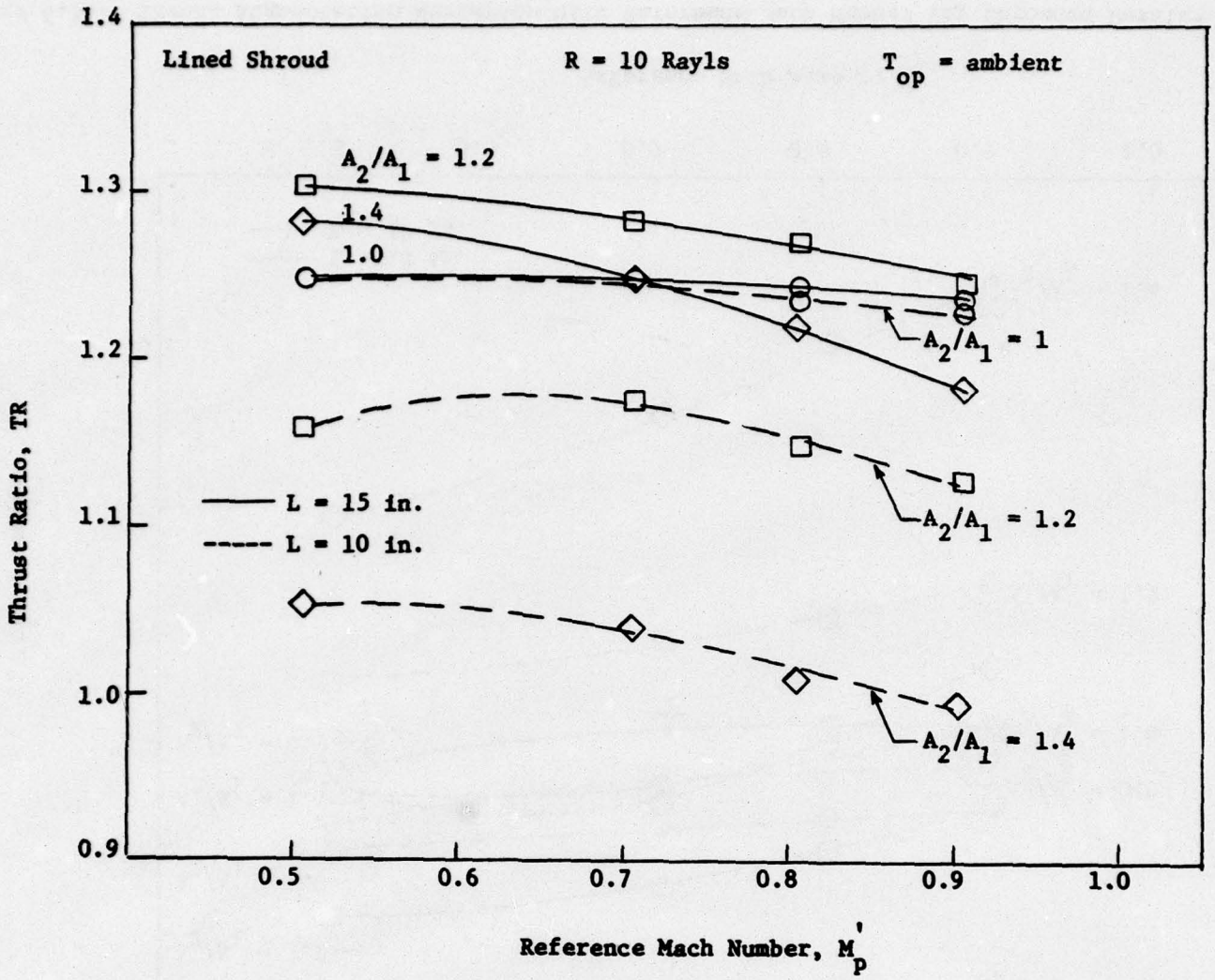

Figure 4.32. Thrust Augmentation Variation with Reference Mach Number for Shrouded Nozzles with 10 Rayl Liners.

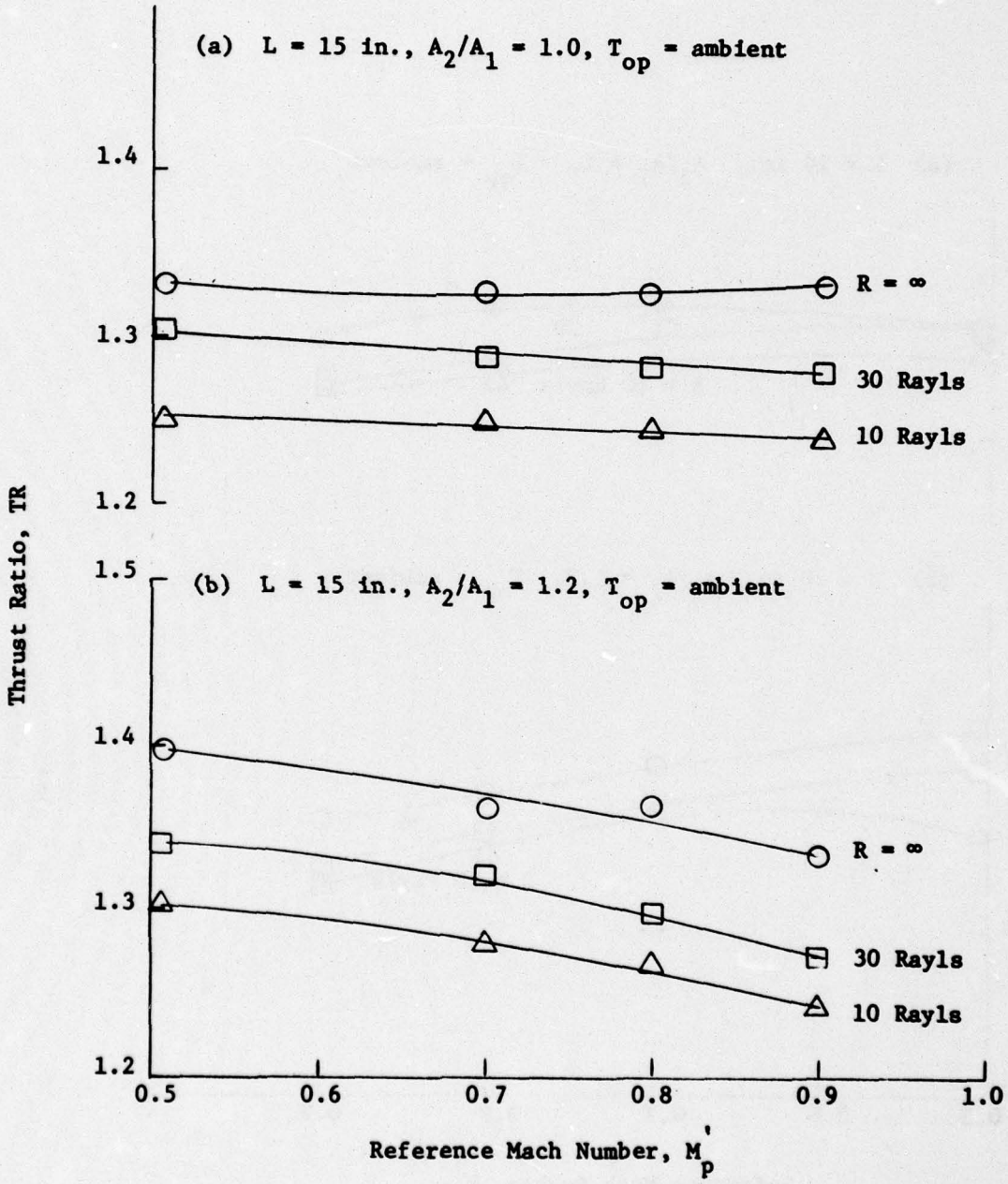

Figure 4.33. Effect of Shroud Wall Resistance on the Thrust Augmentation of 15 Inch Shrouded Nozzle.

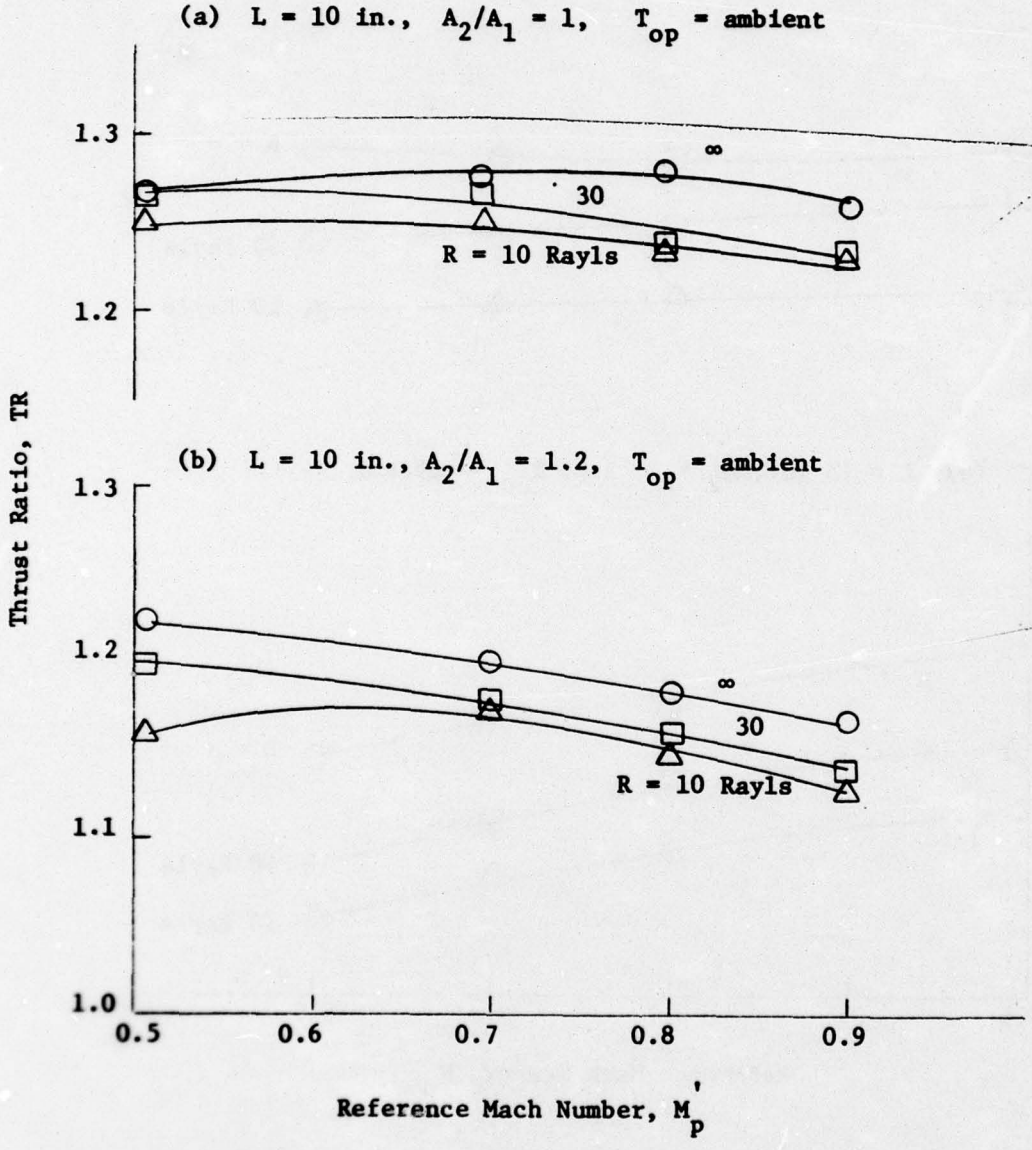

Figure 4.34. Effect of Shroud Wall Resistance on the Thrust Augmentation of 10 Inch Shrouded Nozzles.

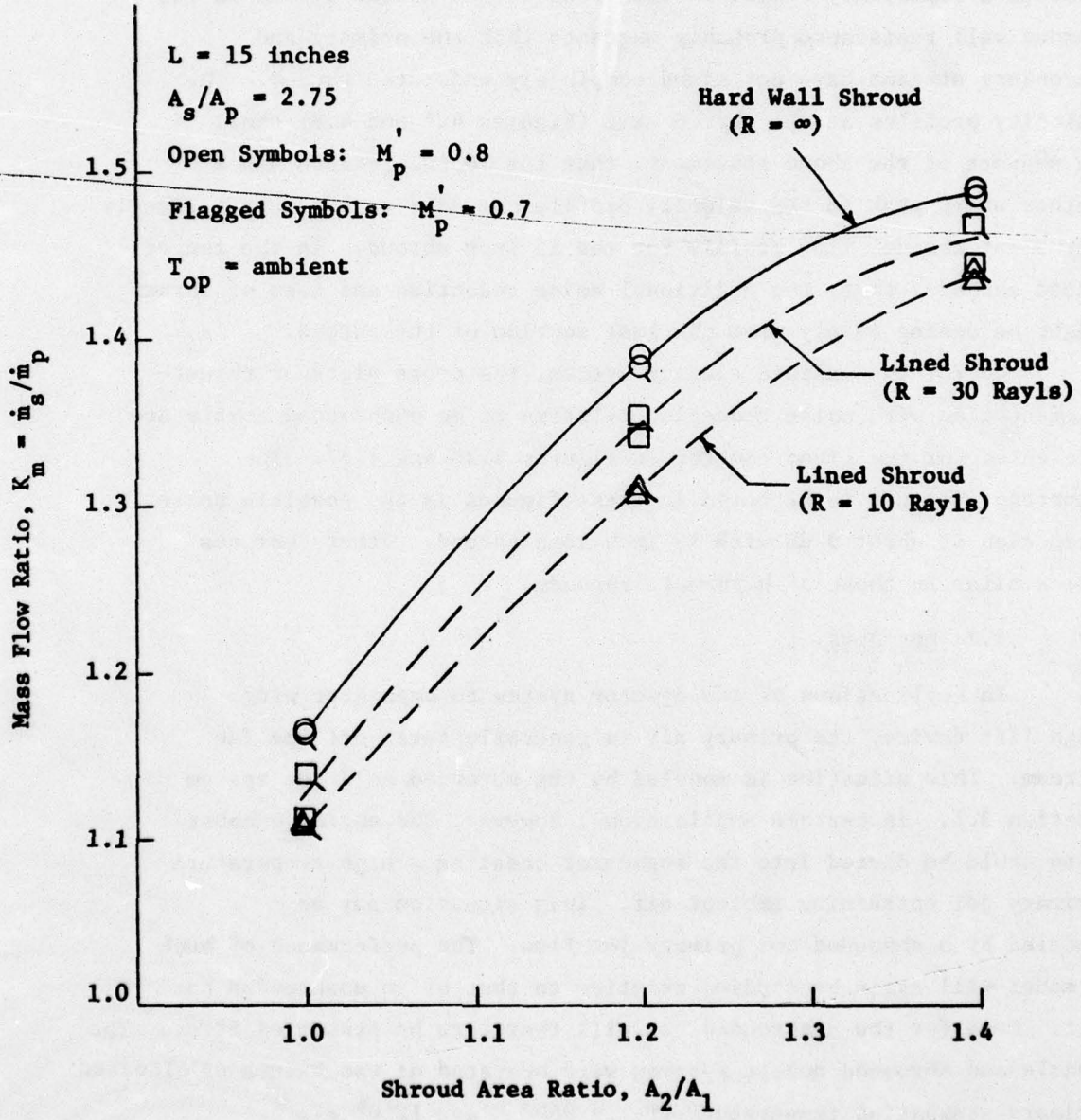

Figure 4.35. Effect of Shroud Wall Resistance on the Mass Induction Capability of 15 Inch Shrouded Nozzles.

induction capability of the shroud. However, the ten percent reduction in thrust augmentation with the present lined ejector system as compared to the 25 percent reduction for the lined ejector system of Ref. 1 is indicative of improved liner construction.

The weak dependence of the thrust augmentation and noise reduction capability of the 10 inch long shroud-nozzle system on the shroud wall resistance probably suggests that the primary and secondary streams have not mixed completely under the shroud. The velocity profiles at the shroud exit (Figures 4.7 and 4.8) show, in support of the above statement, that the 10 inch shroud has a rather sharp peak in the velocity profile compared to the more typically turbulent channel flow profile for the 15 inch shroud. In the longer lined shrouds, thus, the additional noise reduction and loss of thrust might be coming mainly from the last section of the shroud.

As for the unlined ejector system, the cross plots of thrust augmentation with noise reduction relative to an unshrouded nozzle are presented for the lined ejector in Figures 4.36 and 4.37. The important feature to be noted in these figures is the possible noise reduction of about 9 dB with 15 inch long shroud. Other features are similar to those of hard-wall shrouds.

4.2 Hot Jets.

In applications of the ejector system to augmentor wing high lift device, the primary air is generally taken off the fan stream. This situation is modeled by the shrouded cold jet system of Section 3.1. In certain applications, however, the engine exhaust also could be ducted into the augmentor creating a high temperature primary jet entraining ambient air. This situation may be modeled by a shrouded hot primary jet flow. The performance of such a model will again be studied relative to that of an unshrouded hot jet. Data for the unshrouded jet will therefore be presented first. The nozzle and shrouded nozzle systems were operated at two values of elevated primary stagnation temperature (T_{op} = 960° R and 1210° R).

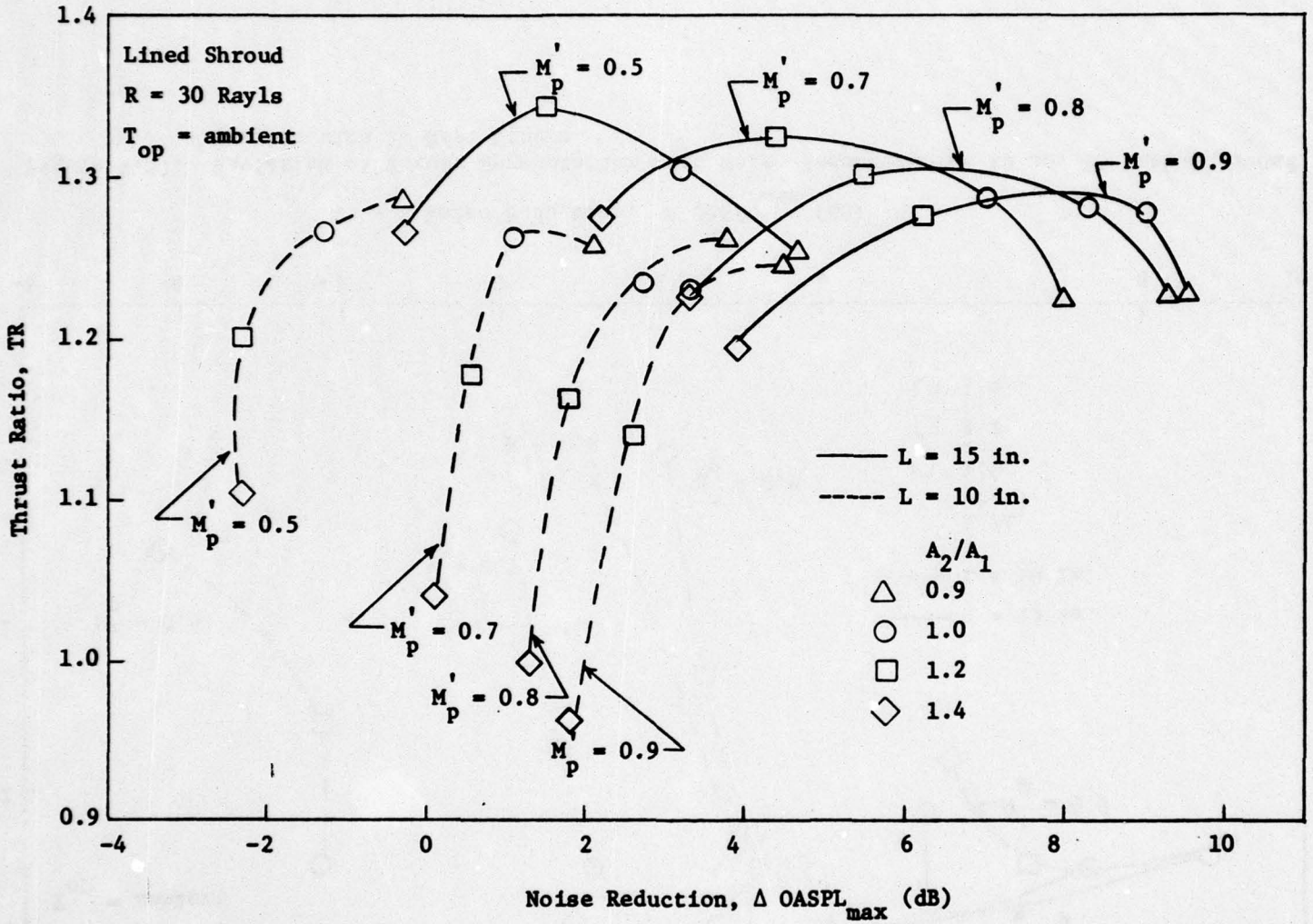

Figure 4.36. Variation of Thrust Augmentation with Noise Reduction for 10 and 15 Inch Shrouded Nozzles with 30 Rayl Liners.

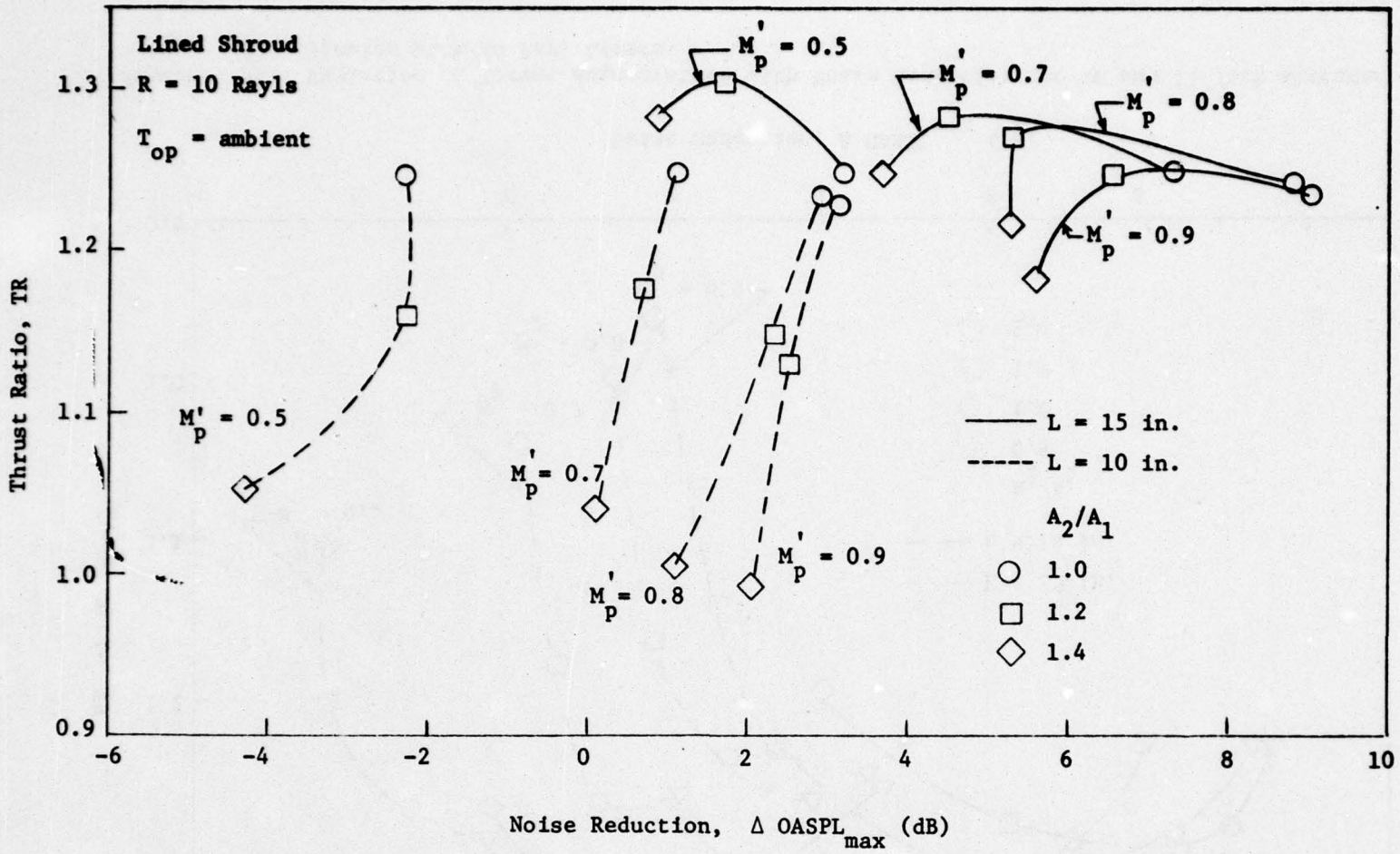

Figure 4.37. Variation of Thrust Augmentation with Noise Reduction for 10 and 15 Inch Shrouded Nozzles with 10 Rayl Liners.

4.2.1 Unshrouded Jets.

Figure 4.38 represents the OASPL directivities in the XZ plane of the unshrouded nozzle exhausting at a Mach number of 0.9 but at different jet temperatures. Among the features to be noted in the figure is the higher noise levels at higher temperature, mainly due to the higher flow velocities for a given Mach number. The higher velocities also cause increased convective amplification. The difference in the maximum OASPL in the plane and the OASPL at $\theta = 90°$ is seen to increase from 9 dB for the cold jet to 12.5 dB at 960° R and 13.5 dB at 1210° R. The directivity of the cold jet peaks at 35° from the jet axis but the peak is around 50° for the hot jets. This may be explained by the increased refraction through the hot jets. The convective-refractive effects cause the maximum noise level in the plane to increase by 12.5 dB as compared to the 8 dB increase in the $\theta = 90°$ direction when the jet temperature is increased from ambient to 1210° R.

The spectral data for the hot jet are shown in Figure 4.39. The major contribution in the direction of the polar peak (near 50°) is due to high frequencies (around 8 kHz). For the cold jet case where the sound level peaks at 35°, the major contribution in the peak direction was seen (Figure 4.2) to be due to components around 3.15 kHz. The peak frequencies in the 30° and 60° directions for the hot jet remain constant at 8 kHz instead of increasing with velocity as would be expected for Strouhal scaling. This was also noted with the cold jet where the peak frequencies were 8 kHz in the 90° and 60° directions and 3.15 kHz in the 30° direction.

Comparison of the spectral data of hot and cold jets (Figures 4.40) shows a uniform increase in sound level over the entire spectrum for the hot jet in the 30° direction. The OASPL directivities in YZ plane for hot and cold jets (Figure 4.41) and the spectral comparison of recordings at $\phi = 0°$ and 90° (Figure 4.42) indicate the shielding of high frequency sound by the jet.

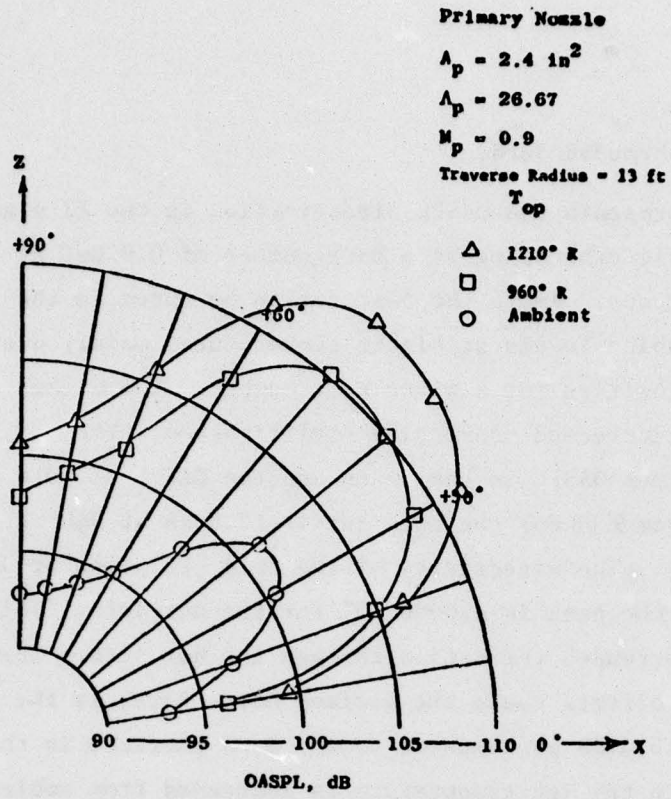

Figure 4.38. OASPL Directivities of the Primary Nozzle in the XZ Plane for Three Stagnation Temperatures (T_{op}).

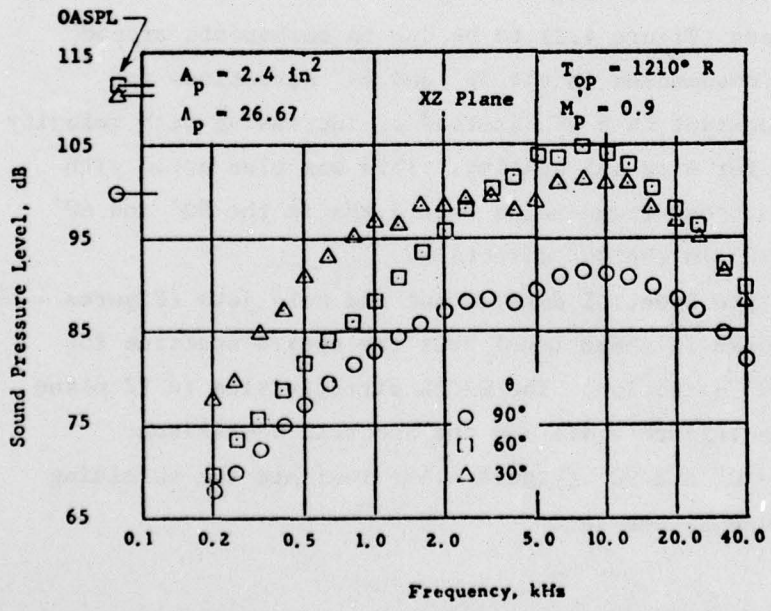

Figure 4.39. Sound Pressure Spectra of the Hot Primary Jet at Three Locations in XZ Plane.

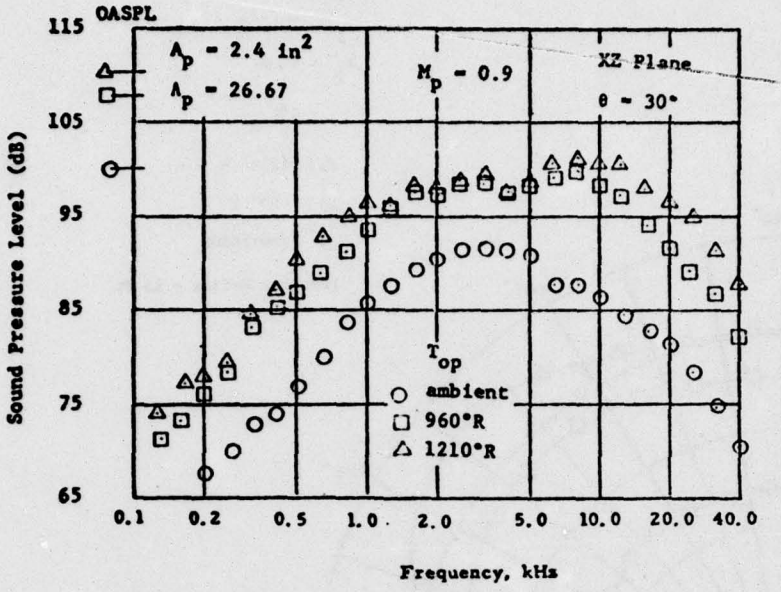

Figure 4.40a. Sound Pressure Spectra for Hot and Cold Primary Jet.

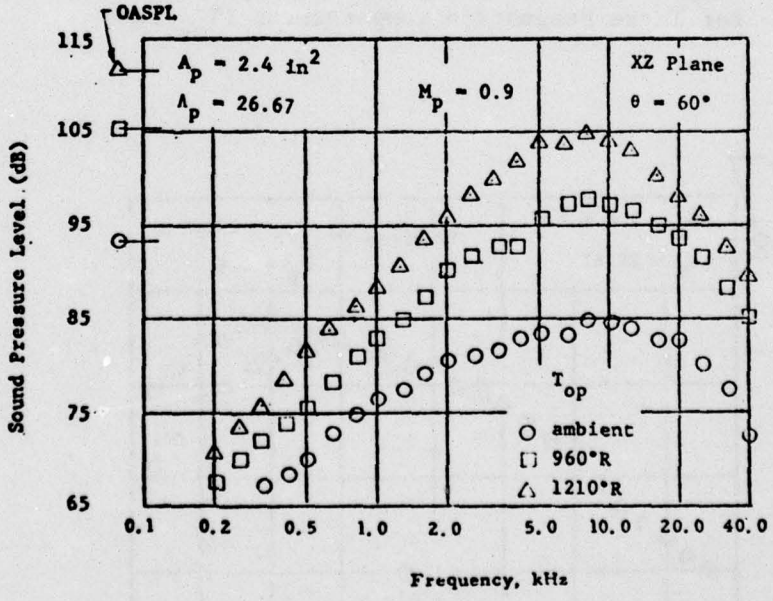

Figure 4.40b. Sound Pressure Spectra for Hot and Cold Primary Jets.

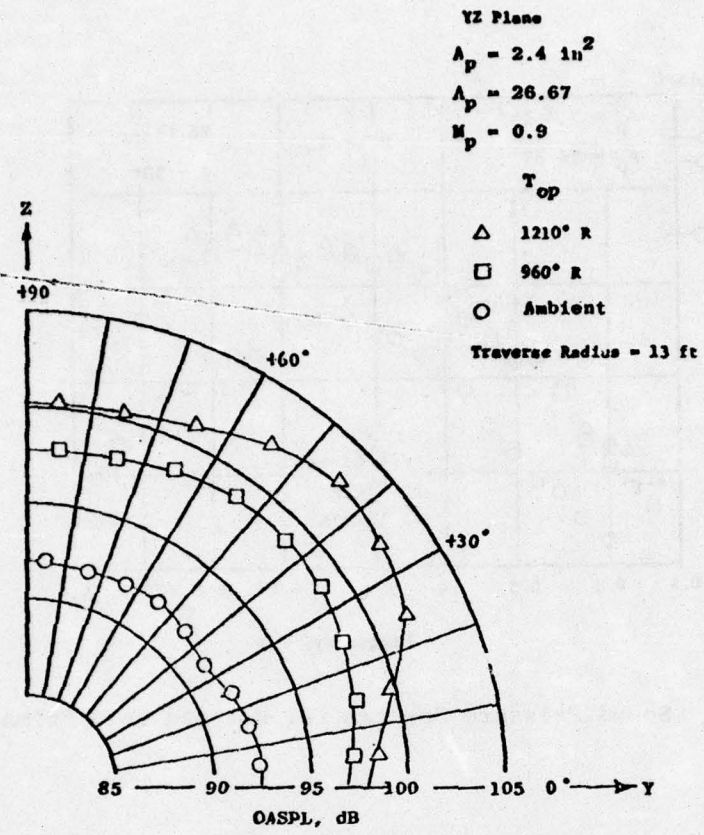

Figure 4.41. OASPL Directivities of the Primary Nozzle in YZ Plane for Three Stagnation Temperatures (T_{op}).

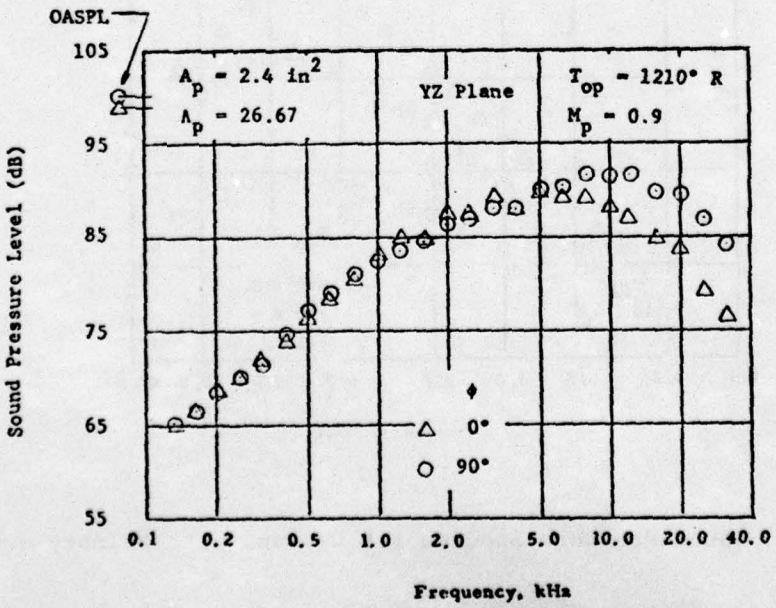

Figure 4.42. Sound Pressure Spectra for the Hot Primary Jet at the Flyover and Sideline Positions in the Exit Plane.

4.2.2 Shrouded Jets with Hard Walls.

The directivities in the flyover plane of hard wall shrouded nozzles are shown in Figures 4.43 and 4.44 for hot and cold jets. In all cases the secondary flow is the entrained flow from the ambient. Among the features to be noted are the increased sound levels at higher jet temperature and change in the direction of maximum noise radiation. For the 10 inch shrouded nozzle the increases in $OASPL_{max}$ (8.5 dB at 960° R and 13 dB at 1210° R) and in the sound level in the $\theta = 90°$ direction (6 dB at 960° R and 8.5 dB at 1210° R) with increasing jet temperature are of the same order as those for the unshrouded nozzle ($OASPL_{max}$: 8.8 dB at 960° R and 12.5 dB at 1210° R, OASPL at $\theta = 90°$: 5 dB at 960° R and 8 dB at 1210° R). For the 15 inch shrouded nozzle the increases in OASPL in the $\theta = 90°$ direction are also of the same order but the increases in $OASPL_{max}$ (11.5 dB at 960° R and 16.5 dB at 1210° R) are greater than those for the 10 inch shroud or the unshrouded nozzle. This causes the maximum OASPL of the 15 inch shrouded hot jet to be almost equal to the $OASPL_{max}$ of the 10 inch shrouded hot jet as shown in Figure 4.45.

Examination of the fluid dynamic data showed that the two shrouded jets have nearly equal flow entrainment. With identical mass flows and areas for two shrouded jets, the longer shroud would produce better mixing of the primary and secondary flows so that the jet exhausting out of the shroud would have a more uniform velocity profile and lower thermal gradients than the 10 inch shroud. Powell (Ref. 17) has shown that a square velocity profile produces less noise than a pipe-flow profile (for a given thrust and jet diameter). Thus the jet exiting from the longer shroud can be expected to be less noisy than the 10 inch shroud.

Note in Figure 4.45 that except near the direction of peak radiation the 15 inch shrouded hot jet is quieter than the 10 inch shrouded hot jet by 3 dB. (Recall that for shrouded cold jets the effect of increased shroud length was to reduce the sound level throughout the plane by more than 3 dB.) The directivity of the 15 inch long shroud thus has a well defined peak, occurring

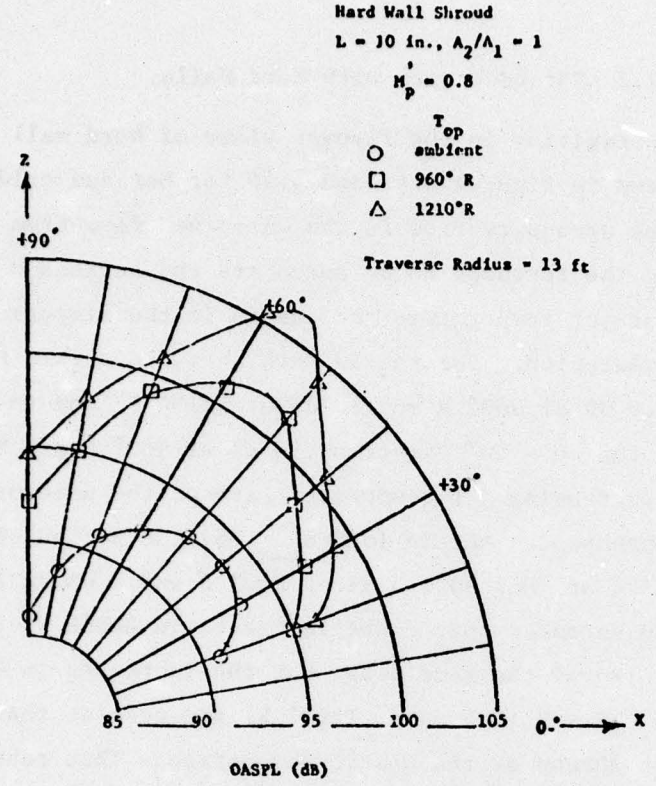

Figure 4.43. OASPL Directivities in the Flyover Plane of 10 Inch Shrouded Nozzles with Hot and Cold Primary Jets.

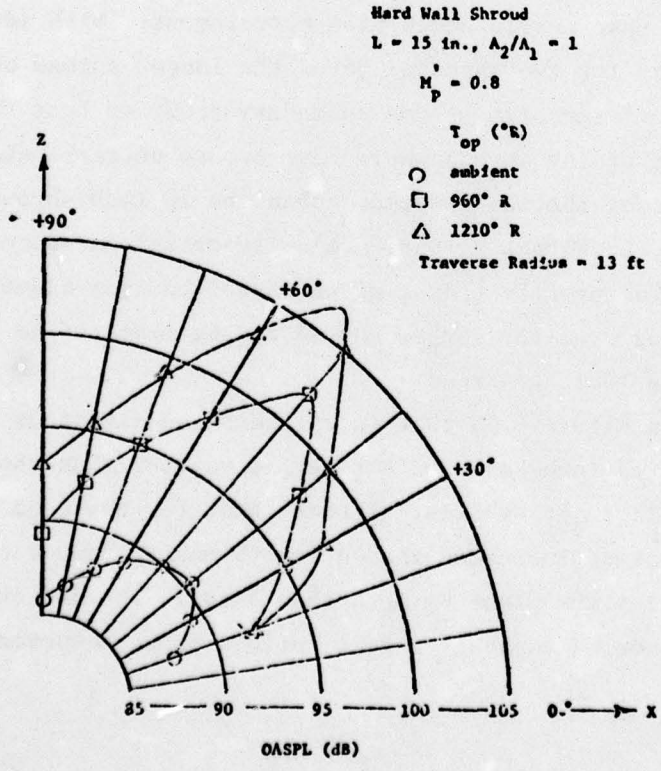

Figure 4.44. OASPL Directivities in Flyover Plane of 15 Inch Shrouded Nozzles with Hot and Cold Primary Jets.

in a direction near $\theta = 50°$ but at a slightly smaller angle than the peak radiation direction of the 10 inch shroud. The shrouded cold jets for both shroud lengths were seen to have peak radiation near $\theta = 40°$ direction. The change in the direction of peak radiation due to increase in jet temperature is somewhat smaller for the shrouded jets than for the unshrouded jets. In the case of shrouded jets the cold air induced into the shroud from the ambient atmosphere after mixing with the hot primary jet reduces the mean temperature of the jet issuing out of the shroud. This might be the reason for the lower change in the peak radiation direction.

Comparing the directivities of the shrouded hot jets with that of the unshrouded hot jet we find (Figure 4.45) considerable reduction in sound level in directions $\theta < 60°$. This is seen in Figure 4.46 to be primarily due to the reduction in mid and high frequency components. Such a behavior was observed for the shrouded cold jets also (Figure 4.11), the reductions were however smaller than for the hot jets. The $OASPL_{max}$ versus M_p' plot of Figure 4.47 indicates that a 5 dB reduction in the maximum noise level can be achieved with a 10 inch shrouded nozzle at 960° R and $M_p' = 0.9$. (Only 3.8 dB reduction was obtained with the shrouded cold jet). Though no additional reduction in $OASPL_{max}$ is obtained by increasing the shroud length, the sound levels in other directions have been seen to decrease by as much as 3 dB.

In order to determine the effect of jet temperature on the acoustic output of a jet we need to have acoustic data on the jet exhausting at different temperatures but at a fixed exit velocity. Fluid dynamic calculations for the shrouded nozzles revealed that for the two operating conditions of $T_{op} = 960°$ R, $M_p' = 0.8$ and $T_{op} = 1210°$ R, $M_p' = 0.7$ the primary jet velocities (V_p) are very nearly the same. This is also true for the unshrouded nozzle. The maximum difference in the velocities in these two conditions is about 1.7% of the lower velocity so that the contribution to the difference in sound levels due to this difference in velocity would be less than 0.5 dB. These two operating conditions thus provide

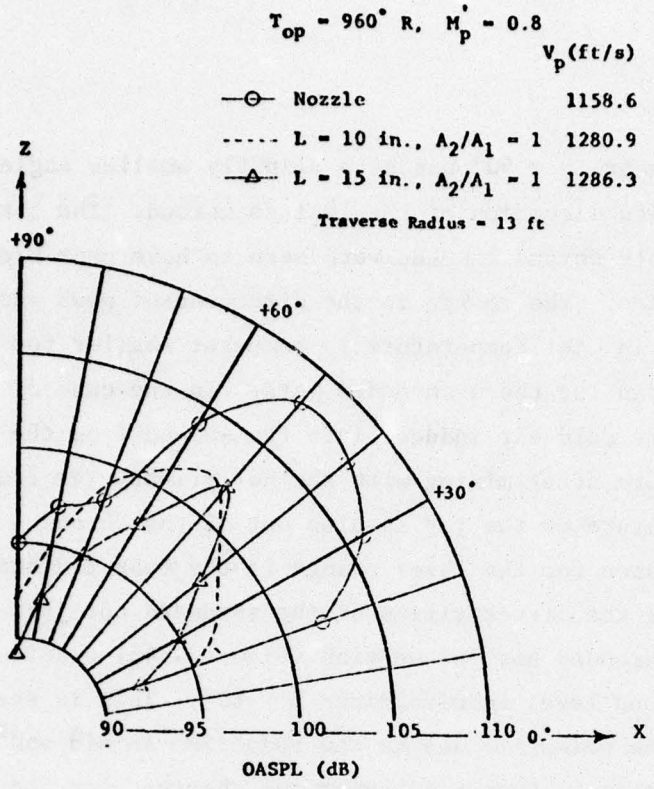

Figure 4.45. OASPL Directivities in Flyover Plane for the Unshrouded Hot Jet and 10 and 15 Inch Shrouded Hot Jets, (Hard Walls).

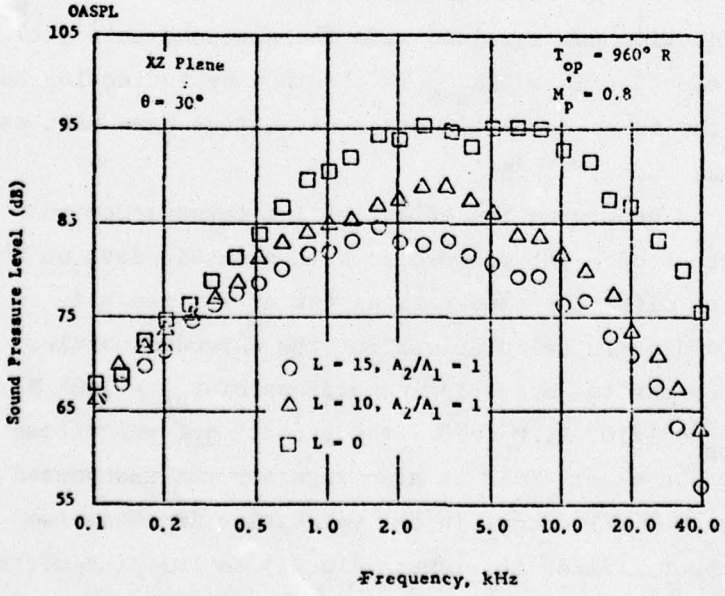

Figure 4.46. Sound Pressure Spectra for Unshrouded Hot Jet and 10 and 15 Inch Shrouded Hot Jets, (Hard Walls).

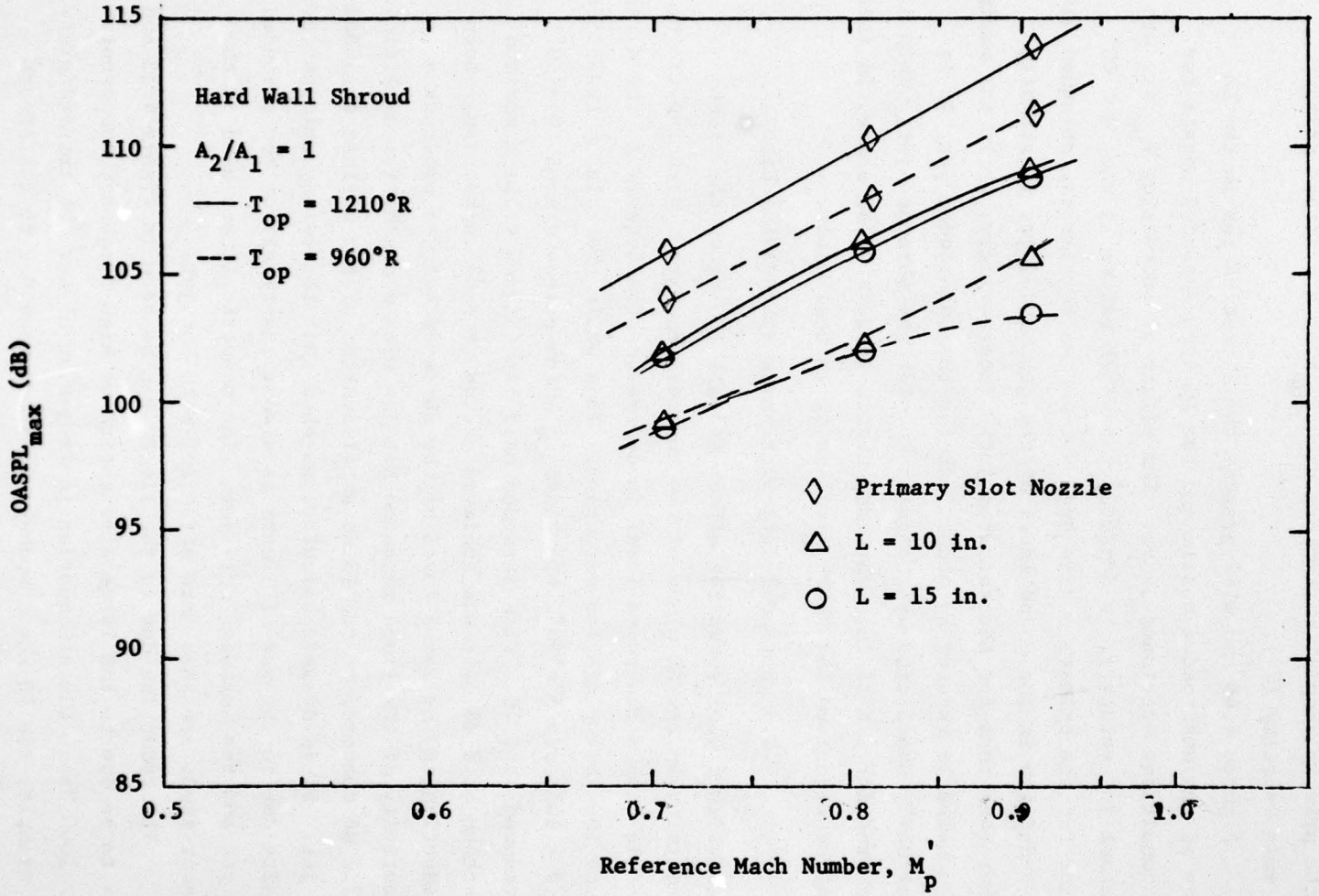

Figure 4.47. Variation of Maximum Sound Level with Reference Mach Number for Shrouded Hot Jets. (Hard Walls).

AD-A041 782 TENNESSEE UNIV SPACE INST TULLAHOMA F/G 21/5
INVESTIGATION OF FEASIBLE NOZZLE CONFIGURATIONS FOR NOISE REDUC--ETC(U)
MAR 77 B H GOETHERT, J R MAUS, W A DUNNILL DOT-FA72WA-3053
UNCLASSIFIED FAA-RD-75-162-3 NL

2 OF 2
ADA
041782

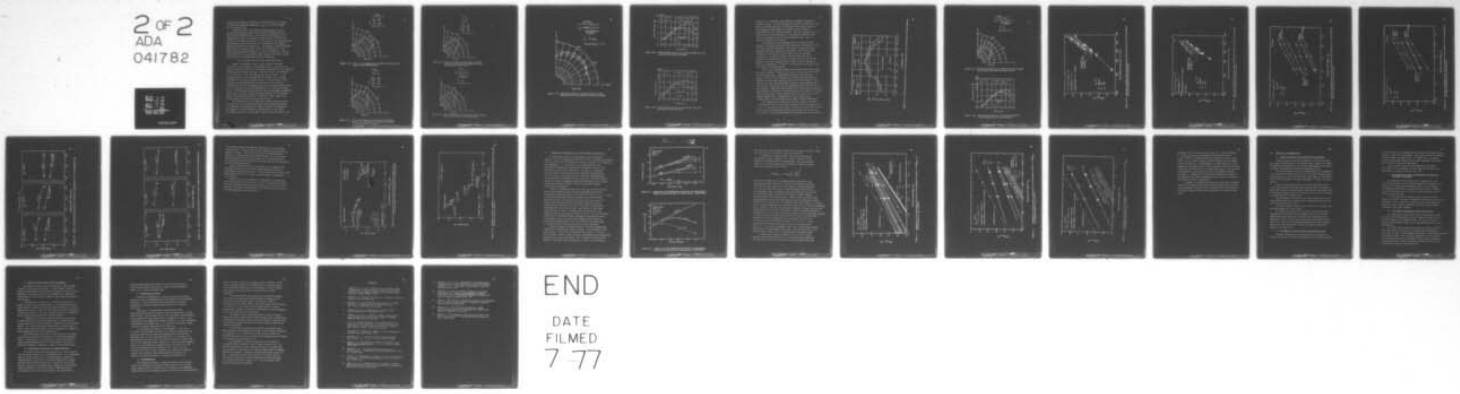

END

DATE
FILMED
7-77

a basis for examining the effect on the noise level due to a change in the primary stagnation temperature (T_{op}) at a constant primary jet exit velocity (V_p).

Figures 4.48 and 4.49 present the directivities in the XZ plane of the unshrouded nozzle and the 10 inch shrouded nozzle for the conditions mentioned above. The effect of increasing T_{op} is, at constant jet velocity, to decrease the OASPL values in the $\theta < 60°$ sector for the primary nozzle and $\theta < 50°$ sector for the shrouded nozzle. The reduction in the sound level of the unshrouded jet is slightly higher than that for the shrouded jet. Interestingly, while the maximum OASPL value is reduced by about 2 dB for the unshrouded jet, it is practically unaffected by change in T_{op} for the shrouded jet. This is also true for the 15 inch shrouded nozzle (Figure 4.50) where, in fact, even the effect on the OASPL directivity is negligible.

4.2.3 Shrouded Jets with Noise Attenuating Liners.

Figure 4.51 shows the effect of wall lining on the OASPL directivity in the XZ plane of the shrouded hot jet. With the use of acoustic liners the sound level is decreased considerably in the directions around the peak radiation direction. Thus while there is no reduction at $\theta = 90°$ and $\theta = 30°$, the $OASPL_{max}$ which occurs around $\theta = 50°$ is reduced by 6 dB. With shrouded cold jet (Figure 4.52) a maximum reduction of 2 dB only was achieved around $\theta = 60°$ direction. Such a reduction in the sound level of the shrouded hot jet produces a directivity of the lined shrouded hot jet with a convective amplification of 7.2 dB compared to the 13 dB amplification of the unlined shrouded hot jet. Fluid dynamic calculations show that the aerodynamic performance penalty due to the use of liners is almost identical for the shrouded hot jet and the shrouded cold jet. The acoustic liners used in the present study are thus more efficient with hot jet.

The reduction due to the liners can be seen in Figure 4.53 and 4.54 to be due to the large attenuation of high frequency components ($f > 2000$ Hz). The attenuation is larger at higher jet temperatures. For example, the 10 kHz component is attenuated due to the liners by 14 dB at 1210° R, by 11 dB at 960° R and 3 dB only for the cold jet

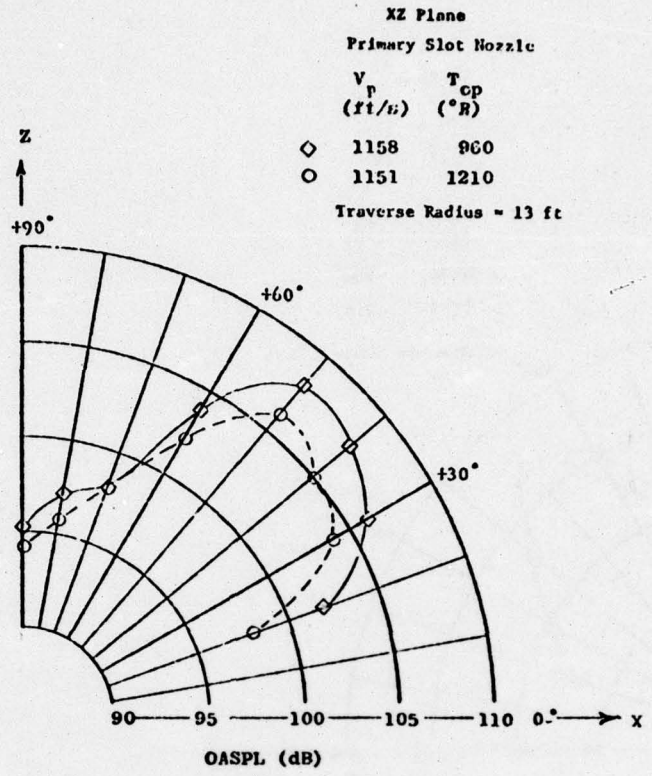

Figure 4.48. Effect of Jet Temperature on OASPL Directivity in XZ Plane for the Primary Nozzle.

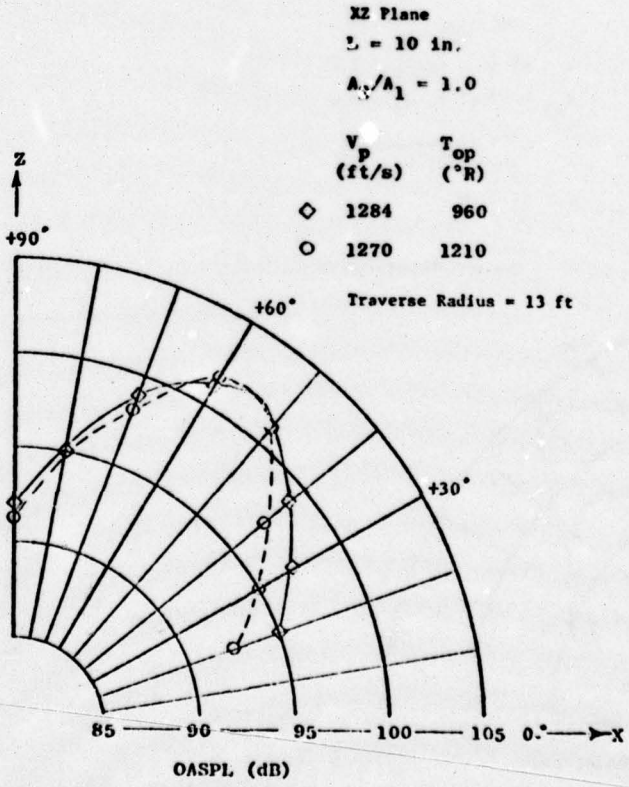

Figure 4.49. Effect of Primary Jet Temperature on the OASPL Directivity in XZ Plane for Augmentor Wing With 10 Inch Long Hard Wall Shroud.

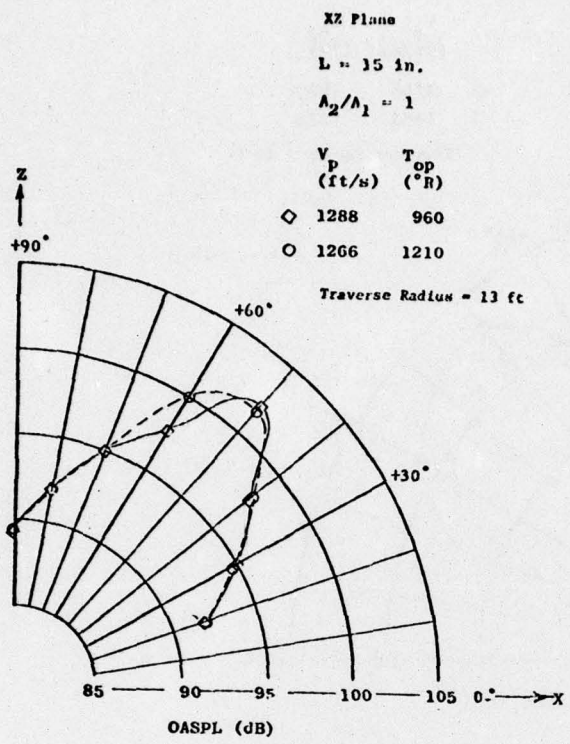

Figure 4.50. Effect of Primary Jet Temperature on the OASPL Directivity in XZ Plane for Augmentor Wing with 15 Inch Long Hard Wall Shroud.

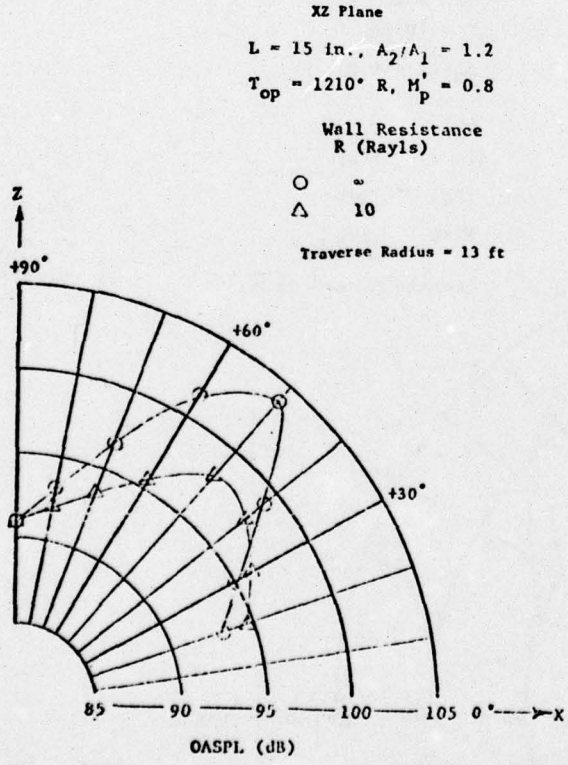

Figure 4.51. OASPL Directivities in XZ Plane of 15 Inch Shrouded Hot Jets with Hard Wall and Lined Shrouds.

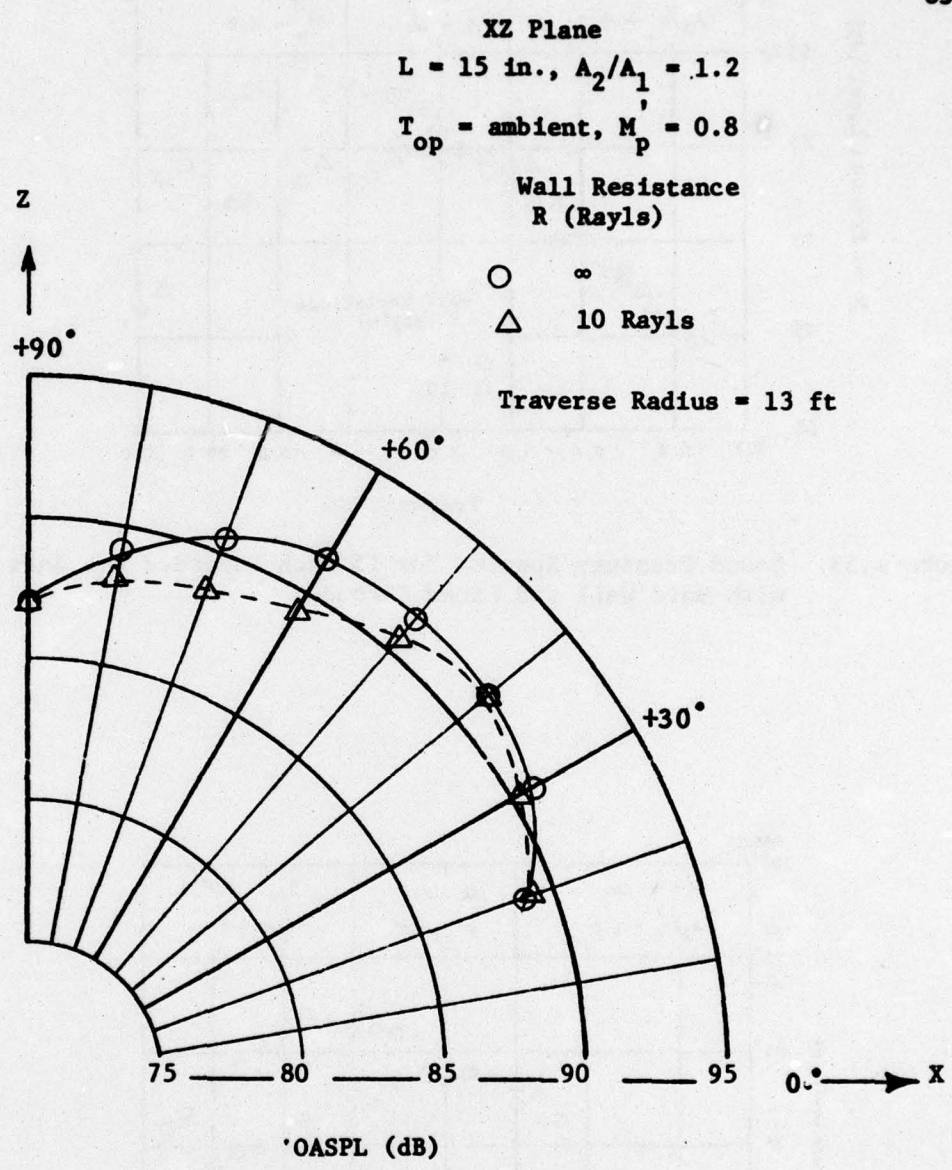

Figure 4.52. OASPL Directivities in Flyover Plane for 15 Inch Shrouded Cold Jets with Hard Wall and Lined Shrouds.

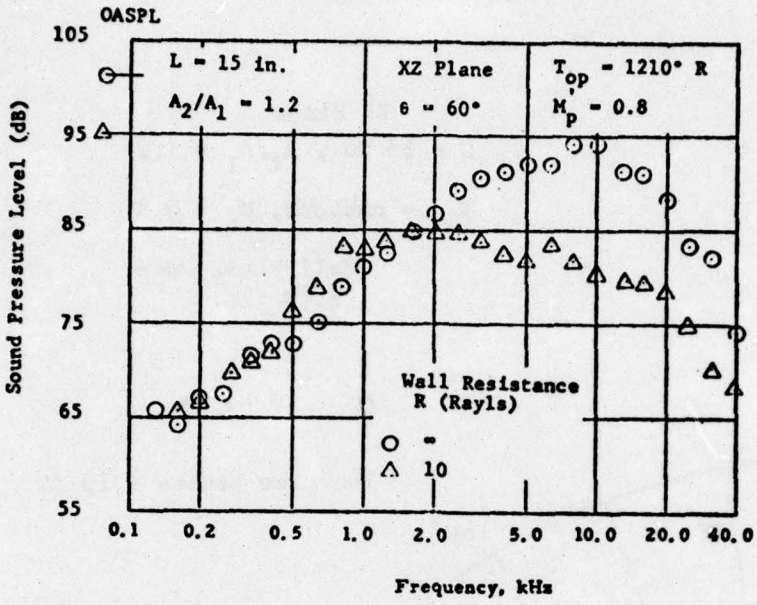

Figure 4.53. Sound Pressure Spectra for 15 Inch Shrouded Hot Jets with Hard Wall and Lined Shrouds.

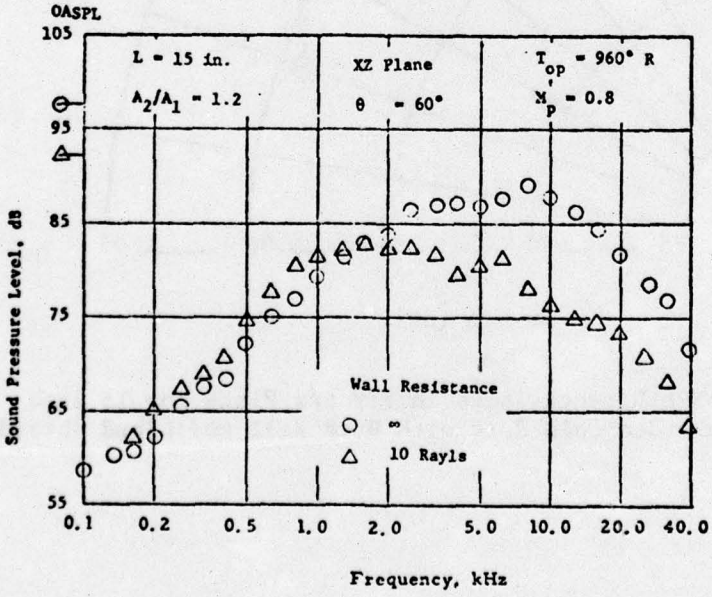

Figure 4.54. Sound Pressure Spectra for Shrouded Hot Jets with Hard Wall and Lined Shrouds.

(Figure 4.55). Components below 2000 Hz are slightly increased by the use of liners. For the lined shroud the major contribution in the direction of peak radiation, as indicated by the spectral peaks, is from components around 1600 Hz as compared to the components around 8000 Hz for the hard wall shroud. The noise attenuation due to liners in the 10 inch shrouded jet is, as would be expected, lower than the attenuation in the 15 inch shrouded jet case. This is obvious from Figures 4.56 and 4.57.

By assuming that jets emerging from the unlined and lined shrouds at the same exit velocity (V_2) make equal contributions to the far field sound, the capability of the liners to absorb the sound generated within the shroud can be evaluated. This has been done in Figures 4.58 and 4.59 for the 10 and 15 inch long shrouds respectively. We notice in Figure 4.58 that while very little internal noise absorption due to the liners occurs with the 10 inch shroud for cold jets, absorptions up to about 3 dB are obtained at higher jet temperatures. For the 15 inch shroud such absorption could be as high as 7 dB (Figure 4.59).

Noise level comparisons based on the reference Mach number (M_p') are given in Figures 4.60 and 4.61 for the 15 inch and 10 inch shrouded hot jets respectively. Considerable additional noise reduction (about 7.5 dB for 15 inch shrouds and 3.5 dB for 10 inch shrouds) is achieved by using lined shrouds in place of hard wall shrouds. This results in a total noise attenuation (relative to the unshrouded hot jet) of about 13 dB for the 15 inch shrouds and about 10 dB for the 10 inch shrouds. Though this noise attenuation is considerably greater than that obtained for cold jets, the thrust penalty due to the use of liners is the same for both the cold and hot jets in the case of the 15 inch shrouds (Figure 4.62). Surprisingly for the 10 inch shrouds (Figure 4.63) the thrust penalty is very high at higher temperatures.

Some comments are in order here about the improved performance of the acoustic liners for hot jets as compared to ambient temperature jets. To a large extent this is due to the fact that the higher velocity hot jets are generating more internal noise beneath the shroud than the cold jets. We have already seen for cold flow that, in some cases,

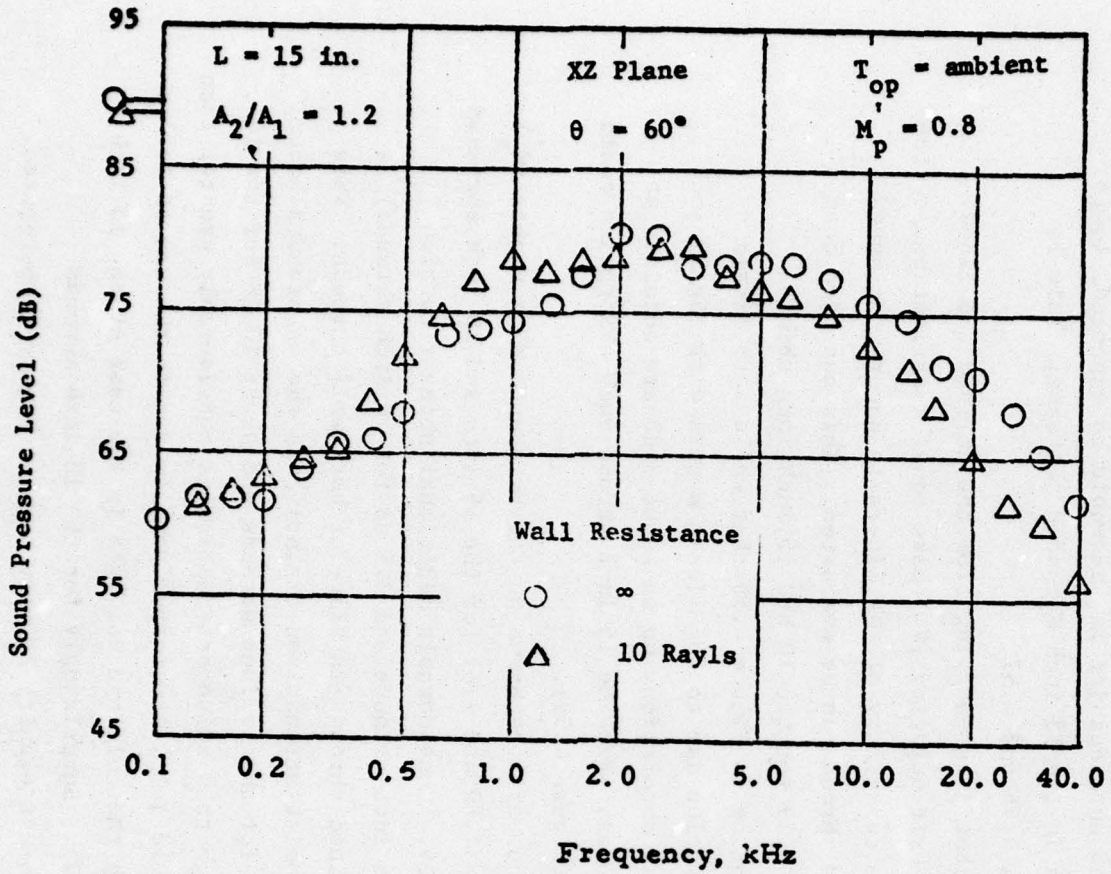

Figure 4.55. Sound Pressure Spectra for 15 Inch Shrouded Cold Jets with Hard Wall and Lined Shrouds.

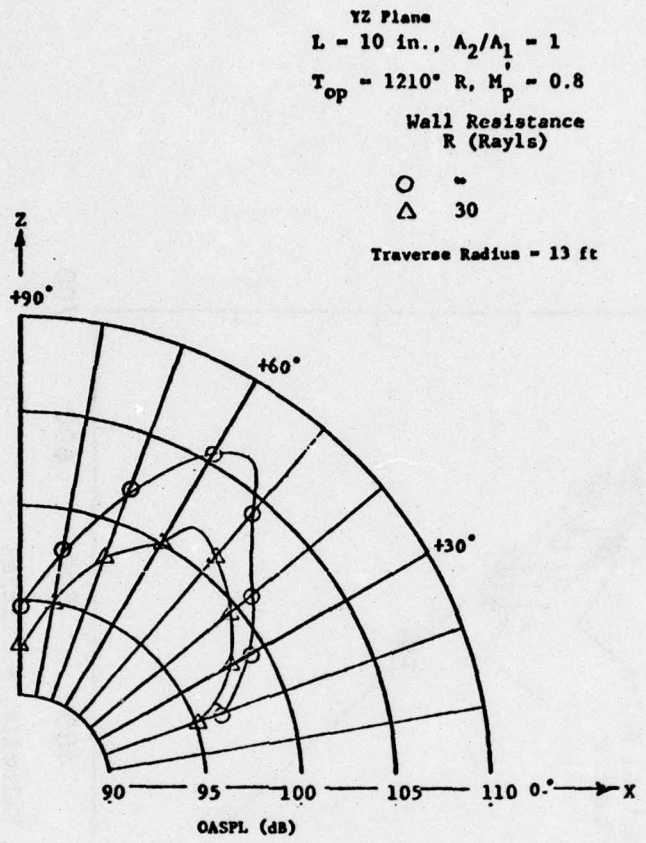

Figure 4.56. OASPL Directivities in XZ Plane of 10 Inch Shrouded Hot Jets with Hard Wall and Lined Shrouds.

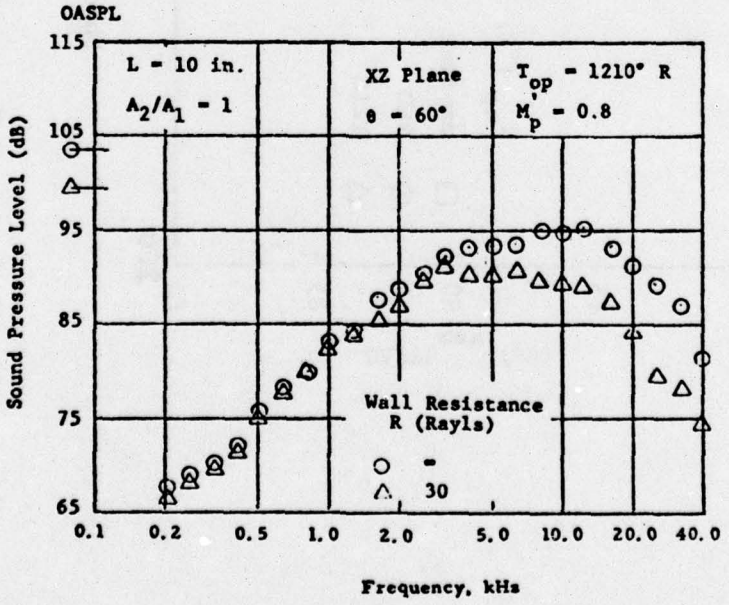

Figure 4.57. Sound Pressure Spectra for 10 Inch Shrouded Hot Jets with Hard Wall and Lined Shrouds.

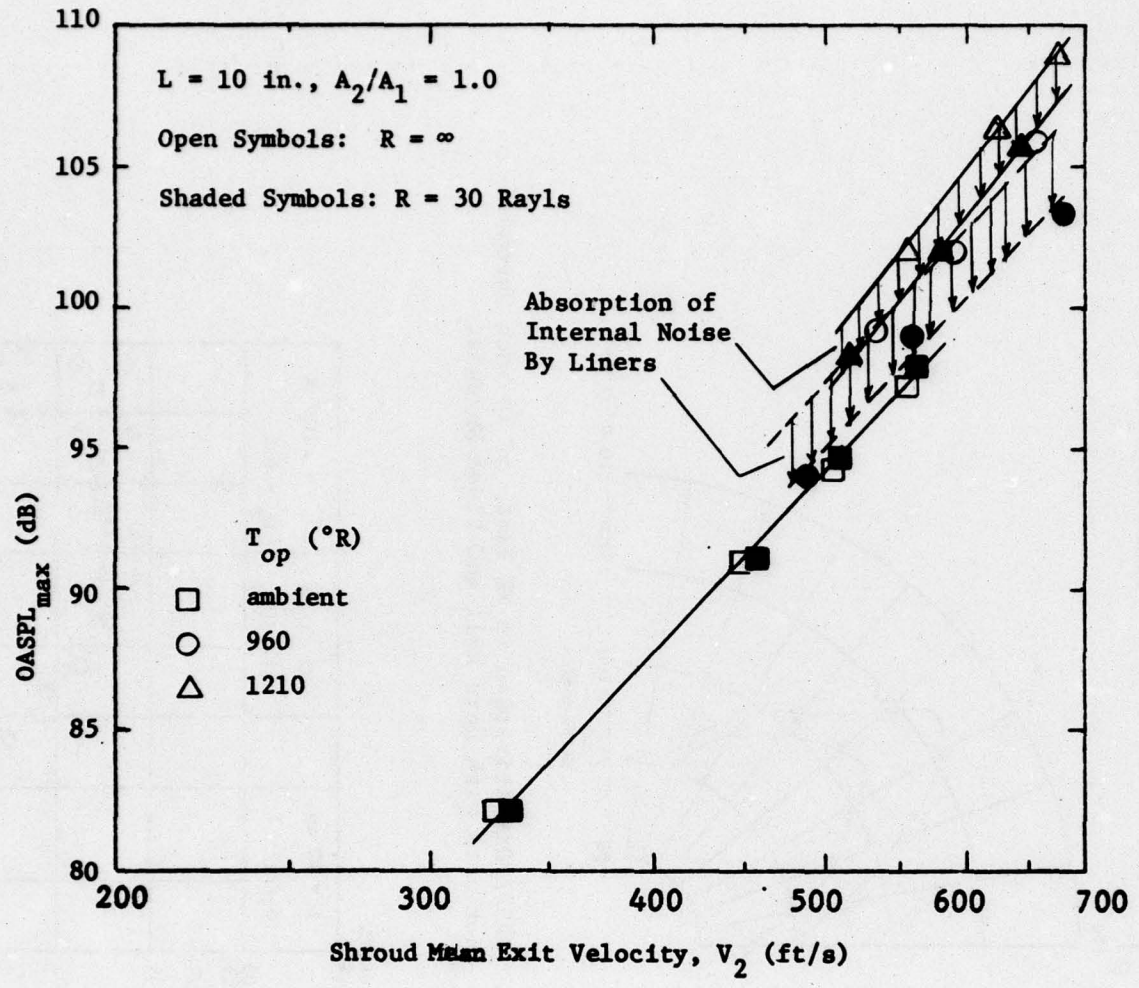

Figure 4.58. Variation of Maximum Sound Level with Shroud Exit Velocity for 10 Inch Shrouded Jets with Hard Wall and Lined Shrouds.

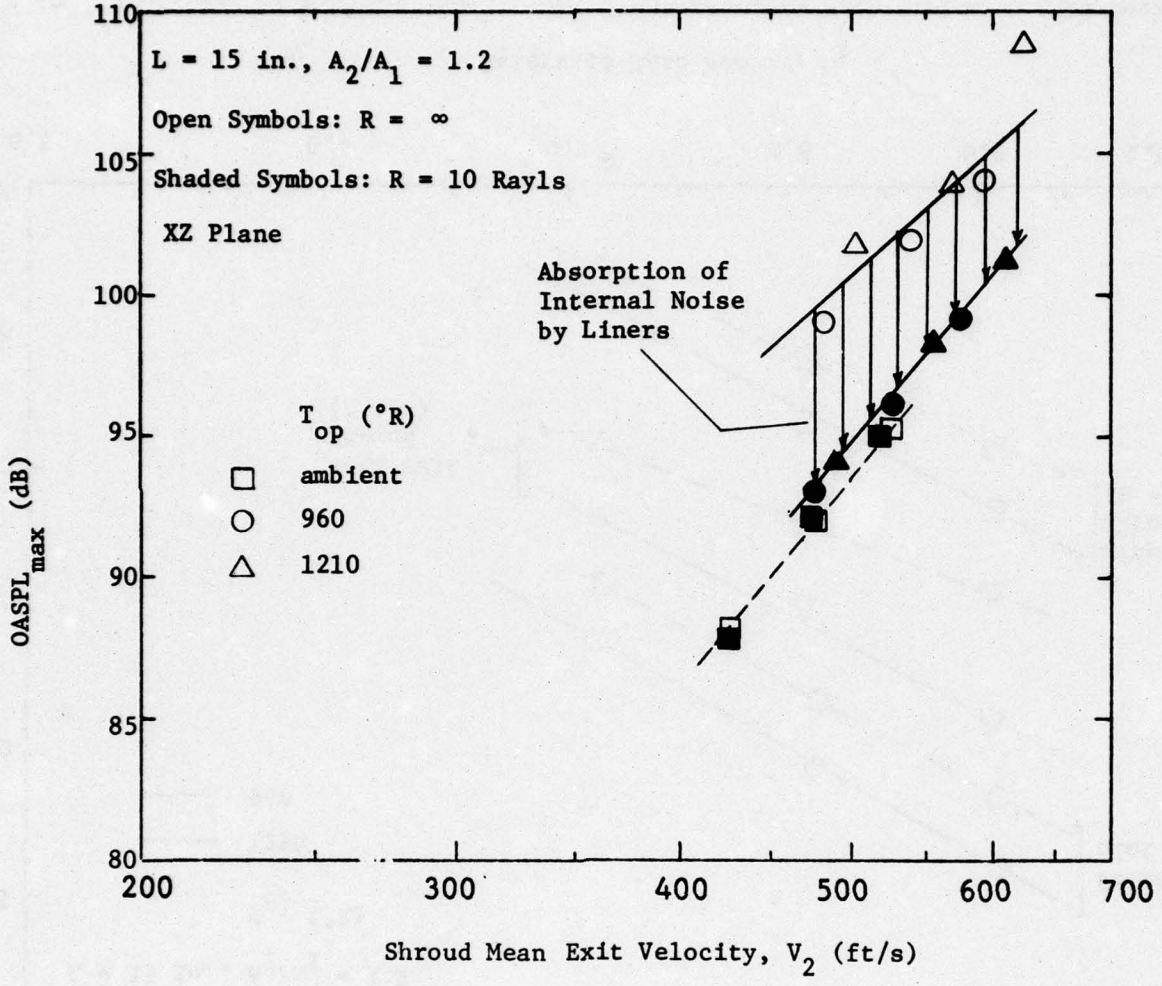

Figure 4.59. Variation of Maximum Sound Level with Shroud Exit Velocity for 15 Inch Shrouded Jets with Hard Wall and Lined Shrouds.

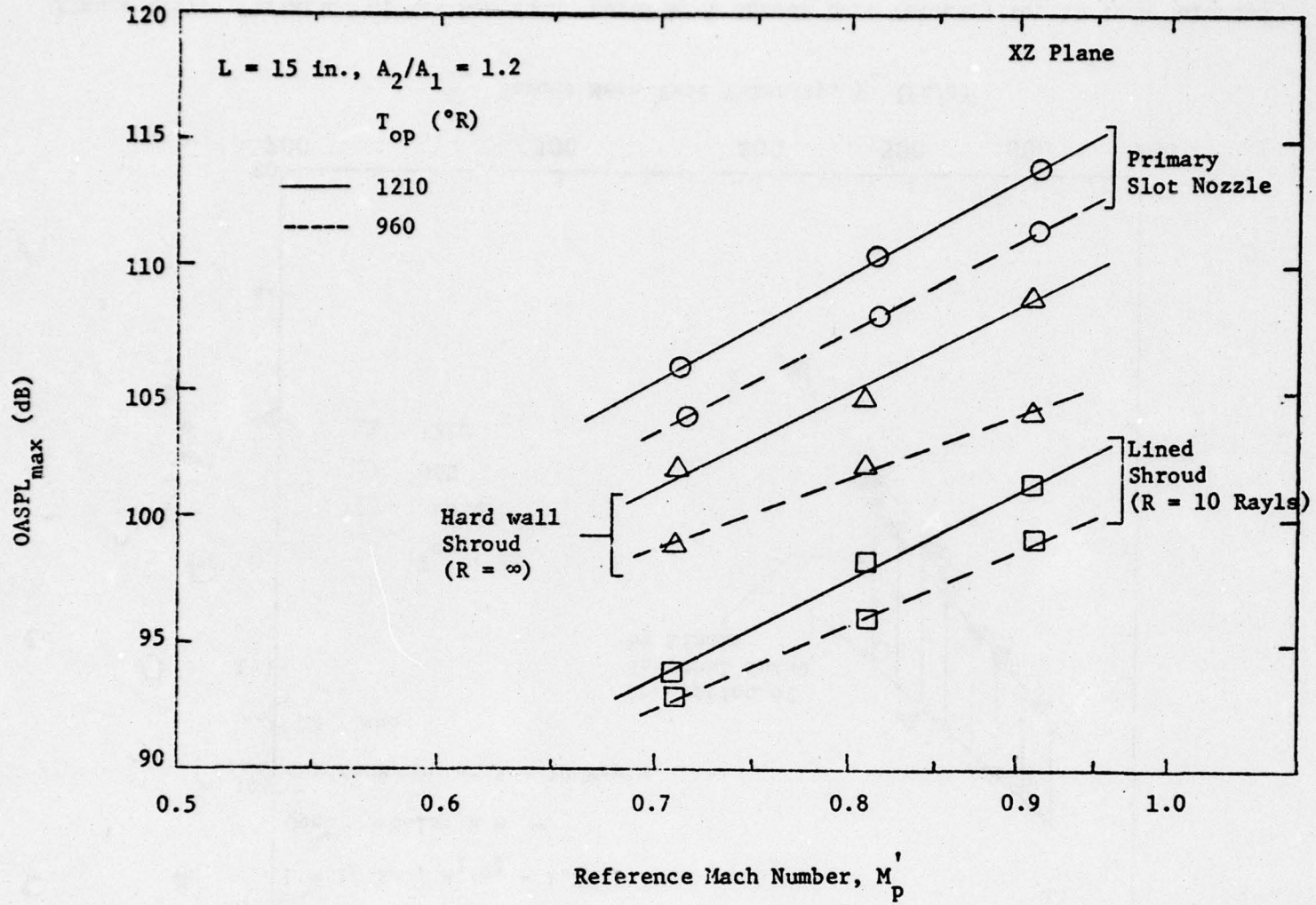

Figure 4.60. Variation of Maximum Sound Level with Reference Mach Number for 15 Inch Shrouded Jets with Hard Wall and Lined Shrouds.

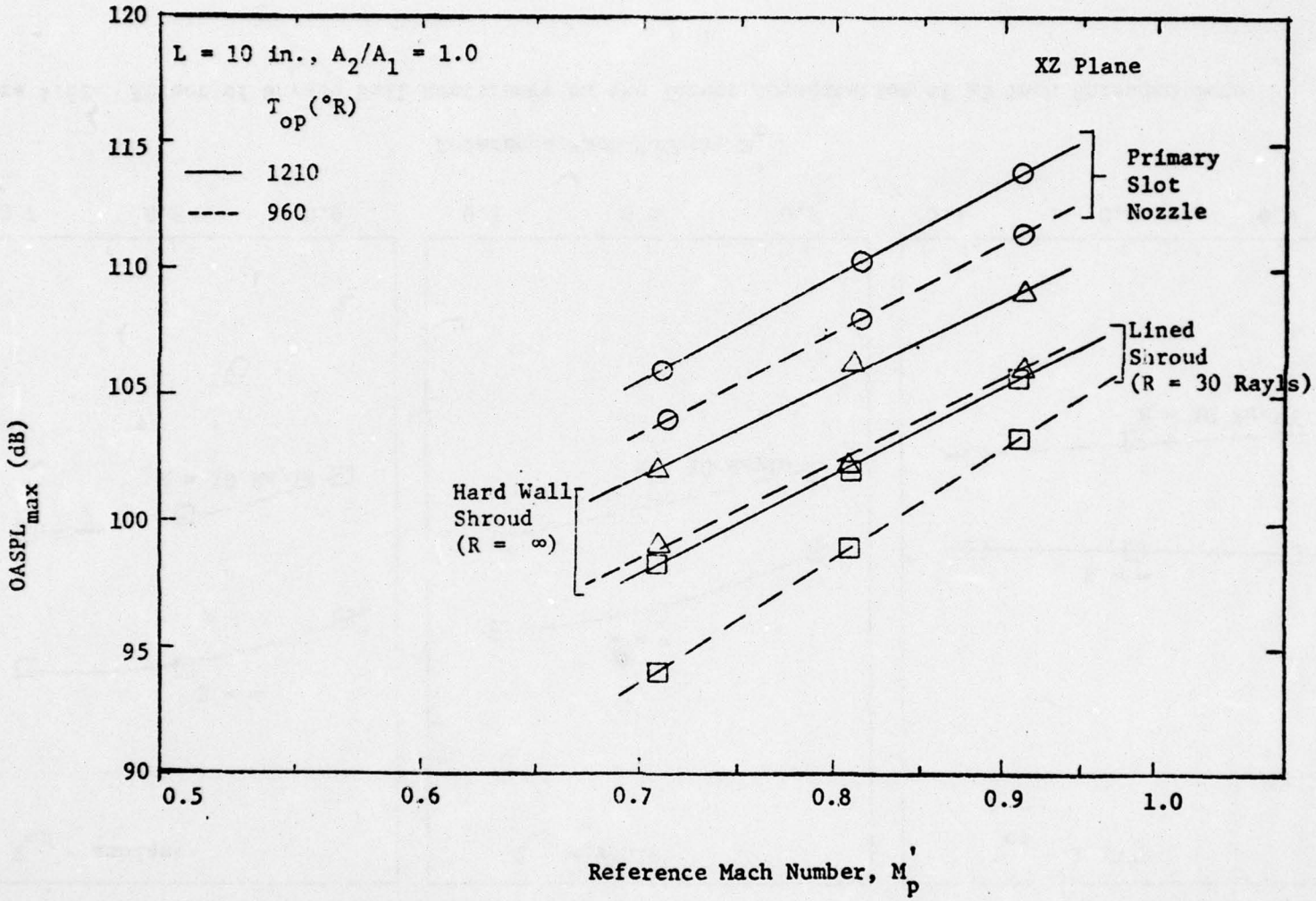

Figure 4.61. Variation of Maximum Sound Level with Reference Mach Number for 10 Inch Shrouded Hot Jets with Hard Wall and Lined Shrouds.

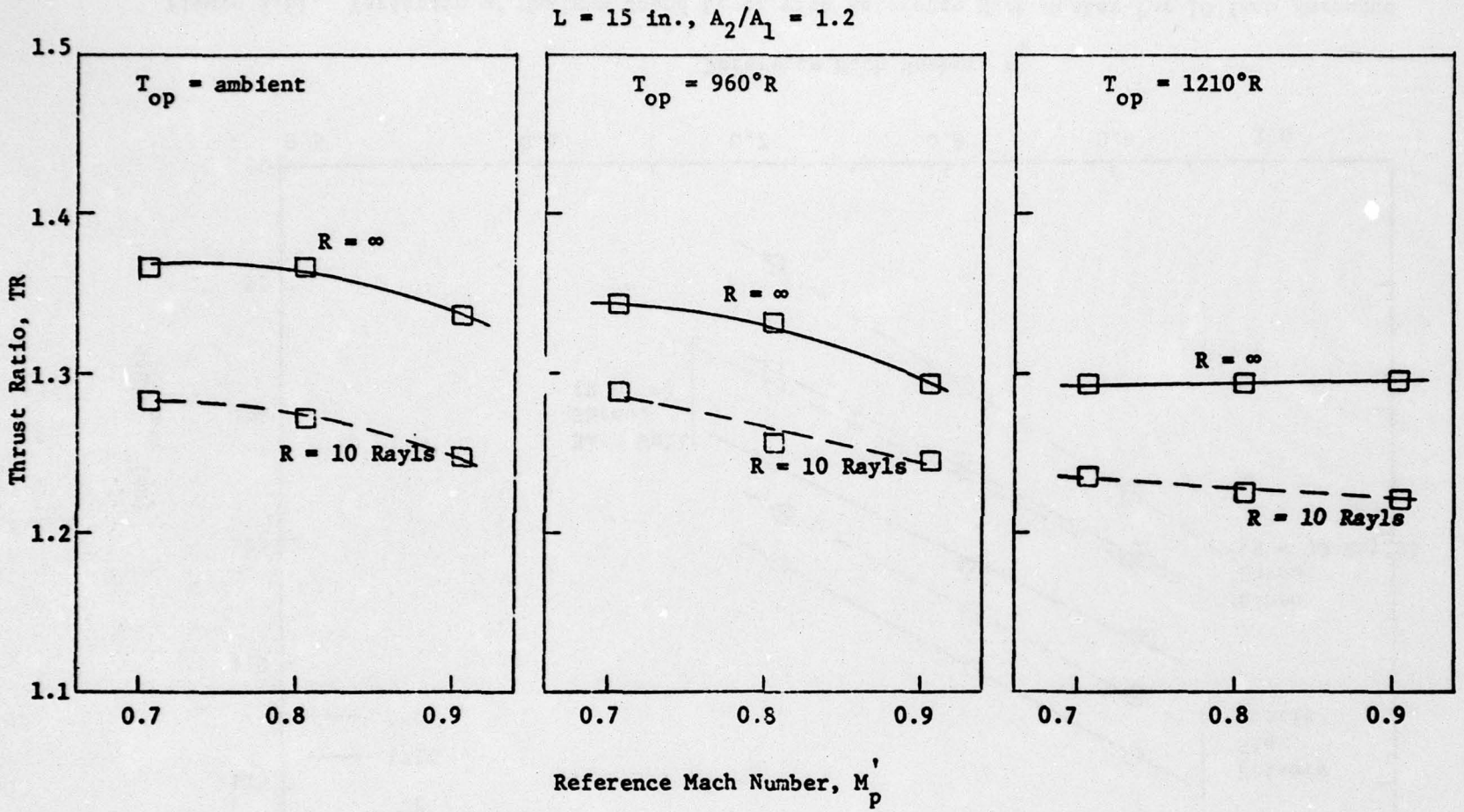

Figure 4.62. Effect of Shroud Wall Resistance on the Thrust Augmentation of 15 Inch Shrouded Jets.

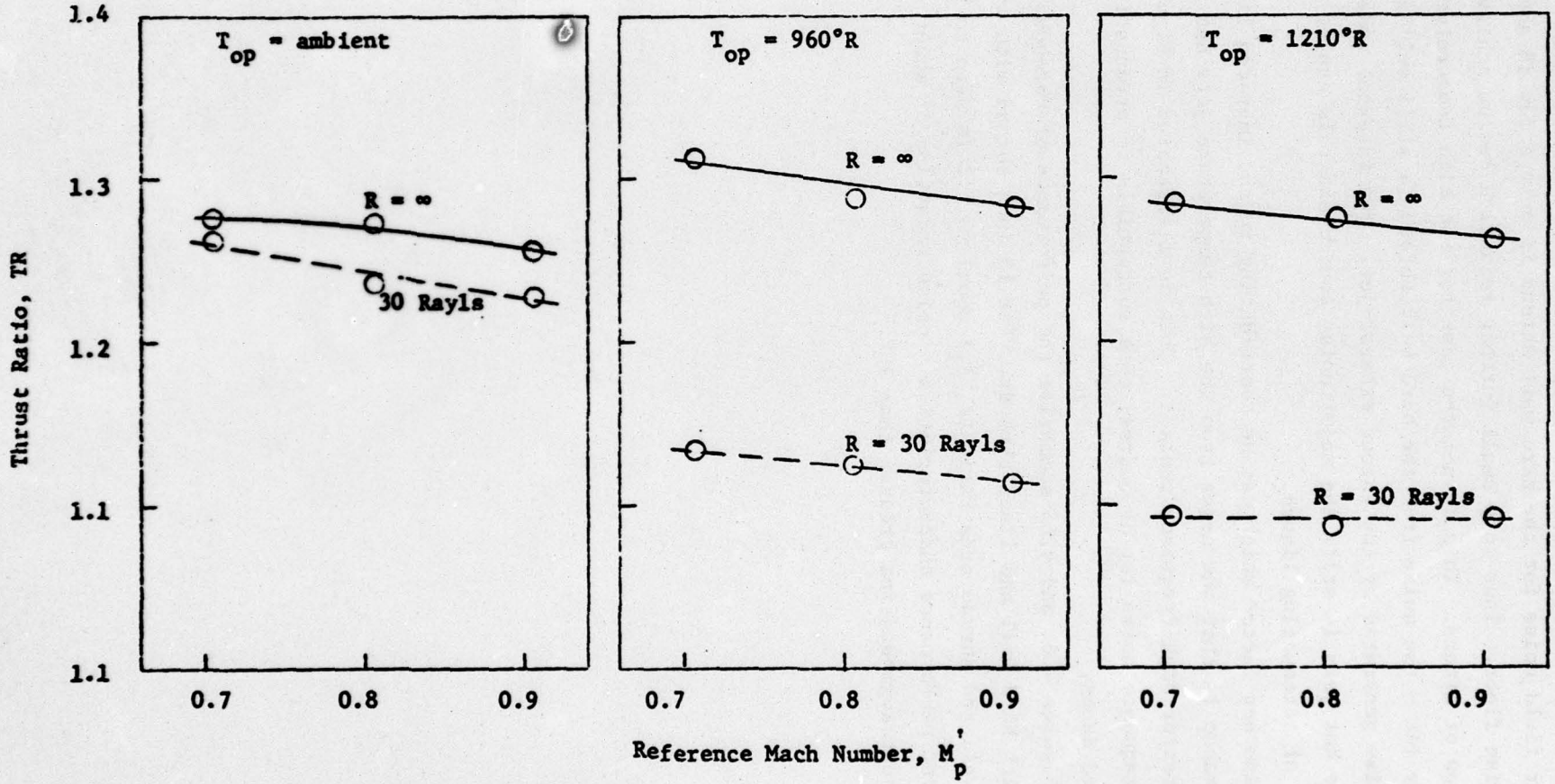

Figure 4.63. Effect of Shroud Wall Resistance on the Thrust Augmentation of 10 Inch Shrouded Jets.

the far field noise for the hard wall shroud is only a few dB above the noise floor. Thus only small further reduction can be achieved by addition of liners. This is not the case for the high temperature primary jet - the noise from the hard wall shroud is still well above the noise generated by the shroud exhaust jet. The internal noise for the hot jets is still the major noise source and this can be reduced by use of attenuating liners.

Another factor which may be contributing to the improved liner performance is that the noise from the high temperature jets has a much greater high frequency content. This is illustrated in Figure 4.40a. High frequency noise is, of course, more susceptible to attenuation in lined ducts.

Figures 4.64 and 4.65 summarize the performance of shrouded hot jets with hard wall and lined shrouds. The 15 inch shroud with 10 Rayl liner wall and shroud area ratio (A_2/A_1) equal to 1.2 is seen to have excellent performance characteristics - noise reduction of about 13 dB and thrust augmentation greater than 20%.

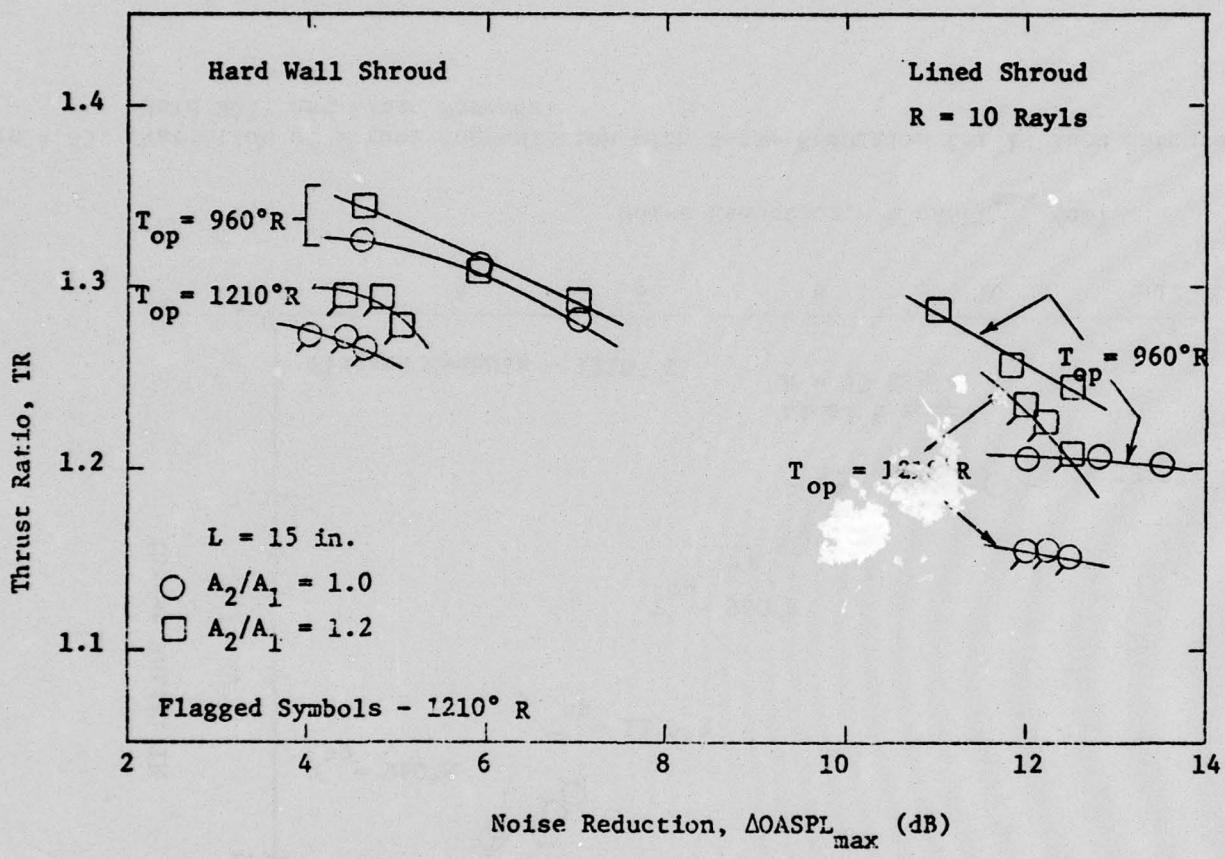

Figure 4.64 Variation of Thrust Augmentation with Noise Reduction for 15 inch Shrouded Hot Jets with Hard Wall and Lined Shrouds

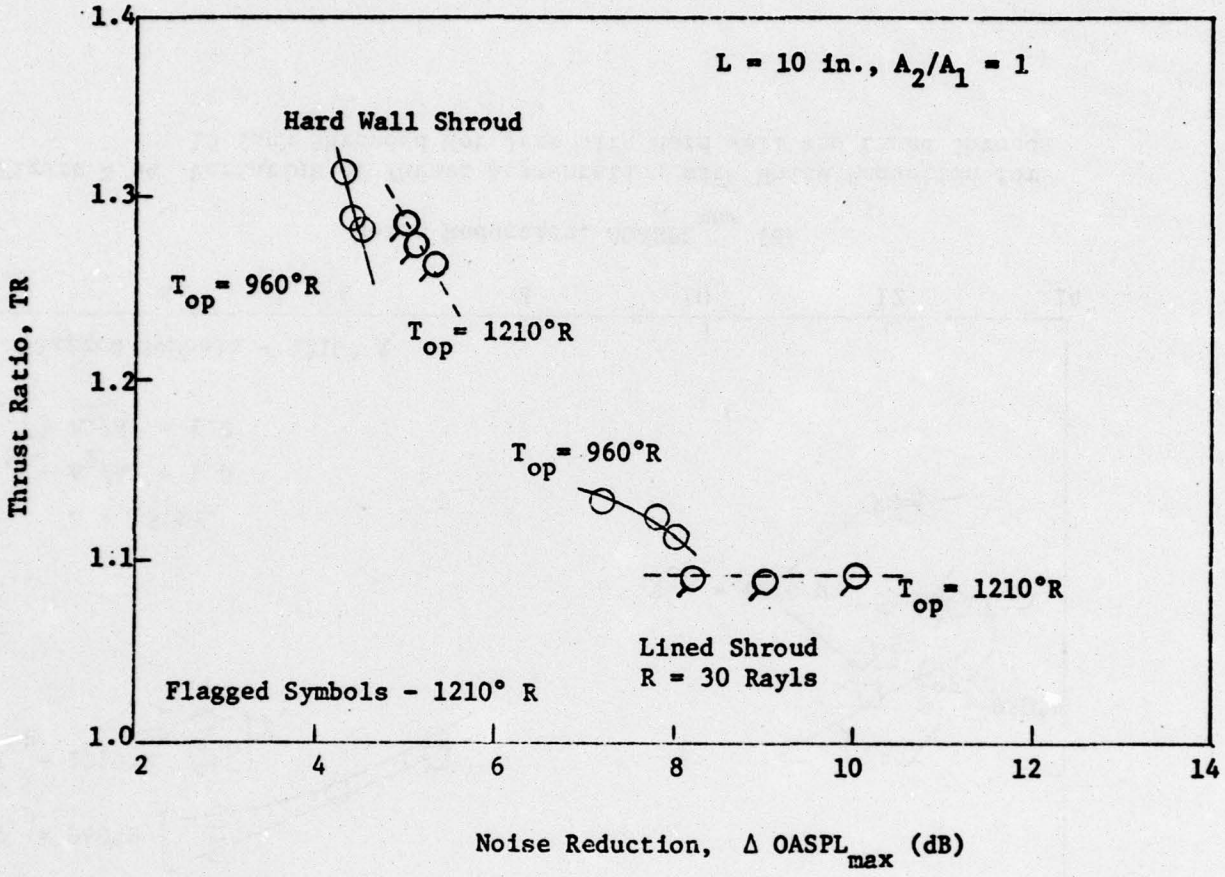

Figure 4.65. Variation of Thrust Augmentation with Noise Reduction for 10 Inch Shrouded Hot Jets with Hard Wall and Lined Shrouds.

5.0 COMPARISON OF EXPERIMENTAL DATA WITH THEORETICAL CALCULATION

In this section some of the experimental data presented in Section 4.0 will be compared with the results of the one-dimensional theory of Section 3.0 where the flow through the shroud is assumed to be frictionless and isoenergetic. In the theory, all the noise generated under the shroud is assumed to be absorbed by the shroud so that the noise radiated to the far field is due only to the mixed jet exhausting from the shroud. The theoretical noise prediction thus represents the noise floor for the ejector system. Since the assumptions made in the theoretical calculations are characteristic of an ideal ejector system, the extent of agreement between the experimental data and these calculations provides a measure of how nearly the model ejector achieves ideal performance.

Figure 5.1 compares the mass flow ratio (K_m) obtained from the model ejector system for both hot and cold shrouded jets with the theoretically predicted values. For low divergent ratios, $A_2/A_1 \leq 1.2$, the 15 inch shroud data shows excellent agreement with the prediction. This indicates that these shrouds are sufficiently long so that the primary and secondary streams mix thoroughly beneath the shroud. Although the mass flow ratio for the 15 inch shroud increases with increasing area ratio over the entire range tested, for the larger values of A_2/A_1 the data is noticably below the prediction. The trends for the 10 inch shroud are similar to those for the 15 inch shroud except that the divergence between experimental and predicted values of K_m begins to occur at an area ratio slightly greater than one. As has been discussed earlier, the 5 inch shroud is not long enough to produce good mass induction and was not tested extensively.

Figure 5.2 shows the measured values of the thrust augmentation compared with theoretically calculated values. The experimental values peak at $A_2/A_1 = 1.2$ for the 15 inch shroud and at $A_2/A_1 = 1$ for the 10 inch shroud. However, these values are considerably below the predicted values even for the 15 inch shroud. This is because the thrust ratio depends on the product $K_m V_2$ and pumping at a lower rate than ideal K_m

BEST AVAILABLE COPY

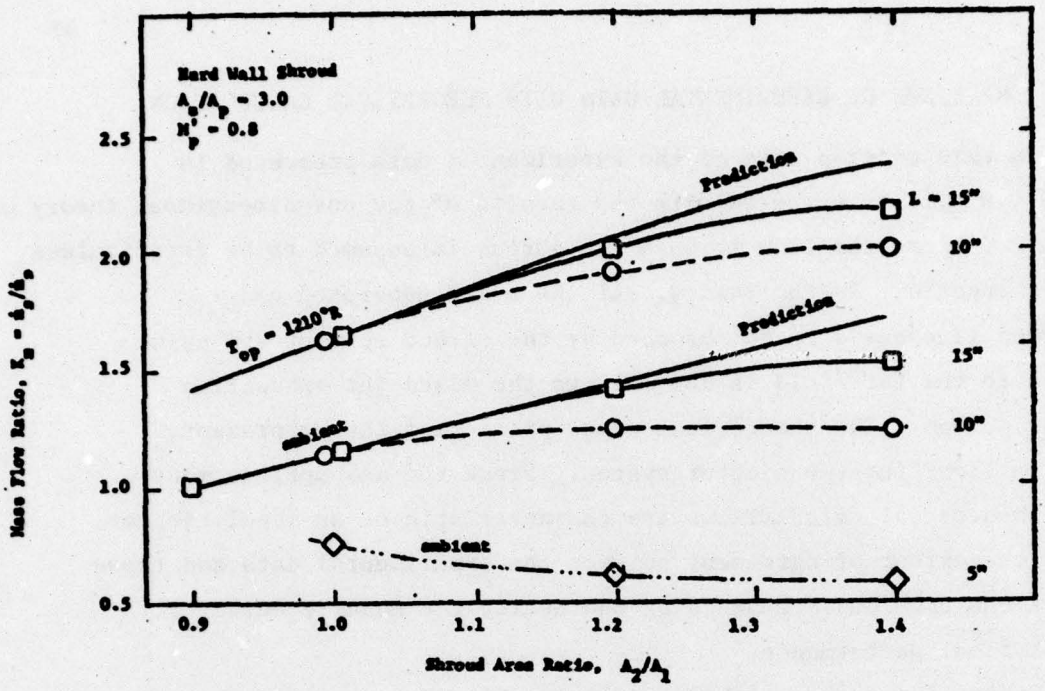

Figure 5.1. Comparison of One-Dimensional Theoretical and Experimental Results of Mass Flow Ratio for Shroud Nozzle, (Hard Walls).

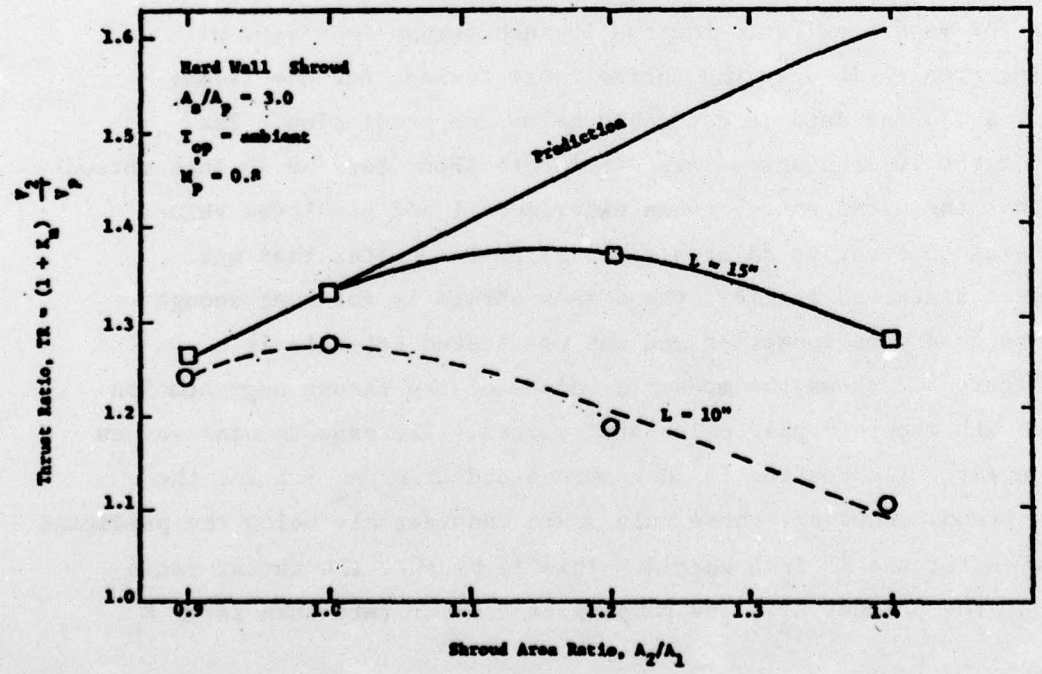

Figure 5.2. Comparison of One-Dimensional Theoretical and Experimental Results of Thrust Ratio for Shroud Nozzle, (Hard Walls).

will also cause the shroud exit velocity V_2 to be lower than ideal. Hence the product $K_m V_2$ is considerably below the ideal case.

Comparison of measured acoustic data with the theoretical predictions is given in Figures 5.3, 5.4 and 5.5 for the 15 inch shrouds at the three primary jet temperatures. The predicted noise levels for the shrouded nozzle were obtained by scaling the primary nozzle data according to the V^8 Law.

$$\Delta OASPL_{max} = 10 \log_{10} \frac{A'_p}{A_2} \left[\frac{V'_p}{V_2} \right]^8$$

This relation assumes that the maximum intensity scales just like the sound power and thus does not account for the forward focussing effect due to source convection. Also ignored in this calculation is the effect of nozzle aspect ratio on the directional characteristics of the radiated sound. Considering these shortcomings, it was felt that the theoretical prediction could not be used to reliably determine the noise floor of the ejector system. For this reason the shroud inlet was modified and acoustic data was taken for flow only through the shroud. These data were taken on the 15 inch, parallel wall shroud ($A_2/A_1 = 1$) for ambient stagnation temperature and a stagnation temperature of 810°R corresponding to $T_{op} = 1210°$ R. The cold flow data were presented in Figure 4.28 as a function of shroud exit velocity. The change in stagnation temperature had no measurable effect on the data shown in that figure as other experiments revealed. By using the relation between V_2 and M'_p given in Figure 4.18 and similar relations for the high temperature jets, the acoustic data for the shroud alone has been replotted in Figures 5.3, 5.4 and 5.5. These data represent the actual noise floor for the 15 inch shroud with $A_2/A_1 = 1$. In all cases the measured noise floor is above that predicted on the basis of scaled primary nozzle data. The calculated values are, however, always within 3 dB of the experimentally determined values.

Of particular interest in Figures 5.3 to 5.5 is how closely the noise level parallel wall for the 15 inch lined shroud approaches the noise floor. For the cold flow case the lined shroud noise level

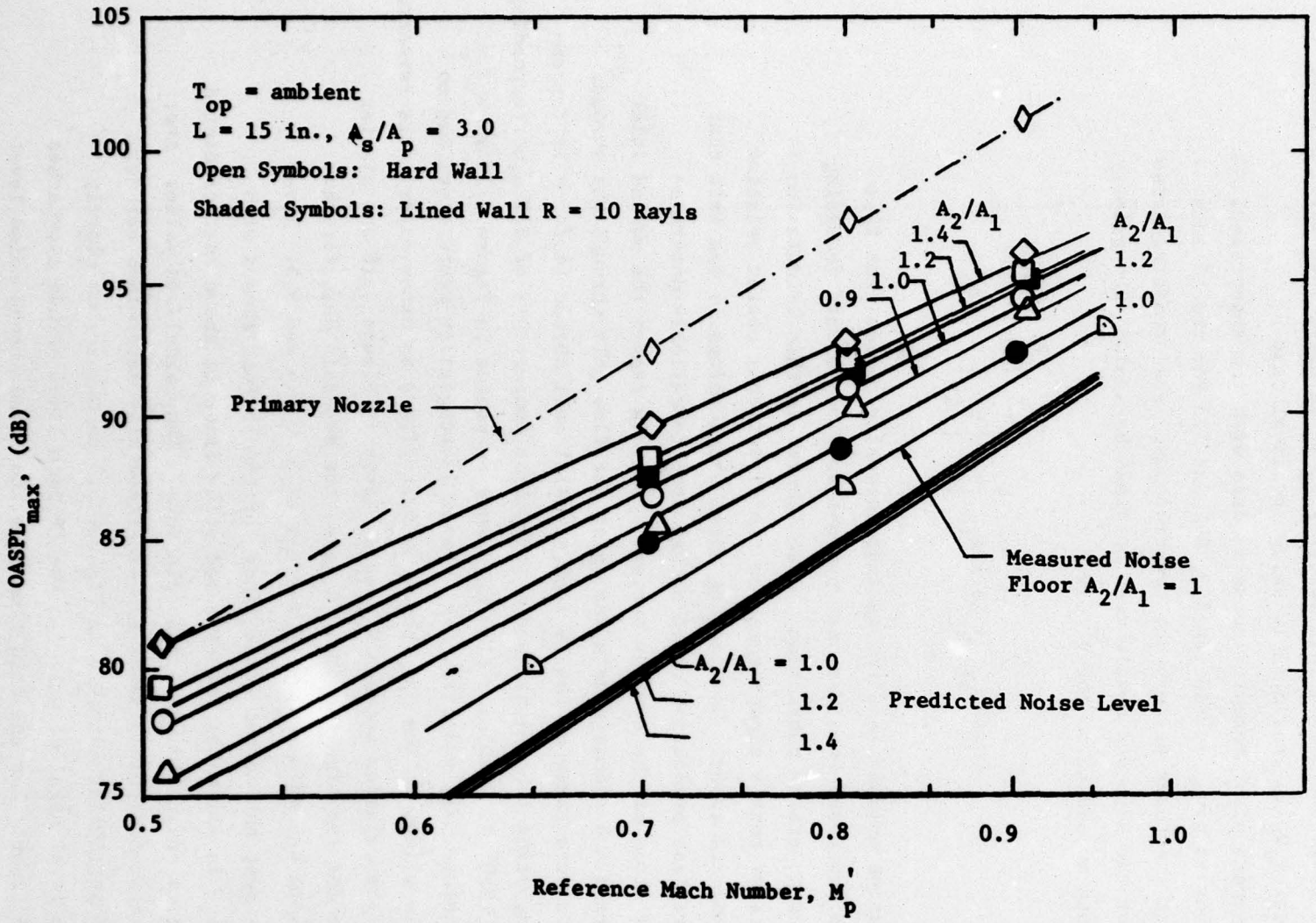

Figure 5.3 Comparison of One-Dimensional Theoretical and Experimental Results of $OASPL_{max}$ for Shrouded Nozzle at T_{op} = ambient.

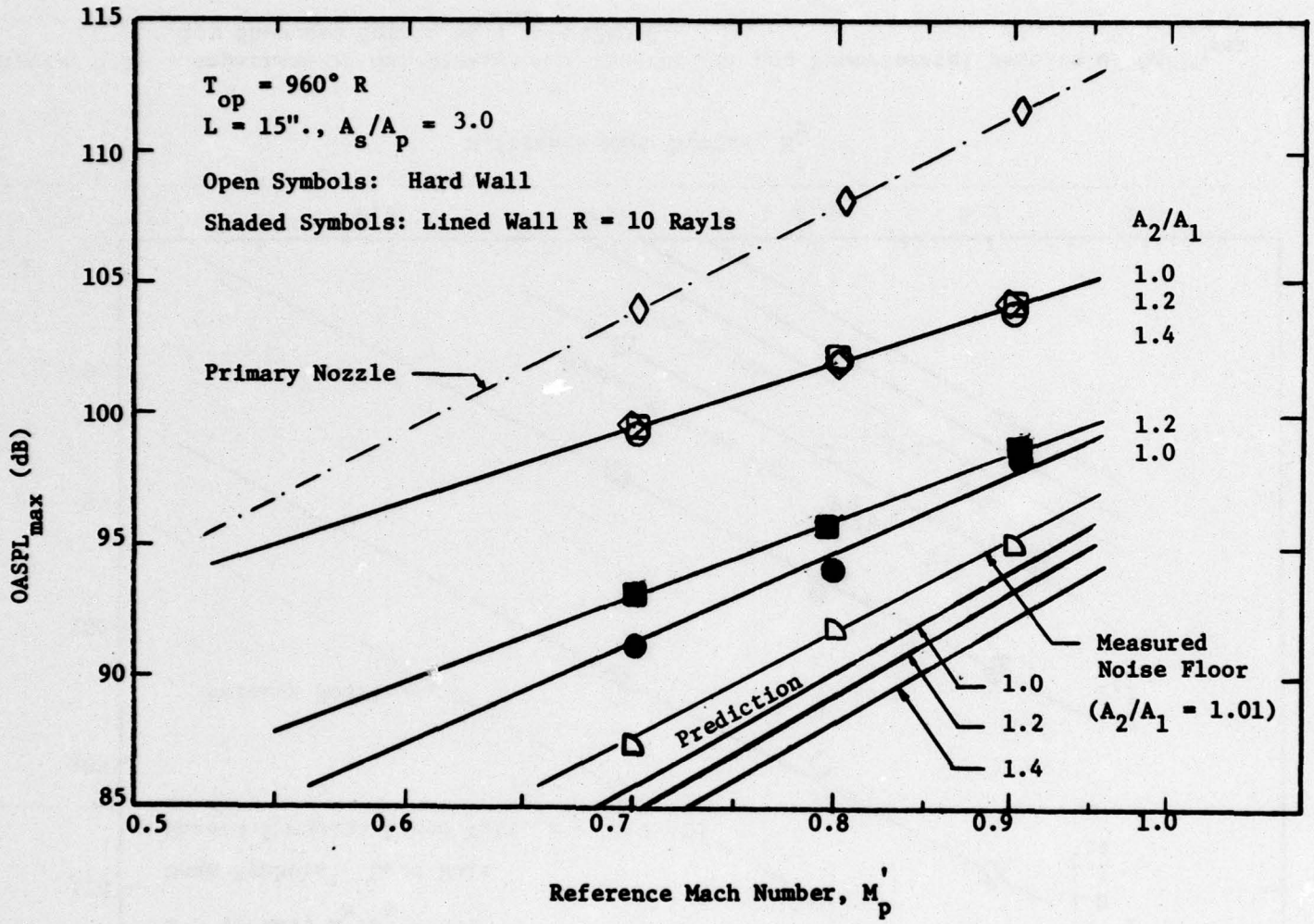

Figure 5.4 Comparison of One-Dimensional Theoretical and Experimental Results of $OASPL_{max}$ for Shrouded Nozzle at T_{op} = 960° R.

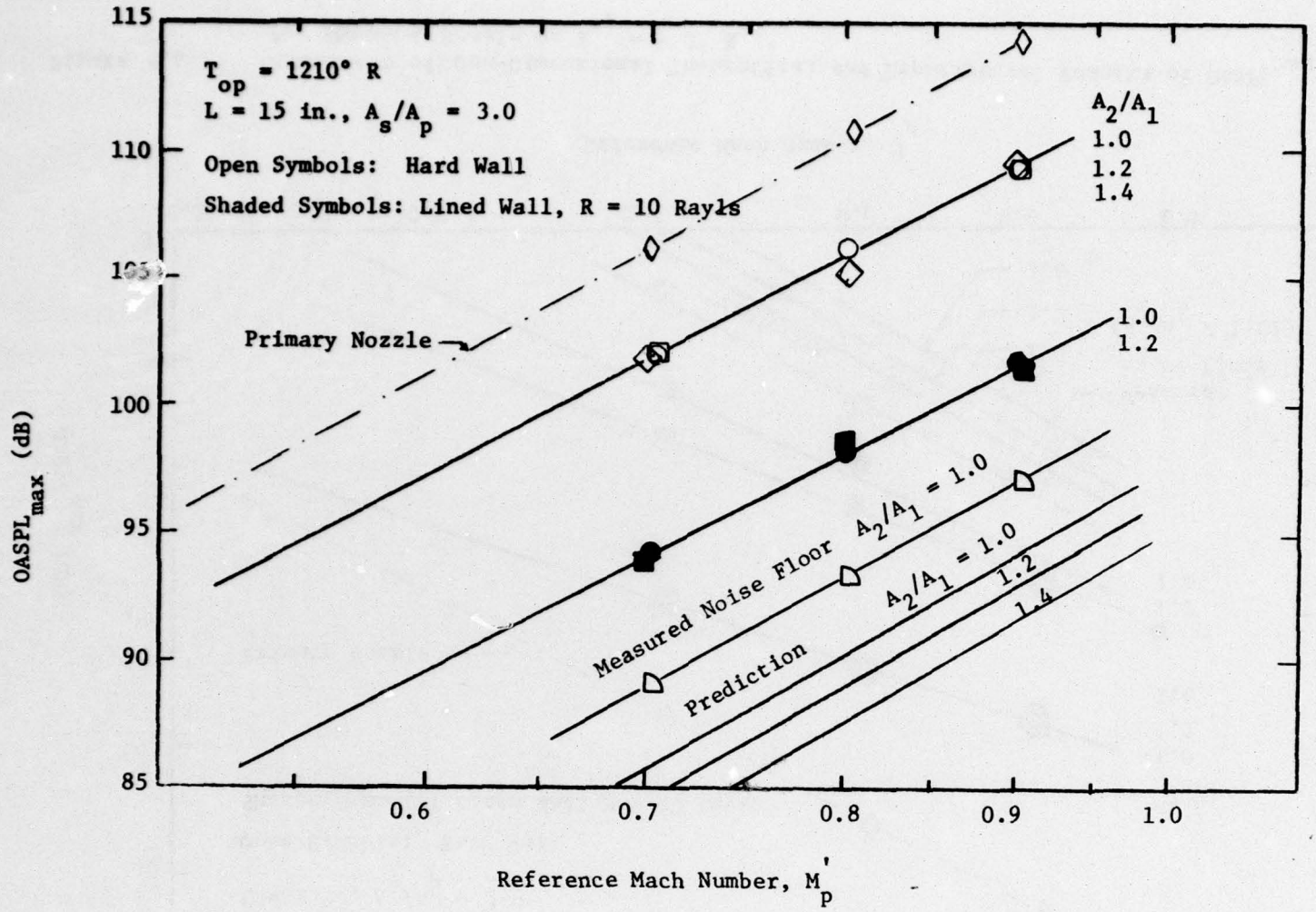

Figure 5.5 Comparison of One-Dimensional Theoretical and Experimental Results of $OASPL_{max}$ for Shrouded Nozzle at T_{op} = 1210°R.

is within 1.5 dB of the noise floor at $M_p' = 0.9$. This corresponds to a noise reduction of 9 dB compared to the primary nozzle. At $T_{op} = 960°$ the 15 inch lined shroud is within 3 dB of the noise floor. At $T_{op} = 1210°$ the noise from the shrouded nozzle is within 5 dB of the noise floor corresponding to a noise reduction of 13 dB compared to the primary nozzle. These comparisons show that the noise attenuating liners for the 15 inch shroud with $A_2/A_1 = 1$ are effective in attenuating a large proportion of the sound generated beneath the shroud. A potential for further noise reduction does exist but such reduction will become progressively more difficult to achieve as the theoretical limit is approached.

In summary, the comparisons presented in this section indicate that for the longest, parallel wall shroud the model ejector used for these experiments comes quite close to achieving the characteristics of the ideal ejector for which the calculations of Section 3.0 were made.

6.0 SUMMARY AND RECOMMENDATIONS.

6.1 Purpose of Research and Description of Experiments.

Previous studies by the UTSI Aeroacoustic Division have shown that ejector shrouds around a dual-circular nozzle assembly are capable of significantly reducing the jet noise and simultaneously increasing the thrust in comparison to equivalent unshrouded nozzles.

The present research series has extended those basic experiments to slot nozzles with aspect area w/h = 27, and ejector shrouds having a total shroud area of four times the area of the primary jet, employing both cold and hot primary jet flows (slot height - 7.6 mm, slot width = 203 mm).

Special attention was given to the noise attenuating liners of the interior surfaces of the shroud to assure that the liners were plane and as smooth as compatible with their function; furthermore, the flow passages through the liner cavities were kept as tight as possible to reduce undesirable secondary flow.

The experiments were carried out without external flow, with a large shield installed to eliminate noise contamination from the inlet of the entrained secondary flow.

The nozzle exhaust velocities were subsonic up to choking, with the noise examined in the far field.

All results for unshrouded and shrouded configurations were compared with the premise that the primary nozzle in both systems operated at the same mass flow, the same total pressure and total temperature. Thus, for the reference mass flow, the equivalent exit area of the nozzle in the shrouded configuration was usually somewhat smaller due to the lower static pressure and higher exhaust Mach number at the nozzle exit.

6.2 Performance of Ejector Shrouds with Internal Liners.

Suitably designed ejector nozzles were found to reduce the external noise by up to 13 dB and simultaneously to increase the thrust

up to 30% for the liner configurations with hot flow and shroud lengths of about 12 times the shroud height. The specific values vary somewhat with Mach number and temperature of the primary flow. In general, the noise attenuation improves and the thrust augmentation decreases with increase of nozzle exit Mach number.

For the primary flow with high temperatures and exhaust Mach numbers close to choking, the noise reduction was about 12 dB accompanied by a thrust increase of about 20%.

6.3 Performance of Shrouds with Hard-Walls and Comparison with Walls with Liners.

As expected, the noise attenuation is substantially lower for hard-wall shrouds, but the thrust augmentation is greater in comparison to the shrouds with attenuating liners. For the highest jet temperature tested and an exhaust Mach number close to choking, the noise attenuation is only 5 dB with a thrust increase of about 28% for hard-wall shrouds.

It is obvious that the liners are very effective in noise reduction. However, the surface roughness of the liners, as used in the experiments, and the inability to stop effectively the leakage flow through the liner cavities, generated thrust losses which should be reducable by more refined designs.

6.4 Directivity and Frequency Spectrum of the Noise.

As in the case of simple slot nozzles, the peak noise in the far field of shrouded nozzles occurs at locations of between 30° and 50° with respect to the primary jet flow. All values for noise reduction, quoted before, refer to the respective peak noise of each configuration.

The shrouds, particularly those with noise attenuation liners, were found to be very effective in attenuating the high frequency noise above 1.0 kHz. In the frequency range below 1.0 kHz, the attenuation was relatively small. Thus, the peak frequencies for the shrouded configurations with liners are shifted to lower values, specifically to the range around 2.0 kHz at far-field locations of about 50° inclination with respect to the nozzle flow.

6.5 Effect of Shroud Length and Wall Divergence.

The overall best results were obtained with a shroud length of about 12 times the shroud height. A shroud length of about 8 times the shroud height gave substantially inferior values for noise attenuation and particularly for thrust augmentation. Obviously, the primary jet is not capable of mixing as well under the shroud of reduced length.

A few tests were conducted for a very short shroud with a length of only 4 times the shroud height. The results imply that the nozzle flow does neither substantially entrain secondary air nor mix appropriately with it. Thus, the short shroud is not only ineffective in noise attenuation, but was also generally found to be accompanied with a thrust reduction instead of a thrust increase.

A comparison of the current shroud results with the results of other investigators on thrust augmentation, including tests on circular nozzles with circular shrouds, showed that a good correlation exists. All of these experiments indicated that a shroud length of about 10 times the shroud height (or shroud diameter) is required for good air-entrainment and thrust augmentation.

The shroud length, required for proper mixing of the primary flow with the entrained flow, depends also on the mixing mechanism itself. Various means for super-mixing are known; when applied to ejector shroud configurations, the required shroud length can be essentially reduced in comparison to those of conventional mixing.

6.6 Shroud Area in Comparison to Primary Flow Area.

The current results have been obtained for a ratio of shroud area over primary nozzle area of approximately four. It is understood that for a given primary nozzle the shroud length, required for complete mixing, in relation to the shroud height will not change very much with increasing shroud area. However, the size of the shroud in relation to the primary nozzle dimensions, will obviously increase directly with the shroud height, making large shroud areas impractical for aircraft application. For application to

STOL-wings with powered lift devices, the ratio of shroud area to primary nozzle area of about four, as used in these experiments, appears to be a practical design value.

6.7 Comparison with Theory.

Theoretical investigations on ejector shrouds were conducted, assuming inviscid one-dimensional flow (with complete mixing underneath the shroud). It was verified by these calculations that thrust augmentation and noise attenuation grow steadily with increasing shroud size.

Comparison of the experimental and theoretical thrust augmentation shows good correlation for the long shroud $L/h_s = 12$ with parallel walls. For divergent walls of the long shroud, the experimental thrust augmentation gets steadily worse in comparison to theory. The experimented thrust augmentation reached a maximum of 1.35 at a divergence corresponding to exit/inlet area = 1.2, whereas the theoretical values continues to increase monotonically with area ratio.

In the theoretical studies, it was assumed as a limit that all noise, generated under the shroud, is completely attenuated by the liners and only the fully mixed flow emerging from the shroud exit generates noise. For the long shroud with $L/h_s = 12$ and liners, the experimental noise reduction by the shroud was found to be about 12 dB for the high temperature nearly choked jets. The theoretically possible value, for those conditions as defined above, was found to be 17 dB based on measurements for the shroud jet only. Thus, it can be concluded that there is still a potential for further noise reduction. However, such reductions will become progressively harder to be achieved in view of the approach to theoretical minimum noise.

6.8 Recommendations.

The remarkable potential or properly designed ejector shrouds, capable of significantly reducing the exhaust noise (12 dB), without thrust penalty but to the contrary with a sizeable thrust augmentation (20%), should be further examined in order to facilitate the incorporation of

superior ejector shrouds in the design of high performance aircraft. In the following a number of recommendations for further research are listed which should improve the performance of ejector shrouds even further beyond the potential identified in the current experiments.

The effectiveness of super-mixing devices should be examined to shorten the mixing length between primary and secondary flow and thus also the required length of the shroud. Based on experiments of other investigators, the shroud length could be reduced to at least 1/2 of its current length without penalty of thrust augmentation. However, the effect of super-mixing on noise attenuation is not known and needs to be determined.

The design of noise attenuating liners for ejector shrouds should be studied in more detail to define optimum liner configurations. Such improved configurations are expected to increase further the noise attenuation of shrouds and reduce the sizeable penalty caused by the current liner design.

In the current experiments, the shrouds are designed either with constant area throughout their length, or with constant divergence or convergence. It is believed that a more effective design for rapid mixing would be to have a constant area upstream section, followed by a suitably selected divergent part.

All experiments on ejector shrouds have been carried out for ambient flight conditions, that is without external flow. For broader applicability of this research, the effect of external flow with velocities in the take-off and landing regime should be examined. Theoretical estimates, conducted by the UTSI Aeroacoustic Group for a Ph.D. - dissertation, showed that the effect of external flow on both noise attenuation and thrust augmentation is relatively small up to flight velocities of about M = .4. This theoretical result should be verified by experiments.

REFERENCES

1. Goethert, B. H., et al., "Investigation of Feasible Nozzle Configuration for Noise Reduction in Turbofan and Turbojet Aircraft, Vol I: Summary and Multi-Nozzle Configurations," Report No. FAA-RD-75-163-I, 1975.

2. Middleton, D., "The Noise of Ejectors," Aeronautical Research Council, R & M No. 3389, 1965.

3. Whittley, D. C., "Ejector-Powered Lift Systems for V/STOL Aircraft," Canadian Aeronautics and Space Journal, Vol. 20, No. 5, May 1974, pp. 179-189.

4. Dorsch, R. G., E. A. Krijsa, and W. A. Olsen, "Blown Flap Noise Research," AIAA Paper 71-745.

5. O'Keefe, J. V. and G. S. Kelley, "Design Integration and Noise Studies for Jet STOL Aircraft, Volume I: Program Summary", NASA CR-114471, May 1972.

6. Ko, S. H., "Sound Attenuation in Lined Rectangular Ducts with Flow and Its Application to the Reduction of Aircraft Engine Noise," Journal of Acoustical Society of America, Vol. 50, No. 6 (Part 1), 1971, pp. 1418-1432.

7. von Karman, T., "Theoretical Remarks on Thrust Augmentation," Reissner Anniversary Volume, 1949.

8. Lighthill, M. J., "Jet Noise" (Wright Brothers Lecture), AIAA Journal, Vol. 1, No. 7, pp. 1507-1517, July 1963.

9. Ribner, H. S., "The Generation of Sound by Turbulent Jets," Advances in Applied Mechanics, Vol. 8, pp. 103-182, Academic Press, 1964.

10. Lighthill, M. J., "On Sound Generated Aerodynamically: I. General Theory," Proceedings of the Royal Society, Vol. 211 A, pp. 564-587, 1952.

11. Lush, P. A., "Measurements of Subsonic Jet Noise and Comparison with Theory," Journal of Fluid Mechanics, Vol. 46, Part 3, pp. 477-500, 1971.

12. Coles, W. D., J. A. Mihaloew and E. E. Callaghan, "Turbojet Engine Noise Reduction with Mixing Nozzle-Ejector Combination," NACA Tech. Note 4317, August 1958.

13. Goethert, B. H., et al., "Investigation of Feasible Nozzle Configurations for Noise Reduction in Turbofan and Turbojet Aircraft, Vol II: Slot Nozzle Configurations," Report No. FAA-RD-75-163-II, 1975.

14. Greatrex, F. B. and D. M. Brown, "Progress in Jet Engine Noise Reduction," Advances in Aeronautical Sciences, Proceedings of First International Congress in Aeronautical Sciences, Madrid, Pergoman Press, 1960.

15. Reid, J., "The Effect of a Cylindrical Shroud on the Performance of a Stationary Convergent Nozzle," Aeronautical Research Council, R & M No. 3320, 1962.

16. Lowson, M. V., "Duct Acoustics and Mufflers," AGARD Lecture Series on Aircraft Noise Generation, Emission and Reduction, AGARD-LS-77, June 1975.

17. Powell, A., "The Influence of Exit Velocity Profile on the Noise of a Jet," Aeronautical Research Council, Report No. A.R.C. 16156, 1953.